Design, Synthesis and Characterization of Artificial Siderophores and their Conjugates

A Thesis

submitted to

Indian Institute of Science Education and Research Pune in partial fulfilment of the requirements for the BS-MS Dual Degree Programme

by

Arjun Jagdish

Indian Institute of Science Education and Research Pune

Dr. Homi Bhabha Road,

Pashan, Pune 411008, India

April, 2024

Supervisor: Prof. Dr. Mark Brönstrup, HZI Braunschweig

Arjun Jagdish

Certificate

This is to certify that this dissertation entitled **"Design, Synthesis and Characterization of Artificial Siderophores and their Conjugates"** towards the partial fulfilment of the BS-MS dual degree programme at the Indian Institute of Science Education and Research, Pune represents study/work carried out by Arjun Jagdish at the Helmholtz Centre for Infection Research (HZI) Braunschweig, under the supervision of Prof. Dr. Mark Brönstrup, Head, Department of Chemical Biology, HZI Braunschweig, during the academic year 2023-2024.

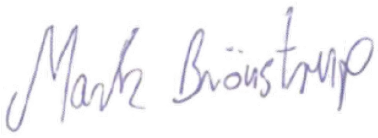

Prof. Dr. Mark Brönstrup

Committee:

Thesis Supervisor: Prof. Dr. Mark Brönstrup

Thesis Expert: Prof. Pinaki Talukdar

This thesis is dedicated to my family

Declaration

I hereby declare that the matter embodied in the report entitled **"Design, Synthesis and Characterization of Artificial Siderophores and their Conjugates"** are the results of the work carried out by me at the Department of Chemical Biology, Helmholtz Centre for Infection Research, Braunschweig, under the supervision of Prof. Dr. Mark Brönstrup, and the same has not been submitted elsewhere for any other degree. Wherever others contribute, every effort is made to indicate this clearly, with due reference to the literature and acknowledgement of collaborative research and discussions.

Arjun Jagdish

20191071

Acknowledgements

This study has been an enriching learning experience, thanks to contributions by several individuals. I would like to express my deepest gratitude to Prof. Dr. Mark Brönstrup for providing me the opportunity to work on this project, to be a part of a remarkable research environment, and for supporting me in this endeavour, in particular during initial stages.

I am deeply indebted to Dr. Vadim Korotkov for mentoring me during this project. In particular, I cannot thank him enough for the unyielding patience towards my queries, his meticulous proofreading of my thesis, and being accommodating throughout. His insights and expertise have been instrumental to my learning experience.

I express my sincere gratitude to Felix Schwenke and Dr. Hazel Fuchs for their cooperation with expediting experiments, and their accommodation in this regard. I also thank Esther Surges and Dr. Kirsten Harmrolfs for their assistance with NMR experiments. Many thanks to Bettina Mehner for easing my onboarding process.

Interactions with colleagues at Department CBIO and COPS at the HZI have further shaped my overall experience. My heartfelt thanks go to Patrick Raunft for his consideration throughout, stimulating technical discussions, and moral support. I am extremely grateful to Simon Hilker and Tamara Ilioska for their valuable resourcefulness and for being welcoming. I also thank Dr. Travis Coyle, Dr. Anna Vetter, Dr. Ravi Kumar Akula, Sarang Mishra, Dr. Jackson Muema, Dr. Pablo Redero Garcia and Dr. Aditya Shekhar for their consideration.

Finally, I thank my family and friends for their continuous moral support.

List of Abbreviations

Ala-OH	Alanine
AMR	Antimicrobial Resistance
ATP	Adenosine Triphosphate
ABC	ATP-Binding Casette
Boc	*tert*-Butoxycarbonyl
CAM	Cerium-Ammonium-Molybdate
CAS	Chrome Azurol S
COSY	homonuclear COrrelation SpectroscopY
CuAAC	Copper (I)-catalyzed Azide-Alkyne Cycloaddition
cUTI	complicated Urinary Tract Infection
DAD	Diode Array Detector
DCC	*N,N'*-Dicyclohexylcarbodiimide
DCM	Dichloromethane
dH_2O	distilled water
DIPEA	*N,N*-Diisopropylethylamine
DMAP	4-Dimethylaminopyridine
DMF	Dimethylformamide
DMSO	Dimethyl sulfoxide
DNA	Deoxyribonucleic Acid
DOTAM	2-[4,7,10-tris(2-amino-2-oxoethyl)-1,4,7,10-tetrazacyclododec-1-yl]acetamide
EA	Ethyl Acetate
ECF	Extracytoplasmic Function
EDC	1-Ethyl-3-(3-dimethylaminopropyl)carbodiimide
eq	equivalent
ESI	Electron Spray Injection
ESKAPE	*Enterococcus faecium, Staphylococcus aureus, Klebsiella pneumoniae, Acinetobacter baumannii, Pseudomonas aeruginosa,* and *Enterobacter spp*
HATU	1-[Bis(dimethylamino)methylene]-1H-1,2,3-triazolo[4,5- b]pyridinium 3-oxide hexafluorophosphate
HDTMA	Hexadecyltrimethylammonium Bromide

HPLC	High-performance Liquid Chromatography
HRMS	High Resolution Mass Spectrometry
IBCF	Isobutyl Chloroformate
KHMDS	Potassium hexamethyldisilazide
LAH	Lithium Aluminium Hydride
LC/MS	Liquid chromatography–mass spectrometry
LPS	Lipopolysaccharide
MECAM	1,3,5-N,N′,N″-tris-(2,3-dihydroxybenzoyl)-triaminomethylbenzene
MIC	Minimum Inhibitory Concentration
min	minute
m/z	mass-to-charge ratio
NMM	*N*-Methylmorpholine
NMR	Nuclear Magnetic Resonance
NOESY	Nuclear Overhauser Enhancement Spectroscopy
OM	Outer Membrane
p-ABSA	4-acetamidobenzenesulfonyl azide
ppm	parts per million
QTOF	Quadrupole Time Of Flight
Rf	Retention factor
$Rh_2(esp)_2$	3-[3-(2-carboxy-2-methylpropyl)phenyl]-2,2-dimethylpropanoic acid
ROS	Reactive Oxygen Species
RP	Reverse Phase
r.t.	room temperature
SAC	Siderophore-Antibiotic Conjugates
TBDT	TonB-Dependent Transporter
TEA	Triethylamine
TFA	Trifluoroacetic Acid
THF	Tetrahydrofuran
THPTA	tris-Hydroxypropyltriazolylmethylamine
TLC	Thin-Layer Chromatography

Contents

List of Figures

List of Schemes

List of Tables

Abstract

An emergence of infections with multidrug-resistant Gram negative bacteria accompanied by a decline in new classes of antibiotics over the past few decades poses a serious concern to global health today. A major technical challenge to the advancement of effective antibiotics targeting Gram-negative bacteria is the low permeability of their outer membrane against small molecules, which represent most drugs currently available. This work employs the Trojan Horse strategy to overcome the challenge, by using drug-loaded siderophores to exploit the active iron transport systems in these pathogens. While artificial siderophores, for example based on DOTAM and MECAM cores, to deliver imaging moieties or antibiotics have been reported, knowledge on the influence of core geometry and size on siderophore activity remains limited. This work describes the design, synthesis and preliminary characterization of artificial tris(catecholate) siderophores with a cyclopropane core of defined stereochemistry. The cyclopropane core includes three *cis*-oriented arms for iron chelation, and one *trans*-oriented arm for the attachment of imaging moieties or antibiotics. The conjugation of one such siderophore to ampicillin, a broad spectrum antibiotic, was also achieved. The iron-binding ability of the synthesized siderophores was assessed in a competitive binding experiment using Chrome Azurol S. Upon further microbiological evaluation, these siderophores and the siderophore-antibiotic conjugate may potentially be developed to candidates for *in vivo* pharmacological studies.

1. Introduction

1.1. Antimicrobial Resistance: A Brief Overview

Throughout history, bacterial infections have posed a global threat to human health. In 2019 out of an estimated 13.7 million infection-related deaths, 7.7 million deaths were associated with 33 monitored bacterial pathogens.[1] Exacerbating this issue, AntiMicrobial Resistance (AMR) has gradually become a formidable challenge. Microbes such as bacteria are said to be “resistant” when they are conferred upon physiological mechanisms that enable survival against antimicrobial treatments that would have previously killed them or stopped their growth. While genes conferring drug resistance did exist millions of years ago,[2] the prevalence of AMR has seen an alarming rise the past few decades. This is an issue that requires urgent intervention primarily since no new classes of antibiotics, especially against Gram-negative bacteria, have reached the public over the past 2-3 decades.[3] AMR notably leads to increased infection rates, higher mortality, prolonged hospitalisation and weaker control over disease spread across the world. Risk levels of healthcare options including major surgery, organ transplantation, treatment of preterm infants, diabetes management and cancer chemotherapy will rise significantly without effective antibiotics.[4,5] The magnitude of risk posed by AMR is thus significant, given the impending economic burden that healthcare centres and governments globally would need to bear.

AMR-associated deaths in 2019 were estimated at 4.95 million, which includes 1.27 million deaths attributable to AMR. Methicillin-resistant *S. aureus* alone was linked to upwards of 100,000 casualties attributable to AMR that year (Fig. 1).[6] At current rates and unless countermeasures are implemented, it has been estimated that deaths attributed to AMR could rise to about 10 million each year by 2050.[7] To provide an impetus towards R&D of antibiotics, in 2017 the WHO released a “priority list” of antibiotic-resistant-pathogens that require urgent attention, which includes 5 of the 6 pathogens belonging to the so-called ESKAPE panel—a group of pathogens that “escape” treatment due to increasing Multi-Drug Resistance (MDR).[8] In 2019, 6 of these pathogens (E. *coli*, S. *aureus*, K. *pneumoniae*, S. *pneumoniae*, A. *baumannii*, and P. *aeruginosa*) were responsible for an estimated 929,000 deaths attributable to AMR and 3.57 million deaths associated with AMR (each of the 6 responsible for over

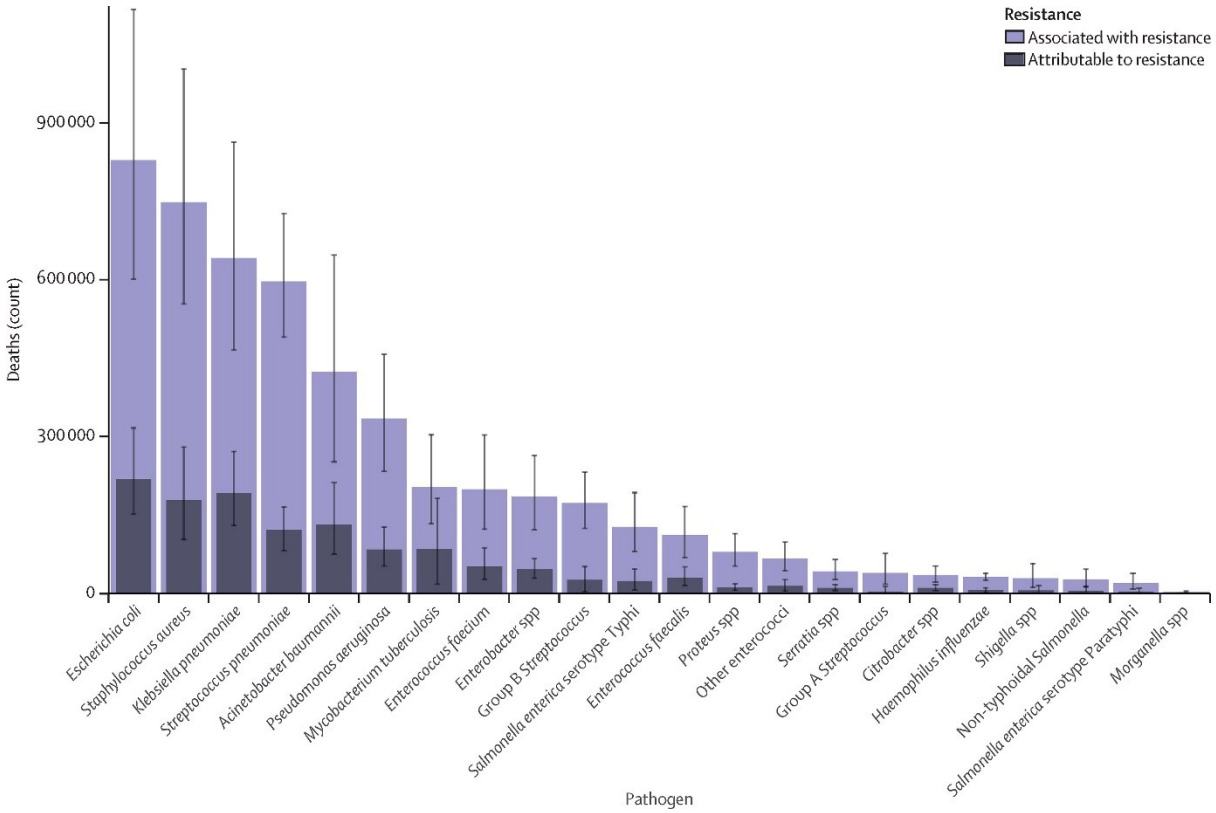

Figure 1: Global deaths attributable to and associated with bacterial antibiotic resistance by pathogen in 2019. Estimates were aggregated across drugs for each pathogen. (ref. 6)

250,000 deaths). Development of AMR in microorganisms is an evolutionarily driven process that has been accelerated by the selective pressure exerted by the misuse and overuse of antibiotics; this may include the administering of antibiotics for either the wrong infection or duration, or either of the wrong type, dosage or route of administration.[4,9] Not to mention, horizontal gene transfer allows bacteria to acquire genetic elements from their external environments—which only accelerates resistance development.[10] At this rate, it would only be a matter of time until resistance is developed against all existing types of antibiotics. Moreover, most of the new classes of antibiotics have been aimed at treating Gram-positive bacteria[4]—easier to tackle compared to Gram-negative bacteria, since the latter possess an additional outer membrane that, apart from reducing overall permeability as a preliminary protective measure, contains lipopolysaccharide (LPS), an essential endotoxin. The LPS may induce an innate immune response in the host, eventually leading to sepsis and septic shock.[11] The outer membrane thus forms the foundation of defences employed by Gram-negative bacteria. Additionally, it can dynamically alter permeability during bacterial growth, as has been revealed in

Enterobacteriaceae.[12] This may result either from one or more mutations altering the structure of a porin,[13] downregulation of porins,[14] or the electric charge within it[15]—effectively attenuating drug permeability. The periplasmic space between the two membranes also contains adapter proteins that aid the efflux, or expulsion, of drug molecules. Efflux pumps along the membranes are particularly important in case of Gram-negative bacteria, since their activity enhances other resistance mechanisms.[16]

A variety of other resistance mechanisms have been reported (Fig. 2).[17] Modification of antibiotics entails either the attachment of chemical moieties to them or their

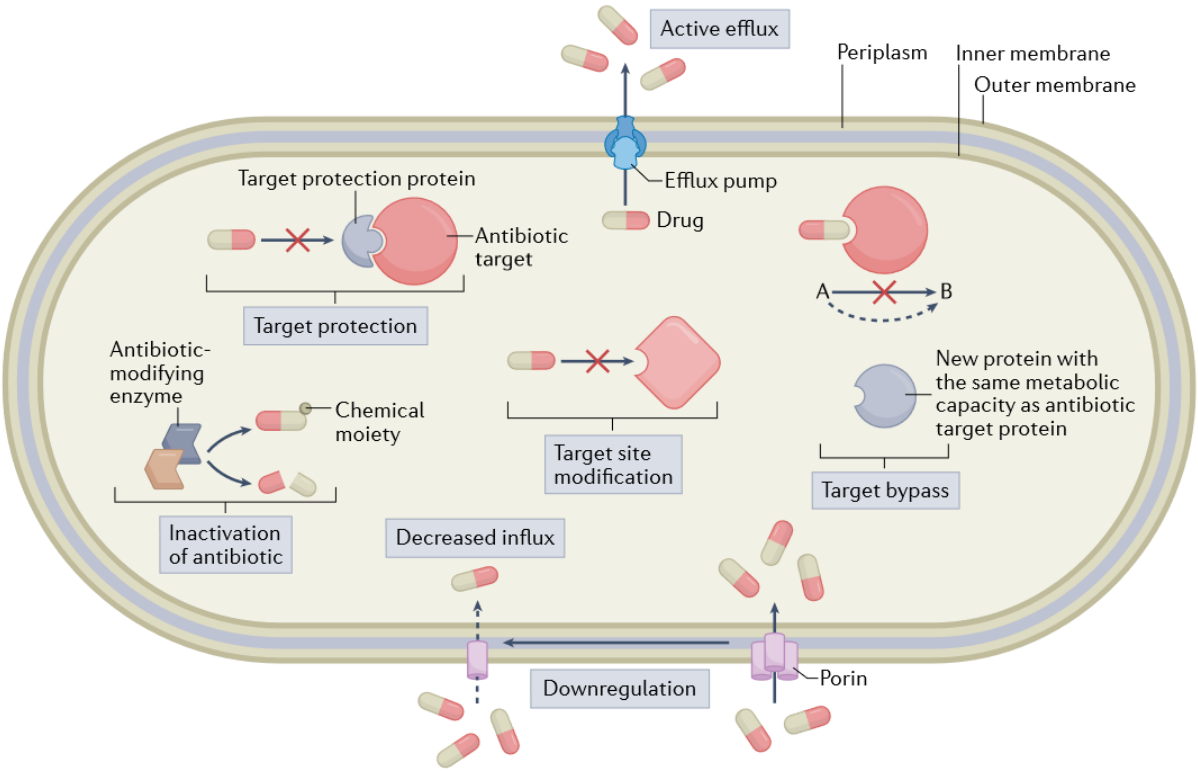

Figure 2: An overview of common antibiotic resistance mechanisms. (ref. 15)

degradation—both by bacterial enzymes.[18] The drug targets may be altered as well—either to reduce binding affinity to the drug,[19] or as a bypass, to ensure functioning is not affected despite the drug binding the original target.[20] While these resistance mechanisms are well-documented and have been countered before, novel resistance mechanisms further challenge antibiotic development.[21,22]

All of these mechanisms are enabled by genetic variation that natural selection operates on. This variation is produced in bacteria primarily by either of two

pathways—mutations and horizontal gene transfer.[23]

1.2. Siderophores for Bacteria

Iron is an essential micronutrient to nearly all microorganisms by virtue of its versatility—it can exist as Fe(II),(III) and (IV), which allows for suitable redox chemistry required by several metabolic pathways. Of note is its role in haemoglobin functioning and its participation in the electron transport chain during respiration through haem groups and Fe-S clusters. It is found in more than 100 enzymes as a cofactor for physiological processes including DNA replication, transcription and ROS regulation.[24,25] Sequestering sufficient amounts of iron for proper function is a challenge that is three-fold—(a) although it is abundant in the earth's crust, its existence predominantly as the insoluble $Fe(OH)_3$ does not allow for its ready absorption from the external environment by bacterial pathogens,[26] (b) free iron levels in the host are too low for acquisition due to high proportions of metal being protein-bound, and (c) selection pressure from host defence mechanisms such as nutritional immunity further limit the availability of iron during infection.[27,28] This challenge has necessitated the development of iron sequestration strategies in bacteria, which broadly comprise haem, siderophore and free Fe^{II}-based acquisition methods.[29] Among these, of particular interest are siderophores, which are small-molecule (<1500 Da) iron chelators with among the highest Fe^{III}-binding affinities—some (e.g. enterochelin **1** (Fig. 3), $K_d = 10^{-49}$ M) with affinities surpassing those of ferric ion-binding glycoproteins such as lactoferrin and transferrin ($K_d \sim 10^{-22}$ M).[30] These molecules are secreted by bacteria to sequester iron from the microenvironment. All siderophores possess high affinities for Fe^{III} as opposed to Fe^{II}. Typical binding moieties in siderophores include catecholates, hydroxamates, and α-hydroxycarboxylates (Fig. 3). The donor atoms of siderophore ligands are predominantly those of oxygen. The electron density on these translates to tighter binding to Fe^{III}, resulting in a strong Lewis acid-base pair.[26] In Gram-negative bacteria, ferrisiderophore complexes enter the periplasmic space through TonB dependent Transporters (TBDTs) in the outer membrane (OM), which, unlike smaller non-selective porins, allow the diffusion of these complexes.

In the absence of ionic gradients and ATP, this step derives the energy it needs from protonmotive force generated at the inner membrane.[31]

(a)

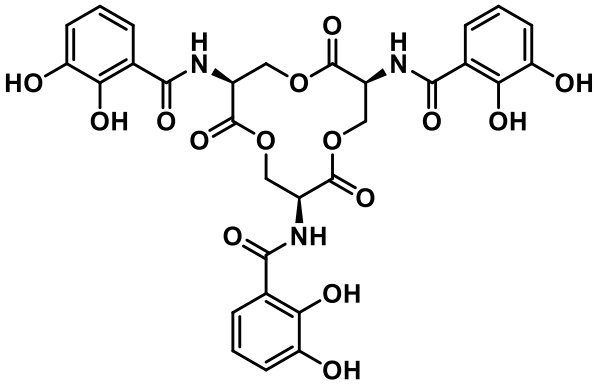

1

(b)

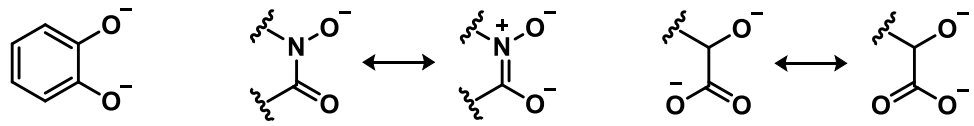

	(i)	(ii)	(iii)
pKa	9.2, 13	9.0	3.0, 14.5

Figure 3: (a) Structure of enterochelin **1**. **(b)** Typical binding moieties in siderophores. (i) catecholate, (ii) hydroxamate, and (iii) α-hydroxycarboxylate. The pKa values of donor atoms are indicated.

The TonB-ExbB-ExbD complex at the inner membrane transduces this energy via TonB, which interacts with the TonB Box of the TBDT. Substrate Binding Proteins (SBPs) in the periplasm then recognise these ferrisiderophore complexes and shuttle them to a complementary ATP-Binding Casette (ABC) transporter for transport through the inner membrane to the cytoplasm. Subsequent dissociation of iron is then ensured either by enzymatic degradation of the siderophore itself, or by reductases that reduce Fe^{III} to Fe^{II}.

Once adequate Fe^{II} has been sequestered in the cytoplasm, further acquisition is attenuated by interplay between Fe^{II}-Fur, ECF σ, an anti-σ factor at the inner membrane, and in some cases a N-terminal extension of the TBDT at the OM (Fig. 4).[29,32]

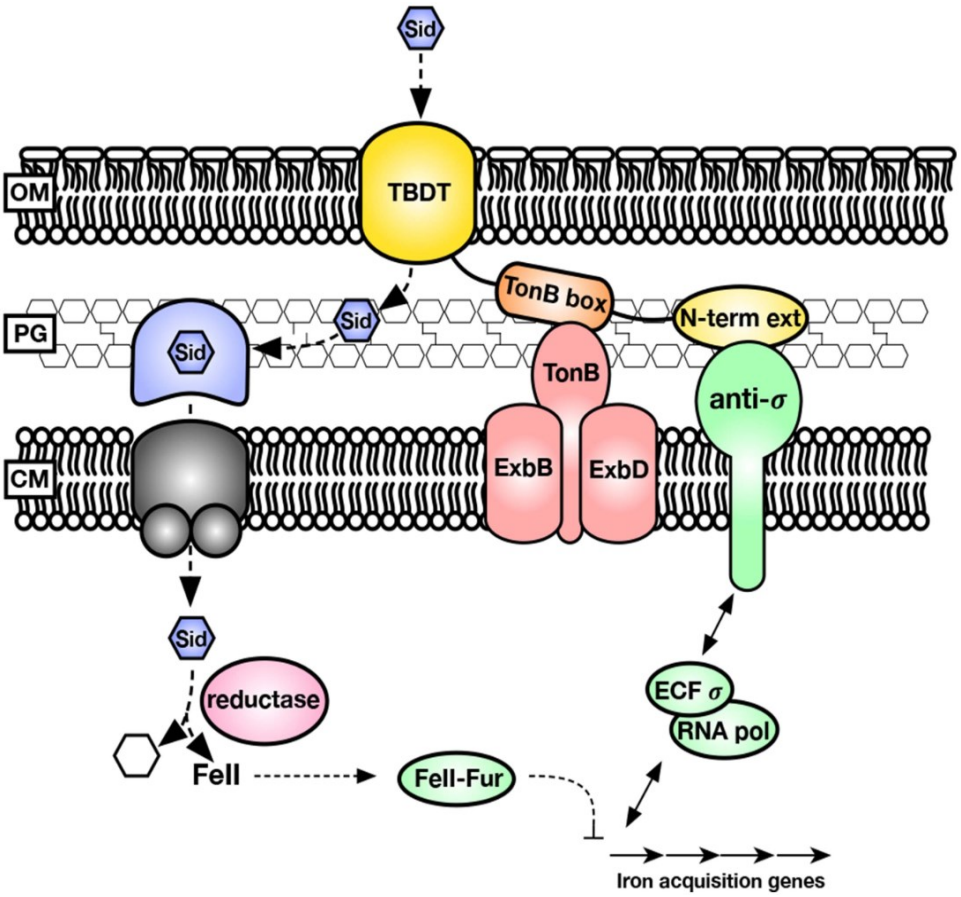

Figure 4: TonB-dependent iron acquisition by siderophores in Gram-negative bacteria (ref. 27).

1.3. Siderophores Against Bacteria: The Trojan Horse Strategy

The low-permeable outer membrane is a notable hurdle that Gram-negative bacteria have posed to the development of effective antibiotics against them. However, it was shown that this problem can be circumvented by conjugating antibiotics to siderophores, which has been termed “Trojan Horse” strategy.[33–36] On one hand, bacterial ferrisiderophore complexes are readily recognised and internalised by bacteria for iron acquisition; on the other hand, the low efficacies of several antibiotics towards Gram-negative bacteria could benefit from greater accumulation at the target sites—either in the periplasmic space or in the cytoplasm. It could then be surmised that conjugating the two via a linker could potentially enable the drugs to “hitch a ride” on the siderophores through the outer membrane. Indeed, the conjugation of siderophore moieties to antibiotics results in a marked enhancement in their uptake, allowing for higher levels of free drug concentrations at their target sites, and thus higher efficacy, evidenced by lower Minimum Inhibitory Concentrations (MICs).[37–39]

Siderophore-antibiotic conjugates (SACs) or sideromycins have also been discovered in nature; For instance, Albomycin (Fig. 5a) (**2**-**4**), produced by a variety of *Streptomyces* species, was discovered in 1947. It was reported as a broad-spectrum antibiotic with potent activity against Gram-negative bacteria as well.[26] Ferrimycins (Fig. 5b) (**5**) were first reported in 1960 after being isolated from *Streptomyces griseoflavus*. They possess a ferrioxamine backbone and are active only against Gram-positive bacteria.

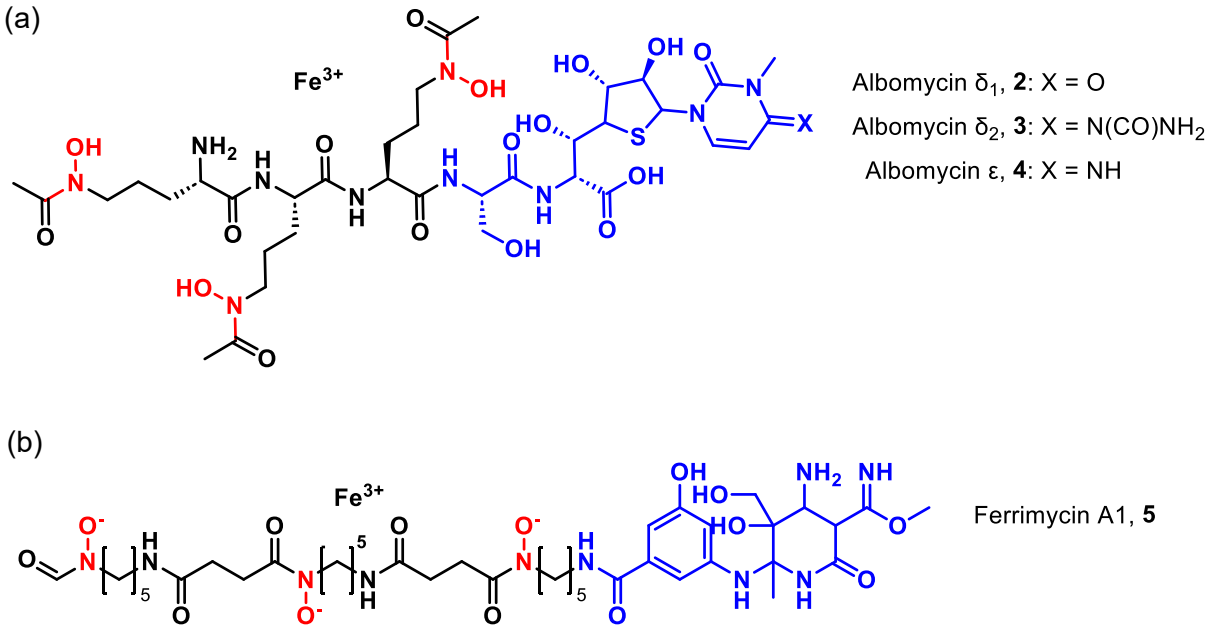

Figure 5: Structures of natural sideromycins. (a) Albomycins **2**-**4**. (b) Ferrimycin A1 **5** (binding moieties in red & bold, antibiotic in blue).

Discoveries of such natural siderophore-antibiotic conjugates provided an impetus towards the synthesis of such conjugates. Beginning in the 1970s, early attempts were aimed at mimicking these by conjugating sulfonamide antibiotics with known natural siderophores such as ferrioxamine B, albeit resulting in no significant activity.[40,41] Later, reports of a significant decrease in MIC against *Pseudomonas aeruginosa* compared to piperacillin upon conjugation of β-lactam antibiotics to single bidentate siderophore moieties (e.g. hydroxamate) sparked a trend towards research on β-lactam-siderophore conjugates in the 1980s and '90s.[42,43] Arguably, this boost in interest has contributed to the eventual approval in 2019 of Cefiderocol (or Fetroja®) **6**—a conjugate of cephalosporin and a single catechol moiety—for treatment of complicated Urinary Tract Infections (cUTIs), owing to its broad spectrum

activity against multiple strains of clinically relevant Gram-negative bacteria (Fig. 6).[44]

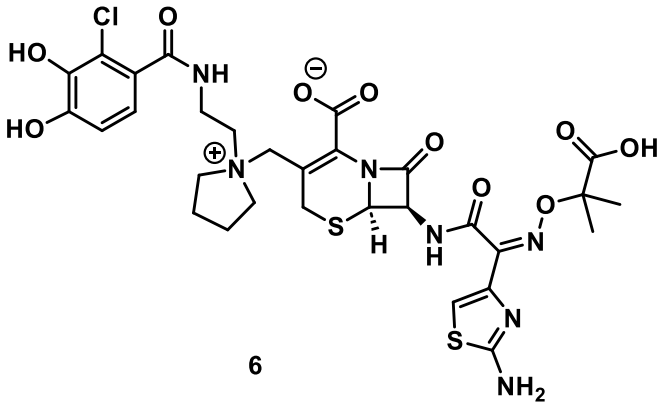

6

Figure 6: Chemical structure of cefiderocol (Fetroja®) **6**, the first clinically approved SAC.

Recent progress towards SACs has witnessed a significant rise in overall variety—of core structure (MECAM[37], **7** and DOTAM[38], **8** among others (Fig. 7)), types of drugs (β-lactams,[45] lipopeptides,[46] anticancer,[47] and fluoroquinolones,[48] among others), and siderophore moieties (desferrioxamine B,[49] citrate,[50] and mixed-ligand bis-catechol-hydroxamate,[51] among others).

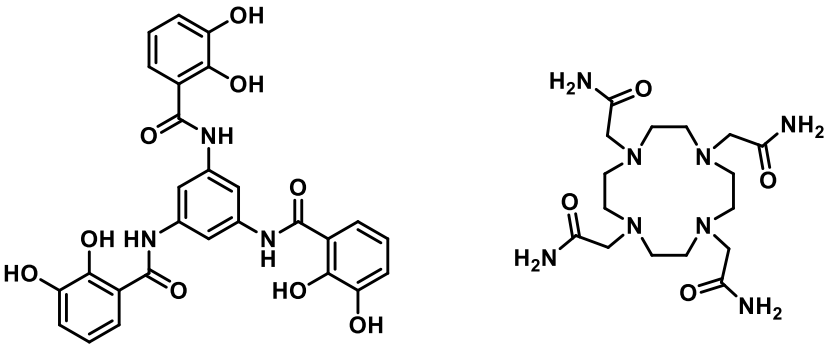

7 8

Figure 7: Examples of artificial siderophore core structures MECAM **7** and DOTAM **8**.

Additionally, linkers between the drug and the siderophore may either be cleavable or non-cleavable, depending on whether release of the free drug to the target site is necessary for therapeutic action, which in turn depends on its target location—β-lactam antibiotics need to only permeate through the outer membrane since they act in the periplasmic space, while a fluoroquinolone-siderophore conjugate may benefit from having a cleavable linker, since it acts in the cytoplasm. Multiple examples of both of these types of linkers are available.[52] Furthermore, SACs with mixed ligands

may circumvent issues where resistance develops to one of the two siderophore-mediated transport pathways.

1.4. Evaluating Fe(III) Binding Ability via a Colorimetric Assay

Chrome Azurol S (CAS) is a red dye that forms a blue ternary complex with Fe(III) and hexadecyltrimethylammonium bromide (HDTMA) with a particularly high molar extinction coefficient ($\varepsilon \sim 10^5$ $M^{-1}cm^{-1}$) at a wavelength of 630 nm and pH 5.6 (Fig. 8).[53]

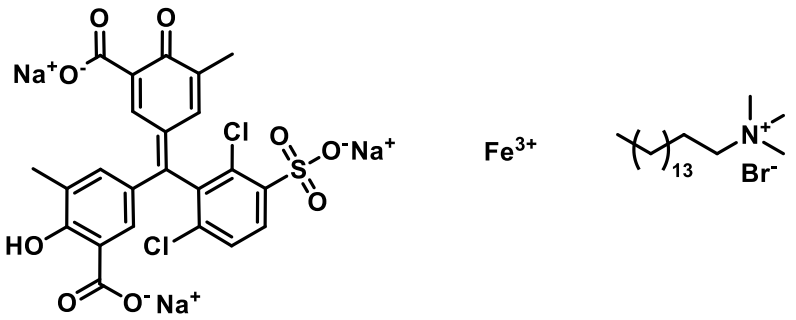

Figure 8: Constituents of the Fe(III)-CAS-HDTMA ternary complex.

However, when the Fe(III) is lost from the complex, a distinct colour change to red (orange, in some cases) is observed, accompanied by a decrease in absorbance at this wavelength. This property has been exploited in a spectrophotometric assay to detect the presence of siderophores in solution.[33] The assay may thus be used to qualitatively evaluate and compare the capability of siderophores to complex Fe(III) in a stable manner in solution.

1.5. Project Objective

An interesting premise is to investigate the smallest possible cyclic core, i.e., cyclopropane, that siderophore systems may be based on, and study its effects on the iron-binding ability of the siderophores. The plan is to design, synthesize and characterize artificial siderophores with a cyclopropane core of defined stereochemistry. The cyclopropane core is envisioned with three *cis*-oriented arms for iron chelation, and one *trans*-oriented arm for the attachment of imaging moieties or antibiotics (Fig. 9).

Upon synthesis, the final compounds will be characterised in microbiological experiments. Their antibacterial activity as well as their ability to deliver iron into bacterial cells will be measured. Initial studies involve *E. coli*, but may extend to other ESKAPE pathogens. Finally, the iron-binding capability of the synthesized siderophores will be assessed in competitive binding experiments.

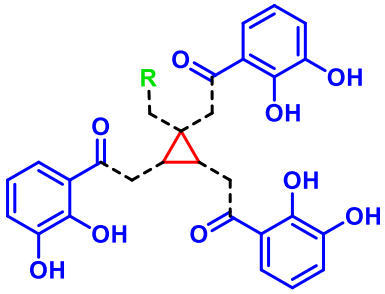

Figure 9: Skeletal structure of the envisioned 1,1,2,3-tetrasubstituted cyclopropane-based siderophore-antibiotic conjugate. Red: cyclopropane core, Blue: catecholamide units, Green: antibiotic payload, Dashed lines: variable linkers.

A principal synthetic route was established previously;[54] however, the synthesis of the final target molecule has not been accomplished.

2. Methods

2.1. General Chemical Information

Unless otherwise mentioned, reagents were purchased and used without further purification. All employed solvents for workups and purifications were of HPLC purity grade. Removal of organic solvents was conducted on a Heidolph Hei-VAP Core rotational evaporator at 40 °C, unless stated otherwise.

Except biphasic reactions or reactions in water, all reactions were carried out with anhydrous solvents stored over molecular sieves. Moisture-sensitive reactions were carried out in oven-dried glassware under argon atmosphere. The reaction progress was monitored either by TLC (silica gel 60 F_{254}, on aluminum/glass, Merck®) or via LC/MS (Single Quadrupole LC/MS System 6130B, Agilent Technologies®). The retention factor R_f indicates the ratio of the distance travelled by an analyte to the distance travelled by the solvent front. Spots on TLC plate were detected either under UV-light (λ = 254 nm) or by staining, either with cerium ammonium molybdate (CAM) solution (12 g of ammonium molybdate, 0.5 g ceric ammonium molybdate, 15 mL conc. sulfuric acid, and 235 mL distilled water) or with potassium permanganate solution (1.5 g $KMnO_4$, 10 g K_2CO_3, and 1.25 mL of 10% NaOH in 200 mL water).

Purifications via column chromatography were carried out using silica gel (Si 60, particle sizes: 40-63 µm, Merck®). Automatic preparative column chromatography was performed on a Grace Reveleris® X2 instrument (Büchi®) with disposable columns (Reveleris® Flash Cartridges Silica 40 µm, Büchi). RP-HPLC purifications were performed on a Dionex Ultimate (Thermo Fisher Scientific) on a phenomenex Gemini C18 RP-column 00G-4435-PO-AX, 5 µm, 110 A, 250×21.20 mm (10 mL/min). Substances were subsequently freeze-dried on an Alpha 2-4 LSCbasic (Christ) instrument.

High resolution mass spectrometry (HRMS) was performed using a Dionex Ultimate 3000 HPLC system equipped with a DAD detector and a Bruker maxis HD QTOF mass detector with electrospray ionization (ESI). Samples were injected directly via an Ultimate 3000RS autosampler (Thermo Fisher Scientific). The mass-to-charge ratios (m/z) are indicated.

NMR spectra were acquired on a 500 MHz (UltraShield Plus) Avance III spectrometer equipped with a 5 mm Nitrogen-cooled cryo probe (Prodigy BBO) by Bruker BioSpin GmbH and a 700 MHz (Ascend) Avance III HD spectrometer equipped with a 5 mm, Helium-cooled cryo probe (TCI) by Bruker BioSpin GmbH. The measured substances were dissolved in the respective deuterated solvent ($CDCl_3$, DMSO-d_6 or MeOH-d_4) and the chemical shifts δ are given in parts per million (ppm). Multiplicities of the individual signals are denoted as: s (singlet), d (doublet), t (triplet), q (quartet), quint (quintet), and combinations thereof: dd (doublet of doublet), tt (triplet of triplet), dt (doublet of triplet), td (triplet of doublet), etc. Others include: s_{br} (broad singlet) and m (multiplet). All NMR spectra were interpreted as spectra of the first order. Coupling constants *J* are reported in hertz (Hz) and refer to ^1H-^1H couplings. All isolated compounds were characterized by ^1H-NMR, ^{13}C-NMR, and ESI-HRMS (selected compounds). The yields were calculated based on substance purity ≥95% as confirmed by NMR and MS.

2.2. CAS Assay to Study Fe(III) Complexation

All used glassware was previously cleaned with 12M HCl and HPLC grade water. Stock solutions of hexadecyltrimethylammonium bromide (HDTMA, 10 mM in water) $FeCl_3$ (1 mM in a 10mM HCl solution) and CAS (2 mM in water) were obtained by adding 3.64 mg in 1mL H_2O, 0.1622 mg in 1mL HCl (10 mM) and 1.211 mg in 1 mL H_2O, respectively. HDTMA (10 mM, 600 µL) was placed in a 10 mL volumetric flask and diluted with water. $FeCl_3$ (1mM in 10mM HCl, 150 µL) and CAS (aq) (2 mM, 750 µL) were slowly added successively under stirring. Anhydrous piperazine (431 mg) was dissolved in water, and HCl (12 M, 625 µL) was carefully added, to form a buffer solution (pH = 5.6). This solution was rinsed into the volumetric flask, which was subsequently filled with water to afford 10 mL of CAS assay solution. 5-sulfosalicylic acid (10.2 mg) was dissolved in the solution to form the Fe(CAS) solution. 100 µM stock solutions of enterobactin and compounds **30**, **50**, **51** and **57** were prepared and added at a final concentration of 9 µM into a 96 well plate (Microplate, 96 well, PS, half area, clear) in 8 replicates. Absorbances were determined after 24 h at 25 °C using an Infinite® 200 PRO (Tecan) spectrometer in a wavelength range from 200 to 1000 nm. Absorbances at 630 nm were determined by averaging those at 620 nm and 640 nm. Data obtained was processed using Microsoft Excel 2016.

2.3. Synthesis Procedures

Dimethyl 2-Diazomalonate (11)

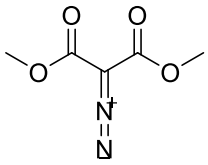

Dimethyl 2-diazomalonate (**11**) was synthesized according to Baum *et al*.[55] Dimethyl malonate **9** (1.83 mL, 2.1 g, 15.9 mmol, 1 eq) and triethylamine (5.31 mL, 38.1 mmol, 2.4 eq) were added to a solution of 4-acetamidobenzenesulfonyl azide (p-ABSA) (5.7 g, 23.9 mmol, 1.5 eq) in MeCN (60 mL) under argon at r.t. and the resulting mixture was stirred for 18 h at r.t. The mixture was filtered and the volatiles were removed under reduced pressure. The residue was triturated with DCM (45 mL), the remaining solids were filtered off, and the volatiles were removed under reduced pressure. The residue was purified by silica gel column chromatography (12-18% EA/cyclohexane) and was isolated as a lime yellow oil (2.2 g, 13.8 mmol, 86%).

TLC: R_f (50% EA/cyclohexane) = 0.76

^{1}H-NMR (500 MHz, CDCl3): δ [ppm] = 3.84 (6H, s). This spectrum is in accordance with literature.[56]

^{13}C NMR (176 MHz, $CDCl_3$): δ 161.62, 65.91, 52.69.

Dimethyl (1*R**,7*S**)-4,4-Dimethyl-3,5-dioxabicyclo[5.1.0]octane-8,8-dicarboxylate (13)

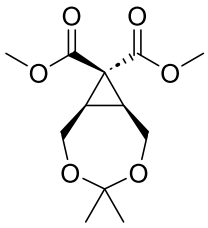

To a mixture of rhodium 3-[3-(2-carboxy-2-methylpropyl)phenyl]-2,2-dimethylpropanoic acid ($Rh_2(esp)_2$) (54 mg, 71 µmol, 7 mol%) and DCM (16 mL) was added 2,2-dimethyl-4,7-dihydro-1,3-dioxepine **12** (1.43 mL, 10.6 mmol, 1 eq) under argon at 0 °C. After 5 min, a solution of dimethyl-2-diazomalonate **11** (2.2 g, 13.8 mmol, 1.3 eq) in DCM (16 mL) was added. The reaction mixture was stirred at 0 °C for 10 min and then stirred at r.t. for 18 h. The crude product was concentrated under

reduced pressure and purified by silica gel column chromatography (7-11% EA/cyclohexane) to afford **13** as a clear oil (2.7 g, 10.3 mmol, 75%).

TLC: R_f (40% EA/cyclohexane) = 0.6 (CAM)

^{1}H-NMR (500 MHz, $CDCl_3$): δ [ppm] = 4.22 – 4.16 (m, 2H), 4.14 – 4.09 (m, 2H), 3.78 (s, 3H), 3.70 (s, 3H), 2.03 – 1.98 (m, 2H), 1.31 (s, 3H), 1.19 (s, 3H). This spectrum is in accordance with literature.[54]

(1*R,7*S**,8*s*)-8-(Methoxycarbonyl)-4,4-dimethyl-3,5-dioxabicyclo[5.1.0]octane-8-carboxylic acid (14)**

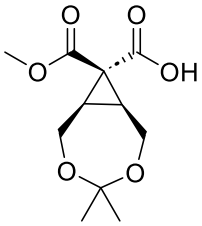

To a solution of **13** (325 mg, 1.3 mmol, 1 eq) in THF (4.5 mL) were added a solution of LiOH·H_2O (106 mg, 2.5 mmol, 2 eq) in MeOH (4.5 mL) and H_2O (1 mL) at r.t. and the mixture was stirred at r.t. for 24 h. Volatiles were then removed under reduced pressure to afford the crude product **14** which was used further without purification.

Methyl (1*R,7*S**,8*s*)-4,4-Dimethyl-8-(prop-2-yn-1-ylcarbamoyl)-3,5-dioxabicyclo [5.1.0]octane-8-carboxylate (16)**

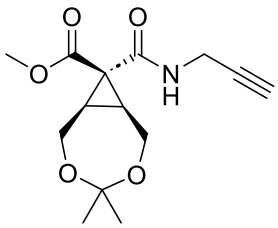

14 (308 mg, 1.3 mmol, 1 eq) was suspended in DMF (18 mL) under argon atmosphere. To this mixture, HATU (718 mg, 1.9 mmol, 1.5 eq) and DIPEA (0.658 mL, 3.8 mmol, 3 eq) were added at 0 °C and stirred. Propargyl amine **15** (0.162 mL, 2.5 mmol, 2 eq) was then added dropwise and the mixture stirred at r.t. overnight. Water (30 mL) was added, and the mixture was extracted with EtOAc (3x15 mL). The combined organic phases were washed with water, brine, dried over Na_2SO_4, filtered and concentrated

under reduced pressure. The crude product was purified by silica gel column chromatography (50% EA/cyclohexane) to yield **16** as a yellow oil (314 mg, 1.1 mmol, 88%).

TLC: R_f (50% EA/cyclohexane) = 0.54 (CAM)

^{1}H NMR (500 MHz, $CDCl_3$): δ 6.26 (s, 1H), 4.16 – 4.13 (m, 4H), 4.01 (dd, *J* = 5.2, 2.6 Hz, 2H), 3.82 (s, 3H), 2.23 (t, *J* = 2.6 Hz, 1H), 2.04 – 2.01 (m, 2H), 1.32 (s, 3H), 1.20 (s, 3H). This spectrum is in accordance with literature.[54]

^{13}C NMR (176 MHz, $CDCl_3$): δ 169.58, 167.42, 102.62, 79.16, 71.73, 57.40, 52.80, 36.21, 29.84, 29.51, 24.23, 23.71.

An attempt to synthesize (1*R,7*S**,8*r*)-8-(Hydroxymethyl)-4,4-dimethyl-*N*-(prop-2-yn-1-yl)-3,5-dioxabicyclo[5.1.0]octane-8-carboxamide (S1)**

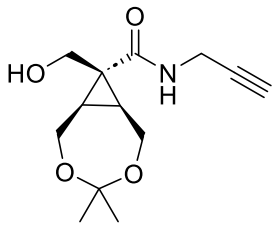

To a solution of **16** (54 mg, 0.19 mmol, 1 eq) in THF (3.6 mL) was added $LiBH_4$ in THF (1.44 mL, 2.88 mmol, 2M, 15 eq) under argon at r.t.. Upon cooling the mixture to 0 ºC, water (142 µL, 7.87 mmol, 41 eq) was added dropwise, and the reaction mixture stirred at r.t.. After 1.5 h, THF (5 mL) was added, and the reaction temperature was increased to 60 ºC. After 24 h, water (30 mL) was added and the mixture extracted with EtOAc (3x15 mL). The combined organic phases were washed with water, brine, and lastly dried over Na_2SO_4, filtered and concentrated under reduced pressure. Purification was performed by silica gel column chromatography (40% EA/cyclohexane) to afford side product **17** as a clear oil.

Methyl (1*R,7*S**,8*s*)-8-(Allylcarbamoyl)-4,4-dimethyl-3,5-dioxabicyclo[5.1.0] octane-8-carboxylate (17)**

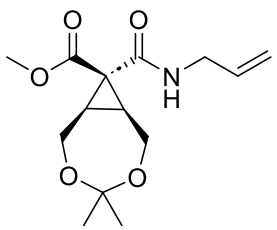

Yield: 17 mg, 0.06 mmol, 31%

TLC: R_f (40% EA/cyclohexane) = 0.45 (CAM)

^{1}H NMR (500 MHz, $CDCl_3$): δ 6.13 (s, 1H), 5.80 (ddt, *J* = 17.1, 10.3, 5.6 Hz, 1H), 5.17 – 5.10 (m, 2H), 4.15 – 4.11 (m, 4H), 3.84 (tt, *J* = 5.6, 1.6 Hz, 2H), 3.80 (s, 3H), 2.03 – 1.99 (m, 2H), 1.31 (s, 3H), 1.19 (s, 3H).

^{13}C NMR (126 MHz, $CDCl_3$): δ 170.13, 167.55, 133.92, 116.51, 102.77, 57.63, 52.91, 42.62, 36.48, 29.37, 24.42, 23.88.

(1*r*,2*R,3*S**)-1,2,3-Tris(hydroxymethyl)-*N*-(prop-2-yn-1-yl)cyclopropane-1-carboxamide (19)**

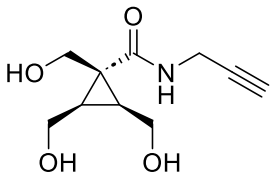

To a solution of $LiBH_4$ in THF (2.1 mL, 4.2 mmol, 2M, 4 eq) was added **16** (296 mg, 1.1 mmol, 1 eq) in THF (6 mL) under argon at r.t.. The mixture was diluted with THF to 20 mL and stirred at 60 °C for 24 h. It was then cooled to r.t. and further to 0°C in an ice-water bath. The reaction was carefully quenched with 2M aq. HCl (6 mL) and stirred for 1 h at r.t.. Solvents were removed under reduced pressure to yield a brown solid crude product (738 mg). An unsuccessful purification attempt via C18 flash column chromatography yielded an impure white solid (573 mg), which was used further without purification.

An attempt to synthesize ((1*r*,2*R,3*S**)-1-(Prop-2-yn-1-ylcarbamoyl) cyclopropane-1,2,3-triyl)tris(methylene)Trimethanesulfonate (22)**

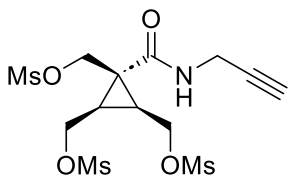

19 (38 mg, 0.18 mmol, 1 eq) was added as a solution in DCM (2 mL), MeCN (2 mL) and DMF (1 mL) to a 25 mL Schlenk flask purged with argon. Upon cooling to 0 ºC, MsCl (42 µL, 62 mg, 0.53 mmol, 3 eq) and TEA (112 µL, 81 mg, 0.80 mmol, 4.5 eq)

were added to the mixture. The reaction mixture was then stirred at r.t. for 21 h. The reaction mixture was then transferred to a separating funnel, and subsequently washed with water, 2M aq. HCl, sat. $NaHCO_3$, and brine solution. The aqueous phases were combined and extracted with DCM (3x10 mL). The organic phases were combined, dried over Na_2SO_4, filtered, and the solvents evaporated to afford a yellow oil (8 mg).

((1*r*,2*R,3*S**)-1-(Prop-2-yn-1-ylcarbamoyl)cyclopropane-1,2,3-triyl) tris(methylene) Tris(3-((*tert*-butoxycarbonyl)amino)propanoate) (24)**

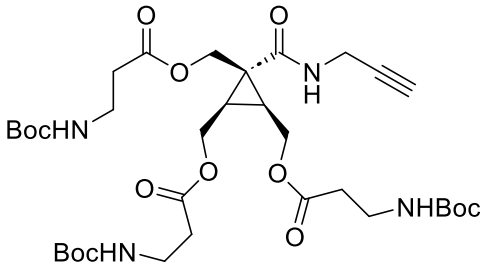

3-((*tert*-Butoxycarbonyl)amino)propanoic acid **23** (572 mg, 3.00 mmol, 4.5 eq), EDC·HCl (387 mg, 2.01 mmol, 3 eq) and DMAP (9 mg, 0.07 mmol, 10 mol%) were dissolved in DMF (10 mL) under argon and the mixture stirred at 0 °C for 10 min. A mixture of **19** (143 mg, 0.67 mmol, 1 eq), DMF (2 mL) and TEA (0.31 mL, 2.21 mmol, 3.3 eq) was then added to this mixture at the same temperature and stirred for 24 h at r.t.. The crude product was concentrated under reduced pressure at 75 °C. Purification was performed by silica gel column chromatography in 45% EA/cyclohexane. The completely pure product could not be obtained. A pale-yellow oil (48 mg) was obtained, which was used further without purification.

TLC: R_f (50% EA/cyclohexane) = 0.33

2,3-Diacetoxybenzoic acid (27)

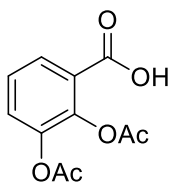

2,3-Dihydroxybenzoic acid (1000 mg, 6.5 mmol, 1 eq) was suspended in THF (10 mL)

under argon. To this mixture were added Ac_2O (1.84 mL, 19.5 mmol, 3 eq), TEA (3.62 mL, 25.9 mmol, 4 eq), and DMAP (79 mg, 0.6 mmol, 0.1 eq) sequentially, at r.t.. Upon dissolution, the reaction mixture was heated to 60 °C and stirred for 24 h at the same temperature. Solvents were removed under reduced pressure and the residue taken up in DCM (30 mL). The organic phase was washed with 1M aq. HCl (3x10 mL), brine (10 mL), dried over Na_2SO_4 and filtered. A few drops of acetic acid were added in flasks before drying and subsequent removal of solvents under reduced pressure to prevent de-acetylation. The residue was dried *in vacuo* overnight to afford **27** as a brown solid, which was used without further purification.

^{1}H NMR (500 MHz, $CDCl_3$): δ 7.98 (dd, *J* = 7.9, 1.7 Hz, 1H), 7.43 (dd, *J* = 8.1, 1.7 Hz, 1H), 7.35 (t, *J* = 8.0 Hz, 1H), 2.33 (s, 3H), 2.32 (s, 3H). This spectrum is in accordance with literature.[57]

^{13}C NMR (126 MHz, $CDCl_3$): δ 168.72, 168.70, 168.50, 168.48, 168.29, 168.27, 143.63, 143.61, 143.17, 129.63, 129.61, 128.75, 128.73, 126.24, 126.22, 123.93, 20.64, 20.62.

3-(Chlorocarbonyl)-1,2-phenylene Diacetate (28)

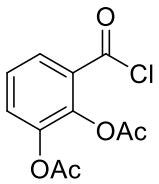

Oxalyl chloride (217 µL, 2.52 mmol, 2 eq) was added dropwise under argon over 5 min to a solution of 2,3-diacetoxybenzoic acid **27** (300 mg, 1.26 mmol, 1 eq) in DCM (7.5 mL) and DMF (100 µL) and the reaction mixture stirred for 10 min at 0 °C, then subsequently for 2 h at r.t.. The crude product was concentrated under reduced pressure and dried *in vacuo* overnight, and used further without purification.

((1*r*,2*R,3*S**)-1-(Prop-2-yn-1-ylcarbamoyl)cyclopropane-1,2,3-triyl) tris(methylene) Tris(3-aminopropanoate) (25)**

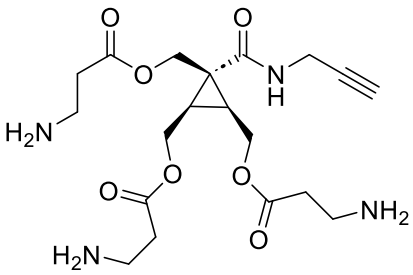

24 (48 mg) was dissolved in 25% TFA/DCM (5 mL) and stirred at r.t. for 1 h. Solvents were removed under reduced pressure to yield a clear oil, which was used further without purification, assuming quantitative yield (28 mg, 0.066 mmol).

((1*r*,2*R,3*S**)-1-(Prop-2-yn-1-ylcarbamoyl)cyclopropane-1,2,3-triyl) tris(methylene) Tris(3-(2,3-dihydroxybenzamido)propanoate) (30)**

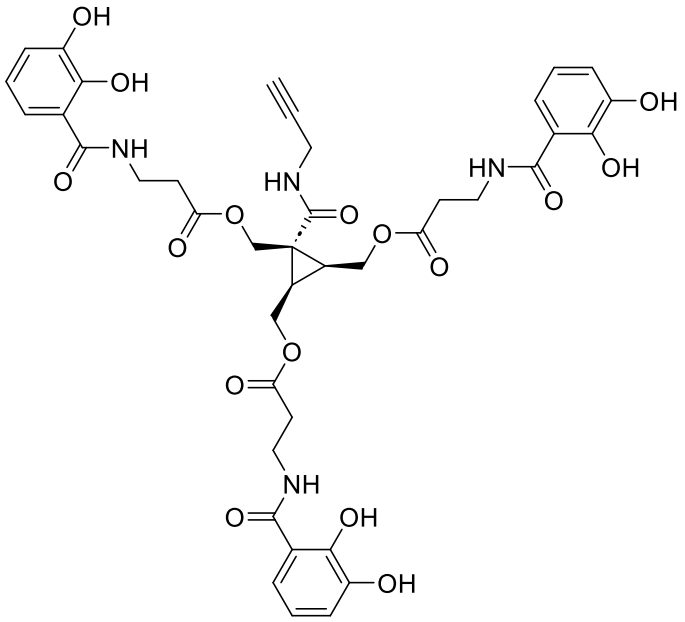

To a solution of **25** (28 mg, 0.07 mmol, 1 eq) in aq. $KHCO_3$ (2 mL, 1 M), a solution of **28** (102 mg, 0.40 mmol, 6 eq) in 1,4-dioxane (1 mL) was added at 0 °C over 10 min. The mixture was then stirred for 20 min at 0 °C and then for 3 h at r.t.. Water was added to the mixture and the aqueous phase was extracted with EtOAc (3x5 mL). The organic phases were combined and washed with brine (2x5 mL), dried over Na_2SO_4 and filtered. The crude product was concentrated under reduced pressure and/ purified by RP-HPLC (H_2O/MeCN, 0.1% AcOH) to afford **30** as a white solid (5 mg, 4.6 µmol, 7%).

^{1}H NMR (500 MHz, MeOD-*d*$_4$): δ 7.19 (m, 3H), 6.91 (dd, *J* = 7.8, 1.4 Hz, 3H), 6.69 (td, *J* = 8.0, 1.9 Hz, 3H), 4.52 (s, 2H), 4.34 – 4.25 (m, 5H), 3.93 (d, *J* = 2.5 Hz, 2H), 3.65 (dt, 6H), 2.69 – 2.63 (m, 6H), 2.52 (t, *J* = 2.5 Hz, 1H), 2.08 – 1.99 (m, 3H).

^{13}C NMR (126 MHz, MeOD-*d*$_4$): δ 173.13, 173.04, 171.55, 171.46, 150.16, 147.33, 119.61, 118.87, 116.75, 116.69, 80.69, 72.01, 61.52, 61.15, 36.59, 36.47, 35.23, 34.84, 32.38, 30.08, 27.68.

HRMS (ESI/Q-TOF) *m/z*: $(M+H)^+$ calcd for $C_{40}H_{44}N_3O_{16}$ 835.2669; found 835.2686.

Methyl (1*R,7*S**,8*s*)-8-(But-3-yn-1-ylcarbamoyl)-4,4-dimethyl-3,5-dioxabicyclo [5.1.0]octane-8-carboxylate (32)**

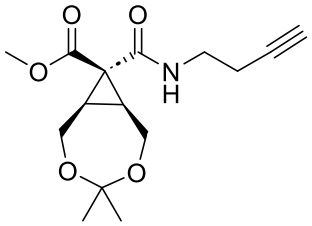

14 was dissolved in DMF (8 mL) under argon. HATU (279 mg, 0.73 mmol, 1.5 eq) and DIPEA (0.255 mL, 1.46 mmol, 3 eq) were added to this solution at 0 °C. But-3-yn-1-amine **31** (0.080 mL, 0.98 mmol, 2 eq) was then added dropwise at 0 °C and the mixture stirred at r.t. overnight. Water (15 mL) was added, and the mixture was extracted with EtOAc (3x8 mL). The combined organic phases were washed with water, brine, dried over Na_2SO_4 and filtered. The crude product was concentrated under reduced pressure and purified by silica gel column chromatography (35% EA/cyclohexane) to afford **32** as a white solid (103 mg, 0.35 mmol, 71%).

TLC: R_f (50% EA/cyclohexane) = 0.56 (CAM)

^{1}H NMR (500 MHz, $CDCl_3$): δ 6.44 – 6.36 (m, 1H), 4.18 – 4.11 (m, 4H), 3.81 (s, 3H), 3.38 (q, *J* = 6.4 Hz, 2H), 2.39 (td, *J* = 6.5, 2.6 Hz, 2H), 2.02 (t, *J* = 2.6 Hz, 1H), 2.01 – 1.99 (m, 2H), 1.32 (s, 3H), 1.20 (s, 3H).

^{13}C NMR (126 MHz, DMSO-d_6): δ 169.94, 167.81, 102.80, 81.26, 70.27, 57.63, 52.89, 38.56, 36.46, 29.40, 27.05, 24.42, 23.91, 19.41.

An attempt to synthesize (1*r*,2*R,3*S**)-*N*-(But-3-yn-1-yl)-1,2,3-tris(hydroxymethyl)cyclopropane-1-carboxamide (33)**

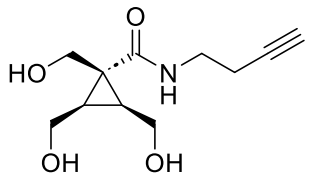

To $LiBH_4$ in THF (0.66 mL,1.33 mmol, 4 eq, 2M) was added **32** (98 mg, 0.33 mmol, 1 eq) under argon. The mixture was diluted with THF to 6 mL, and was then stirred at 60 °C for 24 h. It was then cooled to r.t. and further to 0 °C. The reaction was carefully quenched with 2M aq. HCl (1 mL) and stirred for 1 h at r.t.. The crude product was

concentrated under reduced pressure to a clear oil, which could not be purified via C18 flash column chromatography.

An attempt to synthesise (1*r*,2*R,3*S**)-1,2,3-Tris(hydroxymethyl)-*N*-(prop-2-yn-1-yl)cyclopropane-1-carboxamide (19)**

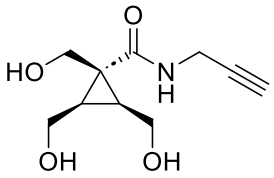

To $LiAlH_4$ (27 mg, 0.71 mmol, 2 eq) was added anhydrous THF (3 mL) under argon and the mixture cooled to 0 °C. TMSCl (0.093 mL, 0.73 mmol, 2 eq) was added dropwise, keeping the reaction temperature below 15 °C. The mixture was stirred at 0 °C for 2 h. A solution of **16** (100 mg, 0.36 mmol, 1 eq) in THF (4 mL) was then added dropwise at 0 °C. This reaction mixture was stirred at -10 °C for 1 h. It was then brought to 0 °C and carefully quenched with EtOAc (4 mL), isopropyl alcohol (2 mL) and then water (1.5 mL). The precipitate was filtered out, and the filtrate was then acidified using 2M aq. HCl (1 mL). The mixture was concentrated under reduced pressure to afford the crude product, which was not the desired product.

An attempt to synthesize (1*r*,2*R,3*S**)-1,2,3-Tris(hydroxymethyl)cyclopropane-1-carboxylic acid (34)**

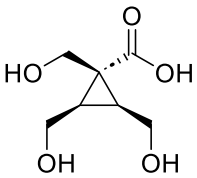

To $LiBH_4$ in THF (0.82 mL, 1.64 mmol, 4 eq, 2M) was added **14** (100 mg, 0.41 mmol, 1 eq) under argon at r.t.. The mixture was diluted with THF to 7 mL, and was then stirred at 60 °C for 24 h. Then, the reaction temperature was increased to 80 ºC and THF (3 mL) was added. After 3 h, 2 drops of water were added. The reaction mixture was stirred at r.t. overnight.

(1*R,7*S**)-4,4-Dimethyl-3,5-dioxabicyclo[5.1.0]octane-8,8-dicarboxylic acid (36)**

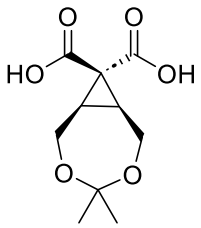

To **13** (200 mg, 0.76 mmol, 1 eq) in EtOH (6 mL) at r.t. was added aq. NaOH (4.8 mL, 4.25 mmol, 11 eq). The reaction mixture was stirred at 80 ºC overnight. Solvents were then removed under reduced pressure to yield an orange solid which was used further without purification.

An attempt to synthesize (1*R,7*S**,8*r*)-8-((But-3-yn-1-yloxy)carbonyl)-4,4-dimethyl-3,5-dioxabicyclo[5.1.0]octane-8-carboxylic acid (38)**

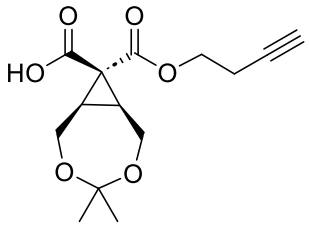

To a suspension of **36** (87 mg, 0.37 mmol, 1.0 eq) in DMF (6 mL) was added but-3-yn-1-ol **37** (0.035 mL, 0.45 mmol, 1.2 eq) under argon at r.t.. To this mixture, DCC (116 mg, 0.56 mmol, 1.5 eq) and DMAP (14 mg, 0.11 mmol, 0.3 eq) were added successively. TEA (0.157 mL, 1.12 mmol, 3 eq) was then added and the reaction mixture stirred at r.t. overnight.

An attempt to synthesize Methyl (1*R,7*S**,8*s*)-8-(Hydroxymethyl)-4,4-dimethyl-3,5-dioxabicyclo[5.1.0]octane-8-carboxylate (35)**

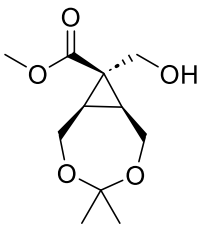

To a mixture of $NaBH_4$ (36 mg, 0.95 mmol, 2 eq) and THF (3 mL) was added a mixture

of **14** (116 mg, 0.47 mmol, 1 eq) and THF (3 mL) dropwise under argon over 10 min at 0 ºC. To this mixture was added $BF_3.OEt_2$ (159 µL, 1.28 mmol, 2.7 eq) dropwise over 10 min and stirred at r.t. overnight.

((1*R,7*S**)-4,4-Dimethyl-3,5-dioxabicyclo[5.1.0]octane-8,8-diyl)dimethanol (39)**

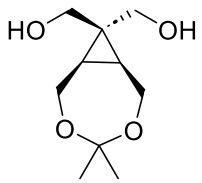

To a suspension of $LiAlH_4$ (0.77 g, 20.5 mmol, 4 eq) in THF (16 mL) was added a solution of **13** (1.32 g, 5.1 mmol, 1 eq) in THF (13 mL) under argon at 0 °C. The reaction mixture was stirred at r.t. for 18 h. It was then carefully quenched at 0 °C by addition of NaOH (11 mL, 1N) then subsequently H_2O (11 mL). The mixture was filtered through celite and the residue washed with MeOH thoroughly. The filtrate was concentrated under reduced pressure to a white solid, which was purified by silica gel column chromatography (90% EA/cyclohexane) to afford **39** as a clear oil (0.68 g, 3.4 mmol, 66%).

TLC: R_f (EA) = 0.3 (CAM)

^{1}H NMR (500 MHz, $CDCl_3$): δ 4.34 (s, 2H), 4.15 (ddd, *J* = 13.6, 3.5, 2.6 Hz, 2H), 3.91 – 3.87 (m, 2H), 3.51 (s, 2H), 1.38 (s, 3H), 1.29 (s, 3H), 1.26 (dt, *J* = 5.2, 2.4 Hz, 2H).

^{13}C NMR (126 MHz, $CDCl_3$): δ 103.65, 72.07, 61.49, 59.05, 32.58, 26.41, 25.81, 23.89.

An attempt to synthesize (1*R,7*S**,8*r*)-8-((But-3-yn-1-yloxy)carbonyl)-4,4-dimethyl-3,5-dioxabicyclo[5.1.0]octane-8-carboxylic acid (38)**

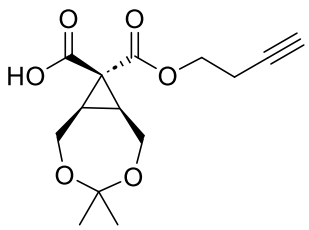

To a mixture of **36** (87 mg, 0.38 mmol, 1 eq) and DMF (5 mL) were added but-3-yn-1-ol **37** (0.03 mL, 0.38 mmol, 1 eq), DMAP (9 mg, 0.08 mmol, 0.2 eq) and TEA (0.108 mL, 0.77 mmol, 2 eq) successively under argon at r.t.. The mixture was then cooled

to 0 ºC and EDC.HCl (90 mg, 0.47 mmol, 1.2 eq) was added. The reaction mixture was then stirred at r.t. overnight.

An attempt to synthesize ((1*R,7*S**,8*r*)-8-((But-3-yn-1-yloxy)methyl)-4,4-dimethyl-3,5-dioxabicyclo[5.1.0]octan-8-yl)methanol (41)**

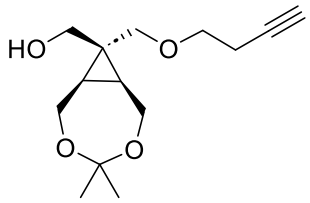

To a suspension of NaH (21 mg, 0.88 mmol, 1.1 eq, 60% w/w in paraffin) in DMF (1 mL) were added a solution of **39** (157 mg, 0.78 mmol, 1 eq) in DMF (2 mL) and THF (4 mL) dropwise at r.t.. The resulting mixture was stirred at 57 ºC for 30 min. To this was added 4-bromo-1-butyne **40** (0.088 mL, 0.94 mmol, 1.2 eq) dropwise over 5 min, and the reaction mixture was then stirred at 57 ºC for 18 h. Water (10 mL) was then added and the mixture extracted with EtOAc (3×5 mL). The organic phases were combined, washed with brine, dried over Na_2SO_4, filtered and concentrated under reduced pressure to afford the crude product.
TLC: R_f (40% EA/cyclohexane) = 0.6

((1*R,7*S**,8*r*)-4,4-Dimethyl-8-((prop-2-yn-1-yloxy)methyl)-3,5-dioxabicyclo[5.1.0] octan-8-yl)methanol (44)**

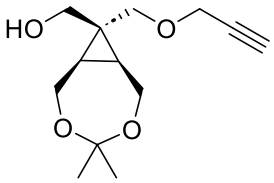

To a suspension of KOH (458 mg, 8.2 mmol, 3 eq) in DMSO (10 mL) was added a solution of **39** (550 mg, 2.7 mmol, 1 eq) in DMSO (5 mL) under argon at r.t.. After stirring for 10 min, propargyl bromide **42** (0.32 mL, 2.7 mmol, 1 eq, 9.2 M in toluene) was added to this mixture at 0 ºC. The reaction mixture was stirred at r.t. for 3 h. Water (30 mL) was added and the mixture extracted with EtOAc (3x15 mL). The organic phases were combined, washed with brine, dried over Na_2SO_4, filtered, and concentrated under reduced pressure. The crude product was purified via silica gel

column chromatography (40% EA/cyclohexane) to afford **44** as a brown oil (180 mg, 0.8 mmol, 27%), along with side products **45** and **46**.

TLC: R_f (40% EA/cyclohexane) = 0.48

^{1}H NMR (500 MHz, DMSO-*d*$_6$): δ 4.38 (t, *J* = 5.0 Hz, 1H), 4.07 (d, *J* = 2.4 Hz, 2H), 4.00 – 3.94 (m, 2H), 3.88 (d, *J* = 5.0 Hz, 2H), 3.79 – 3.74 (m, 2H), 3.40 (t, *J* = 2.4 Hz, 1H), 3.24 (s, 2H), 1.26 (s, 3H), 1.18 (s, 3H), 1.13 – 1.10 (m, 2H).

^{13}C NMR (126 MHz, CDCl$_3$): δ 103.59, 79.38, 78.57, 75.01, 60.74, 58.98, 58.31, 31.07, 26.65, 25.77, 23.91.

((1*R,7*S**,8*s*)-4,4-Dimethyl-8-((prop-2-yn-1-yloxy)methyl)-3,5-dioxabicyclo[5.1.0] octan-8-yl)methanol (45)**

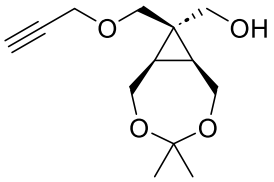

Yield: 30 mg, 0.13 mmol, 5% (brown oil)

TLC: R_f (40% EA/cyclohexane) = 0.38

^{1}H NMR (500 MHz, CDCl$_3$): δ 4.21 (d, *J* = 2.4 Hz, 2H), 4.20 (s, 2H), 4.15 – 4.10 (m, 2H), 3.88 – 3.82 (m, 2H), 3.43 (s, 2H), 2.46 (t, *J* = 2.4 Hz, 1H), 1.37 (s, 3H), 1.31 – 1.28 (m, 5H).

^{13}C NMR (126 MHz, CDCl$_3$): δ 103.62, 79.91, 74.88, 71.14, 68.37, 58.99, 58.55, 31.56, 26.42, 25.89, 23.85.

(1*R,7*S**)-4,4-Dimethyl-8,8-bis((prop-2-yn-1-yloxy)methyl)-3,5-dioxabicyclo [5.1.0]octane (46)**

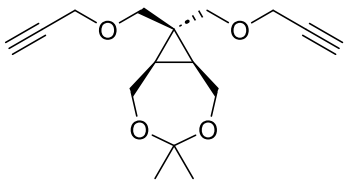

Yield: 31 mg, 0.11 mmol, 4% (yellow oil)

TLC: R_f (20% EA/cyclohexane) = 0.65

^{1}H NMR (500 MHz, CDCl$_3$): δ 4.19 (d, *J* = 2.4 Hz, 2H), 4.13 – 4.09 (m, 4H), 4.08 (s,

2H), 3.92 – 3.86 (m, 2H), 3.34 (s, 2H), 2.43 (t, *J* = 2.4 Hz, 1H), 2.40 (t, *J* = 2.4 Hz, 1H), 1.36 (s, 3H), 1.29 (s, 3H), 1.29 – 1.26 (m, 2H).

^{13}C NMR (126 MHz, $CDCl_3$): δ 103.57, 80.43, 79.97, 75.12, 74.43, 74.36, 65.54, 59.01, 58.41, 58.17, 29.87, 26.33, 25.92, 23.93.

((1*s*,2*R,3*S**)-1-((Prop-2-yn-1-yloxy)methyl)cyclopropane-1,2,3-triyl)tris(methylene) Tris(3-((*tert*-butoxycarbonyl)amino)propanoate) (48**)

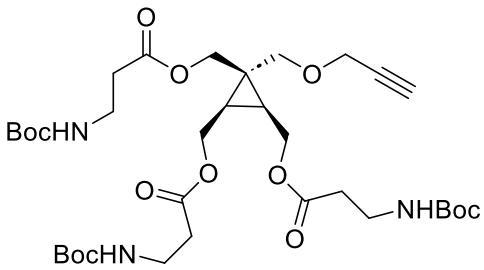

To **44** (180 mg, 0.75 mmol, 1.0 eq) was added 1M aq. HCl (4 mL) and the mixture stirred for 1 h at r.t.. The intermediate **47** was concentrated under reduced pressure. To 3-((*tert*-butoxycarbonyl)amino)propanoic acid **23** (781 mg, 4.13 mmol, 5.5 eq) were added EDC.HCl (791 mg, 4.13 mmol, 5.5 eq), DMAP (10 mg, 0.08 mmol, 10 mol%) and DMF (5 mL) under argon at r.t. and the mixture stirred at 0 °C for 10 min. A solution of **47** (150 mg, 0.75 mmol, 1.0 eq) in DMF (7 mL), and TEA (0.63 mL, 4.52 mmol, 6.0 eq) were then added to the mixture at 0 ºC and the reaction mixture stirred overnight at r.t.. The crude product was concentrated under reduced pressure and purified by silica gel column chromatography (40% EA/cyclohexane) to yield a pale yellow oil (474 mg, 0.66 mmol, 89%).

TLC: R_f (50% EA/cyclohexane) = 0.52

^{1}H NMR (500 MHz, $CDCl_3$): δ 5.19 – 5.07 (m, 3H), 4.31 (s, 2H), 4.30 – 4.18 (m, 4H), 4.16 (d, *J* = 2.0 Hz, 2H), 3.44 – 3.32 (m, 8H), 2.53 (dd, *J* = 12.1, 6.0 Hz, 6H), 2.44 (t, *J* = 2.3 Hz, 1H), 1.53 – 1.49 (m, 2H), 1.43 (s, 27H).

^{13}C NMR (126 MHz, $CDCl_3$): δ 172.28, 155.95, 79.57, 79.35, 75.15, 74.31, 61.46, 60.63, 58.07, 36.29, 36.22, 34.84, 34.76, 27.51, 27.05, 23.83.

HRMS (ESI/Q-TOF) *m/z*: $(M+H)^+$ calcd for $C_{34}H_{56}N_3O_{13}$ 714.3808; found 714.3806.

((1*s*,2*R,3*S**)-1-((Prop-2-yn-1-yloxy)methyl)cyclopropane-1,2,3-triyl) tris(methylene) Tris(3-aminopropanoate) (49)**

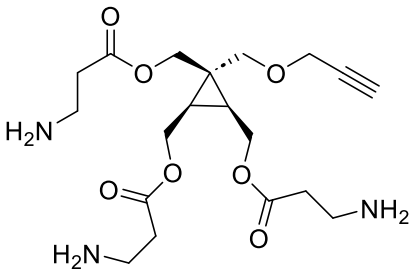

48 (156 mg, 0.22 mmol) was dissolved in 25% TFA/DCM (12 mL) and stirred at r.t. for 1 h. The crude product was concentrated under reduced pressure and used further without purification, assuming 100% yield (90 mg, 0.22 mmol).

((1*s*,2*R,3*S**)-2,3-Bis((2-(2,3-bis(methylcarbonyloxy)phenylcarbonylamino) ethylcarbonyloxy)methyl)-1-((prop-2-ynyloxy)methyl)cyclopropyl)methyl 3-(2,3-Bis (methylcarbonyloxy)phenylcarbonylamino)propanoate (50)**

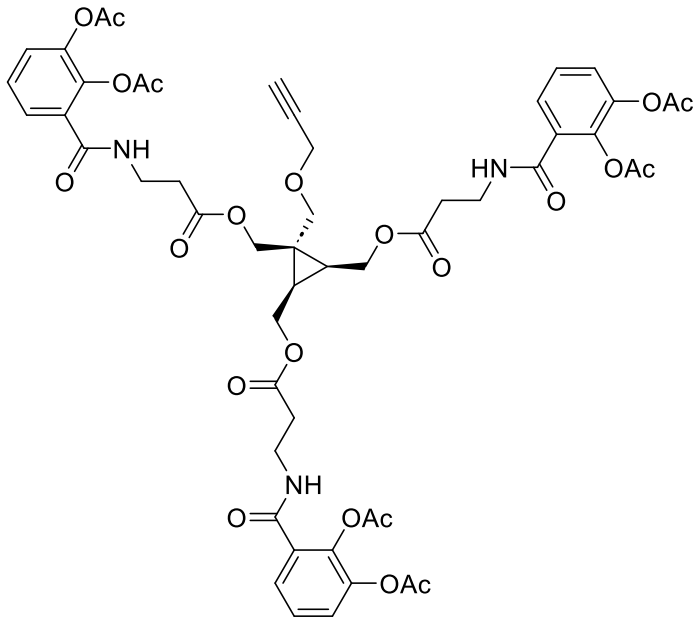

To a solution of **49** (90 mg, 0.22 mmol, 1 eq) in aq. $KHCO_3$ (5 mL, 1 M), a mixture of **28** (336 mg, 1.31 mmol, 6 eq) and 1,4-dioxane (5 mL) was added at 0 °C over 10 min. The mixture was then stirred for 5 min at 0 °C and then for 1 h at r.t.. Water (20 mL) was added and the aqueous phase was extracted with EtOAc (3x10 mL). The combined organic phases were washed with brine (5 mL), dried over Na_2SO_4, and

filtered. The crude product was concentrated under reduced pressure and purified by RP-HPLC (H_2O/MeCN, 0.1% AcOH) to afford **50** as a white solid (41 mg, 0.04 mmol, 18%).

^{1}H NMR (500 MHz, DMSO-d_6): δ 8.43 (t, *J* = 5.5 Hz, 3H), 7.43 (dt, *J* = 7.0, 2.3 Hz, 3H), 7.39 – 7.31 (m, 6H), 4.31 – 4.21 (m, 6H), 4.11 (d, *J* = 2.3 Hz, 2H), 3.46 – 3.39 (m, 7H), 3.33 (s, 2H), 2.56 (dt, *J* = 14.0, 7.1 Hz, 6H), 2.28 (s, 9H), 2.23 (s, 9H), 1.44 (p, *J* = 8.8 Hz, 2H).

^{13}C NMR (176 MHz, DMSO-d_6): δ 171.54, 168.73, 168.24, 165.04, 143.23, 140.45, 131.18, 126.67, 126.48, 125.92, 80.56, 77.69, 73.35, 61.25, 60.80, 57.50, 35.72, 34.00, 27.15, 23.36, 20.80, 20.69.

HRMS (ESI/Q-TOF) *m/z*: $(M+H)^+$ calcd for $C_{52}H_{56}N_3O_{22}$ 1074.3350; found 1074.3353.

tert-Butyl (*E*)-(4-Bromobut-2-en-1-yl)Carbamate (64)

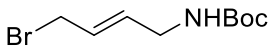

To a suspension of NaH (0.21 g (0.12 g), 5.1 mmol, 60% w/w in mineral oil, 1 eq) in THF (10 mL) were added *tert*-butyl carbamate **63** (0.60 g, 5.1 mmol, 1 eq) and (*E*)-1,4-dibromo-2-butene **62** (3.30 g, 15.4 mmol, 3 eq) under argon at r.t. and the reaction mixture stirred at the same temperature for 18 h. Water (20 mL) was added to the mixture, which then was extracted with EtOAc (10x3 mL). The organic phases were combined and washed with brine, dried over Na_2SO_4, filtered, and concentrated under reduced pressure. The crude product was purified by silica gel column chromatography (8-10% EA/cyclohexane) to yield **64** as a white solid (151 mg, 0.6 mmol, 12%).

TLC: R_f (15% EA/cyclohexane) = 0.42 (potassium permanganate)

^{1}H NMR (500 MHz, $CDCl_3$): δ 5.84 – 5.71 (m, 2H), 4.72 (s, 1H), 3.91 (d, *J* = 6.6 Hz, 2H), 3.78 – 3.66 (m, 2H), 1.41 (s, 9H).

^{13}C NMR (126 MHz, $CDCl_3$): δ 155.77, 132.19, 127.62, 79.70, 41.66, 32.15, 28.46.

3-Azidopropanoic acid (53)

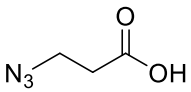

3-Bromopropanoic acid **52** (0.76 g, 5 mmol, 1 eq) was dissolved in dH_2O (10 mL). To this solution was added sodium azide (1.30 g, 20 mmol, 4 eq) and the reaction mixture stirred for 24 h. The reaction mixture was acidified with 12M aq. HCl to pH ≈ 1 and extracted with Et_2O (3×25 mL). The combined organic phases were washed with brine (25 mL), dried over Na_2SO_4, filtered, and concentrated under reduced pressure at 25°C to afford **53** as a clear oil that was used further without purification.

(2*S*,5*R*,6*R*)-6-((*R*)-2-(3-Azidopropanamido)-2-phenylacetamido)-3,3-dimethyl-7-oxo-4-thia-1-azabicyclo[3.2.0]heptane-2-carboxylic acid (56)

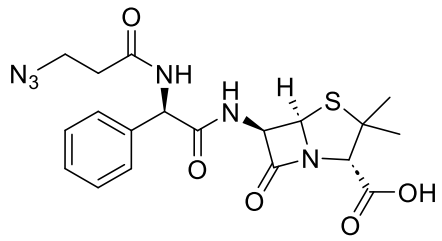

N-Methylmorpholine (0.02 mL, 22 mg, 0.22 mmol, 1 eq) and isobutyl chloroformate (0.03 mL, 30 mg, 0.22 mmol, 1 eq) were added to **53** (25 mg, 0.22 mmol, 1 eq) in THF (8.0 mL) under argon at 0 °C. The mixture was stirred at 0 °C for 2 h. To the mixture were added a solution of ampicillin **54** (85 mg, 0.24 mmol, 1.1 eq) and TEA (0.09 mL, 65 mg, 0.65 mmol, 3 eq) in THF (4.0 mL), and water (0.8 mL) under argon at 0 °C and the reaction mixture stirred at the same temperature for 1 h, and at r.t. for another 1 h. Excess solvent was removed under reduced pressure and the residue dissolved in water (16 mL) and acidified carefully at 0 °C with 1M aq. HCl to pH ≈ 2. The resulting mixture was extracted with EtOAc (3x10 mL). The organic phases were combined, washed with brine, dried over Na_2SO_4, filtered, and concentrated under reduced pressure. The crude product was purified via RP-HPLC (H_2O/MeCN, 0.1% HCOOH) to afford **56** as a white solid (23 mg, 0.05 mmol, 24%).

^{1}H NMR (500 MHz, DMSO-d_6)*: δ 13.35 (s, 1H), 9.19 (d, *J* = 7.9 Hz, 1H), 8.76 (d, *J* = 8.3 Hz, 1H), 7.44 – 7.40 (m, 2H), 7.35 – 7.30 (m, 2H), 7.29 – 7.25 (m, 1H), 5.77 (d, *J* = 8.2 Hz, 1H), 5.52 (dd, *J* = 7.9, 4.0 Hz, 1H), 5.39 (d, *J* = 4.0 Hz, 1H), 4.20 (s, 1H), 3.50 (td, *J* = 6.4, 1.4 Hz, 2H), 2.53 (td, *J* = 6.3, 2.4 Hz, 2H), 1.55 (s, 3H), 1.41 (s, 3H).

^{13}C NMR (176 MHz, DMSO-d_6)*: δ 173.40, 170.03, 169.34, 168.91, 138.12, 128.20, 127.56, 127.05, 70.29, 67.21, 63.75, 58.11, 55.37, 46.94, 34.20, 30.35, 26.62.

This spectrum is in accordance with literature.[58]

***Note:** A minor impurity—most likely (2*S*,5*R*,6*R*)-6-((*R*)-2-(3-bromopropanamido)-2-phenylacetamido)-3,3-dimethyl-7-oxo-4-thia-1-azabicyclo[3.2.0]heptane-2-carboxylic acid—was present along with **56** at the time of recording NMR spectra. However, this did not affect the next reaction with **56**.

(2*S*,5*R*,6*R*)-3,3-Dimethyl-7-oxo-6-((*R*)-2-phenyl-2-(3-(4-((((1*s*,2*R,3*S**)-1,2,3-tris(((3-(2,3-diacetoxybenzamido)propanoyl)oxy)methyl)cyclopropyl)methoxy)methyl)-1*H*-1,2,3-triazol-1-yl)propanamido)acetamido)-4-thiazabicyclo[3.2.0]heptane-2-carboxylic acid (57)**

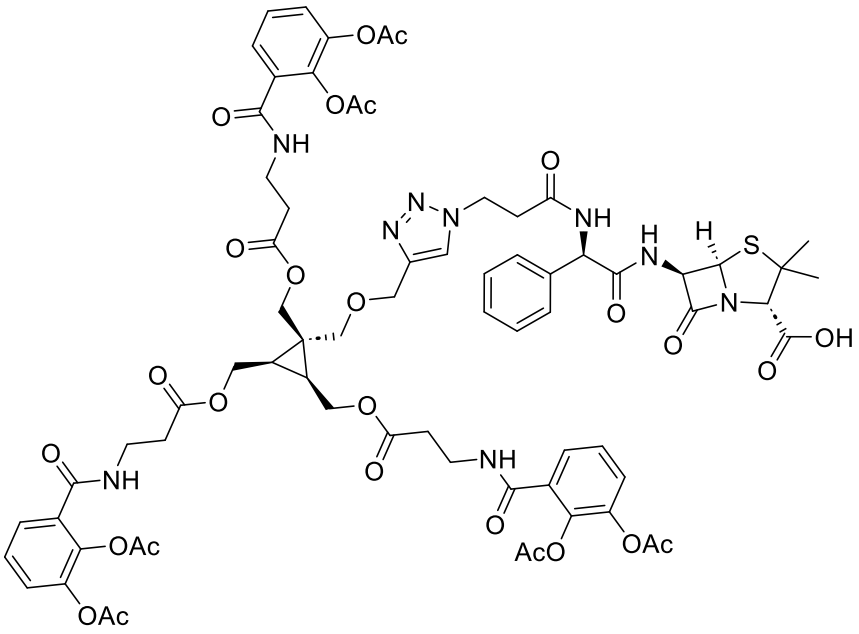

To a solution of **50** (7.0 mg, 6.5 µmol, 1.0 eq) in DMSO (150 µL) were added AcOH (3 µL) and a solution of **56** (4.4 mg, 9.8 µmol, 1.5 eq) in DMSO (75 µL) under argon at r.t.. To this mixture was added a pre-mixed solution of copper sulfate pentahydrate (1.2 mg, 4.9 µmol, 0.8 eq), sodium ascorbate (2.6 mg, 13.0 µmol, 2.0 eq), and tris(3-hydroxypropyltriazolylmethyl)amine (THPTA) (1.4 mg, 3.3 µmol, 0.5 eq) in degassed dH_2O (37 µL) at r.t. and stirred at the same temperature for 1 h. Then, the same amount of this pre-mixed solution was added and the reaction mixture stirred at r.t. for 15 minutes. The mixture was filtered using a syringe filter and then purified by RP-HPLC (H_2O/MeCN, 0.1% AcOH) to afford **57** as a white solid (4 mg, 2.6 µmol, 40%).

^{1}H NMR (700 MHz, DMSO-d_6): δ 9.18 (d, *J* = 7.9 Hz, 1H), 8.73 (d, *J* = 8.1 Hz, 1H), 8.41 (dd, *J* = 11.2, 5.6 Hz, 3H), 7.94 (s, 1H), 7.44 – 7.40 (m, 3H), 7.38 – 7.24 (m, 11H),

5.72 (d, *J* = 8.1 Hz, 1H), 5.51 (dd, *J* = 7.9, 4.0 Hz, 1H), 5.39 (d, *J* = 4.0 Hz, 1H), 4.53 (ddd, *J* = 20.4, 13.8, 7.0 Hz, 4H), 4.46 (s, 2H), 4.29 – 4.21 (m, 6H), 4.20 (s, 1H), 3.44 – 3.32 (m, 8H), 2.57 – 2.52 (m, 6H), 2.27 (s, 6H), 2.22 (d, *J* = 3.7 Hz, 6H), 1.55 (s, 2H), 1.45 – 1.42 (m, 2H), 1.40 (s, 2H).

^{13}C NMR (176 MHz, DMSO-*d*$_6$): δ 171.30, 171.11, 170.51, 170.01, 168.54, 168.29, 167.79, 164.59, 143.63, 142.77, 139.98, 130.72, 128.17, 128.00, 127.28, 127.00, 126.21, 126.04, 125.46, 123.87, 73.14, 70.29, 67.20, 62.98, 60.87, 60.39, 58.10, 57.17, 55.41, 45.72, 35.25, 33.51, 30.31, 26.81, 26.65, 22.80, 20.34, 20.21.

HRMS (ESI/Q-TOF) *m/z*: $((M+2H)/2)^{2+}$ calcd for $C_{71}H_{79}N_9O_{27}S$ 760.7398; found 760.7402.

tert-Butyl (*R*)-(4-Bromobut-2-en-1-yl)(*tert*-Butoxycarbonyl)Carbamate (66)

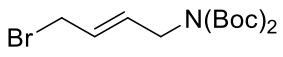

To a suspension of di-*tert*-butyl iminodicarbonate **65** (0.75 g, 3.5 mmol, 1 eq) in DMF (16 mL) were added Cs_2CO_3 (2.25 g, 6.9 mmol, 2 eq) and (*E*)-1,4-dibromo-2-butene **62** (3.69 g, 17.3 mmol, 5 eq) under argon at r.t. and the reaction mixture stirred at the same temperature for 18 h. The reaction mixture then was poured onto water (30 mL) and extracted with EtOAc (3x15 mL). The combined organic phases were washed with brine, dried over Na_2SO_4, filtered, and concentrated under reduced pressure. The crude product was dry loaded onto silica and purified by flash column chromatography (10% EA/cyclohexane) to afford **66** as a clear oil (0.73 g, 2.1 mmol, 60%).

^{1}H NMR (500 MHz, $CDCl_3$): δ 5.90 – 5.74 (m, 2H), 4.18 (d, *J* = 5.4 Hz, 2H), 3.94 (d, *J* = 7.0 Hz, 2H), 1.50 (s, 18H).

^{13}C NMR (176 MHz, $CDCl_3$): δ 152.19, 130.72, 128.64, 82.70, 47.12, 32.11, 28.16.

An attempt to synthesize (2*S*,5*R*,6*R*)-6-((*R*)-2-(3-Azidopropanamido)-2-(4-hydroxyphenyl)acetamido)-3,3-dimethyl-7-oxo-4-thia-1-azabicyclo[3.2.0] heptane-2-carboxylic acid (59)

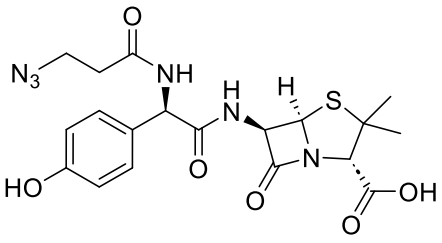

N-Methylmorpholine (0.06 mL, 56 mg, 0.55 mmol, 1 eq) and isobutyl chloroformate (0.07 mL, 76 mg, 0.55 mmol, 1 eq) were added to a solution of **53** (64 mg, 0.55 mmol, 1 eq) in THF (3.0 mL) under argon at 0 °C. The mixture was stirred at 0 °C for 30 min and at r.t. for 30 min. To the mixture were added a solution of amoxicillin **58** (221 mg, 0.61 mmol, 1.1 eq) and TEA (0.23 mL, 167 mg, 1.65 mmol, 3 eq) in THF (2.0 mL), and water (0.3 mL) under argon at 0 °C and the reaction mixture stirred at the same temperature for 30 min, and at r.t. for 30 min. Excess solvent was removed under reduced pressure and the residue taken up in water (5 mL) and acidified carefully at 0 °C with 1M aq. HCl to pH ≈ 2. The resulting mixture was extracted with EtOAc (3x4 mL). The organic phases were combined, washed with brine, dried over Na_2SO_4, filtered, and concentrated under reduced pressure. Purification was performed by RP-HPLC (H_2O/MeCN, 0.1% HCOOH) to yield **59** in trace amounts (<1 mg, <1%).

An attempt to synthesize *tert*-Butyl ((*E*)-4-(((1*r*,2*R,3*S**)-2,3-Bis((((*E*)-4-(bis(*tert*-butoxycarbonyl)amino)but-2-en-1-yl)oxy)methyl)-1-((prop-2-yn-1-yloxy)methyl) cyclopropyl)methoxy)but-2-en-1-yl)(*tert*-butoxycarbonyl)carbamate (67**)

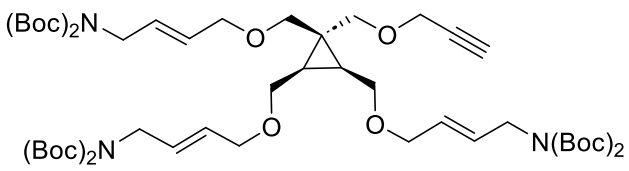

To **44** (113 mg, 0.5 mmol, 1.0 eq) was added 1M aq. HCl (4 mL, 4.0 mmol, 8.5 eq) and the mixture stirred at r.t. for 1 h. Excess solvent was removed under reduced pressure to afford the intermediate **47** as a brown oil. To a suspension of NaH (84 mg (50 mg), 2.1 mmol, 4.4 eq, 60% w/w in mineral oil) in DMF (2 mL) was added a solution of **47** (94 mg, 0.5 mmol, 1 eq) in DMF (4 mL) under argon and the mixture stirred for 15 min at 0 ºC. To this was added **66** (731 mg, 2.1 mmol, 4.4 eq) slowly at 0 ºC. The reaction mixture was stirred at r.t. overnight. The reaction was quenched at 0 ºC with MeOH and water. Water (10 mL) was then added to the mixture and the crude product extracted with EtOAc (3x10 mL). The organic phases were combined, washed with brine, dried over Na_2SO_4 and concentrated under reduced pressure to afford the crude product.

((1*s*,2*R,3*S**)-1-((Prop-2-yn-1-yloxy)methyl)cyclopropane-1,2,3-triyl)tris(methylene) Tris(3-(2,3-dihydroxybenzamido)propanoate) (51)**

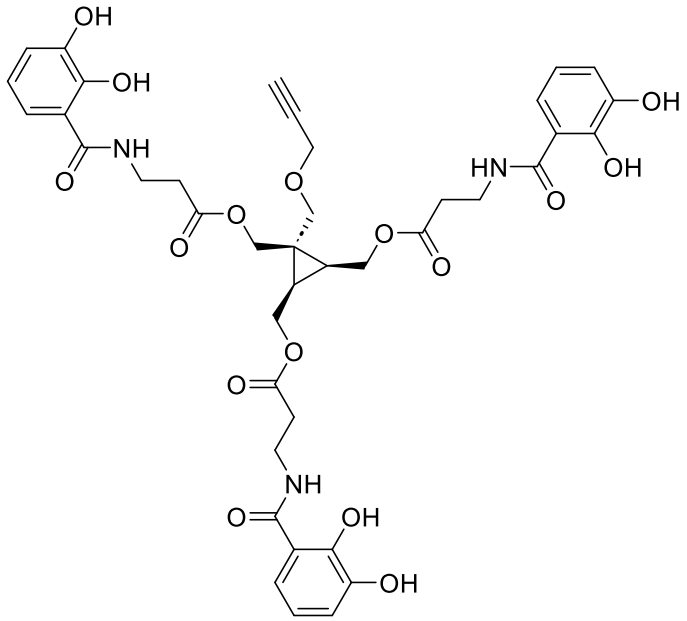

To **50** (23 mg, 21 μmol) in MeOH (0.75 mL) was added TEA (0.25 mL) under argon at 0 ºC. The reaction mixture was stirred at this temperature for 5 min and then at r.t. for 10 min. The crude product was concentrated under reduced pressure and the residue purified by RP-HPLC (H_2O/MeCN, 0.1% HCOOH) to afford **51** as a white solid (11 mg, 13 μmol, 62%).

^{1}H NMR (700 MHz, DMSO-d_6): δ 12.53 (s, 3H), 9.16 (s, 3H), 8.84 – 8.80 (m, 3H), 7.25 – 7.22 (m, 3H), 6.92 – 6.88 (m, 3H), 6.66 (td, *J* = 7.9, 2.6 Hz, 3H), 4.26 – 4.18 (m, 6H), 4.06 (d, *J* = 2.3 Hz, 2H), 3.55 – 3.49 (m, 6H), 3.37 (t, *J* = 2.2 Hz, 1H), 3.27 (s, 2H), 2.63 (t, *J* = 7.1 Hz, 2H), 2.61 (t, *J* = 7.0 Hz, 4H), 1.40 – 1.35 (m, 2H).

^{13}C NMR (176 MHz, DMSO-d_6): δ 171.50, 170.14, 149.89, 146.63, 119.27, 118.42, 117.73, 115.44, 80.50, 77.67, 73.34, 61.28, 60.81, 57.46, 35.64, 33.88, 27.11, 23.35.

HRMS (ESI/Q-TOF) *m/z*: $(M+H)^+$ calcd for $C_{40}H_{44}N_3O_{16}$ 822.2716; found 822.2714.

3. Results and Discussion

3.1. Synthesis of Artificial Siderophores

To assemble the cyclopropane core, dimethyl malonate **9** was diazotized using *p*-ABSA **10**, a known diazotransfer reagent (both commercially available) to yield dimethyl 2-diazomalonate **11**, a carbenoid precursor.[59] This was reacted with commercially available 2,2-dimethyl-4,7-dihydro-1,3-dioxepine **12** in the presence of $Rh_2(esp)_2$, a chiral rhodium (II) complex-based catalyst reported to enantioselectively catalyse olefin cyclopropanations with carbenoid precursors,[59] to yield the cyclopropane core system **13** (Scheme 1). This reaction was optimized previously as part of a Master's thesis.[54] This cyclopropanation is a key step as it involves the

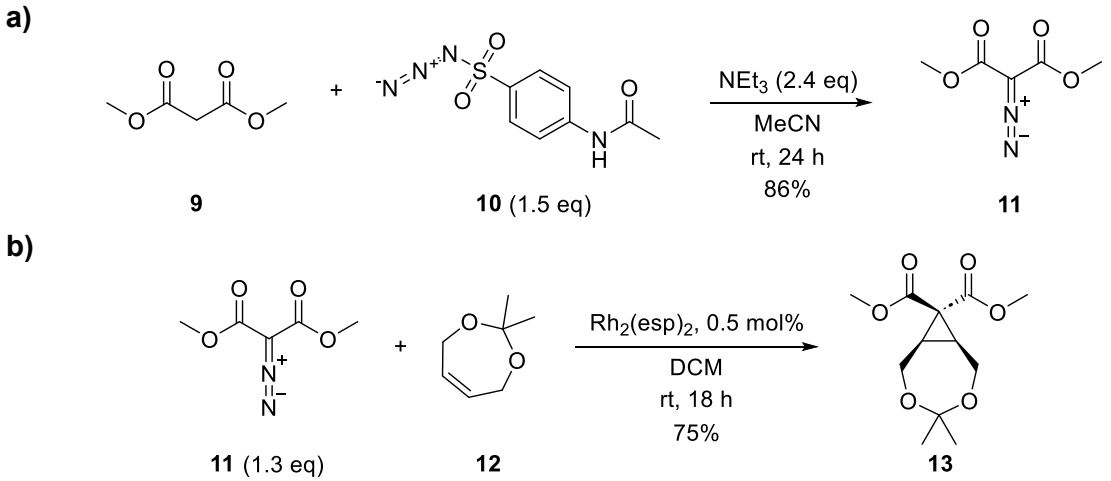

Scheme 1: (a) Diazotization of **9** to dimethyl 2-diazomalonate **11** using *p*-ABSA **10**. (b) Cyclopropanation of **12** with **11** in the presence of $Rh_2(esp)_2$ catalyst to cyclopropane core system **13**.

assembly of the cyclopropane core, which is essential for all subsequent transformations. The next focus was to generate 3 identical *cis*-oriented arms and one *trans*-oriented arm for reasons explained above. Subsequent transformations were carried out towards this aim: **13** was treated with $LiOH \cdot H_2O$ as a base to yield mono-acid **14** via stereoselective partial hydrolysis.[54] To functionalize the newly generated carboxylic acid with a moiety for eventual attachment of an antibacterial payload, **14** was subjected to amide coupling with commercially available propargylamine **15** using HATU as a coupling reagent in the presence of DIPEA as a base, to yield the corresponding amide **16** (Scheme 2). The alkyne moiety installed in this step would enable an azide-alkyne cycloaddition to later attach the payload.

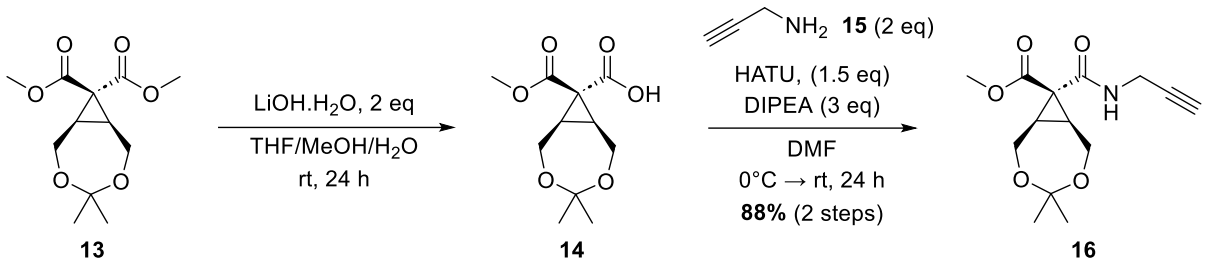

Scheme 2: Partial hydrolysis of **13** to mono-acid **14** and amide coupling of **14** with propargylamine **15** using HATU and DIPEA to yield amide **16**.

It is important to note that sufficient evidence was previously obtained[54] to conclude that **16** and, by extension, **14** were diastereomerically pure. The stereochemistry of **16** could not be confirmed via ^{1}H-^{1}H NOESY owing to a large distance between the methyl ester H and the ring H, which prevented their correlation. However, treating **16** with 1M aq. HCl led to the formation of lactone **17** as the major product, with the hydrolysis product **18** formed in trace amounts (Scheme 3). This is possible only if the methyl ester of **16** is *cis*-oriented with respect to the 7-membered ring.

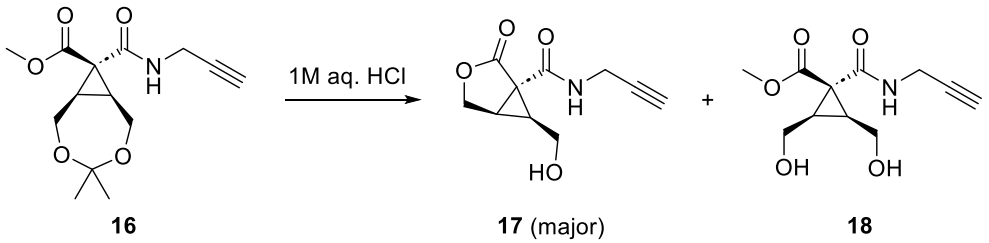

Scheme 3: Acid-catalysed lactonization of **16** to lactone **17**.

To obtain the 3 *cis*-oriented arms, a triol-based system was pursued for two reasons: a) there are several possible options to subsequently functionalize the alcohols, and b) previous work[54] had described a partially successful synthesis of this triol-based system. Optimizing this synthesis step would be an interesting task to pursue. Towards this direction, in an attempt to reduce the methyl ester to an alcohol, **16** was treated with $LiBH_4$ in THF in the presence of a few drops of H_2O and the mixture was stirred at 60 °C overnight. However, this resulted in the reduction of the alkyne on the amide arm to an alkene in **17**, without any formation of the ester reduction product**.** A second attempt without H_2O and subsequent quenching at 0 °C with 1M aq. HCl was performed in close analogy to a previously reported procedure[54]. While the triol **19** did indeed form upon hydrolysis, it could not be purified and was used further as a

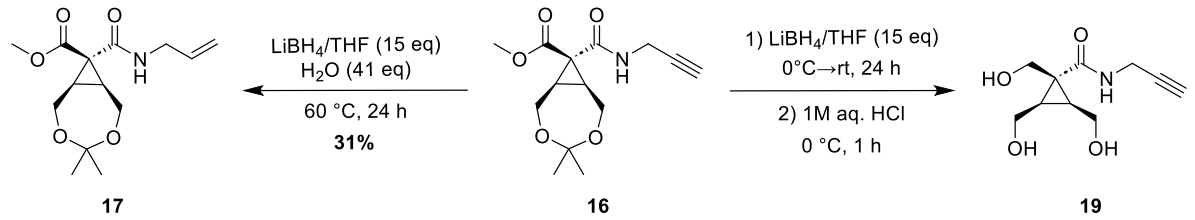

Scheme 4: Chemoselective reduction of **16** to side product alkene **17** and alternatively to triol **19**.

crude product (Scheme 4). The initial plan to functionalize the triol **19** involved converting it to a triamine system **20**, followed by amide coupling with a catechol acid (or acyl chloride) to eventually afford **21**, a cyclopropane-based tris(catecholate) siderophore (Scheme 5).

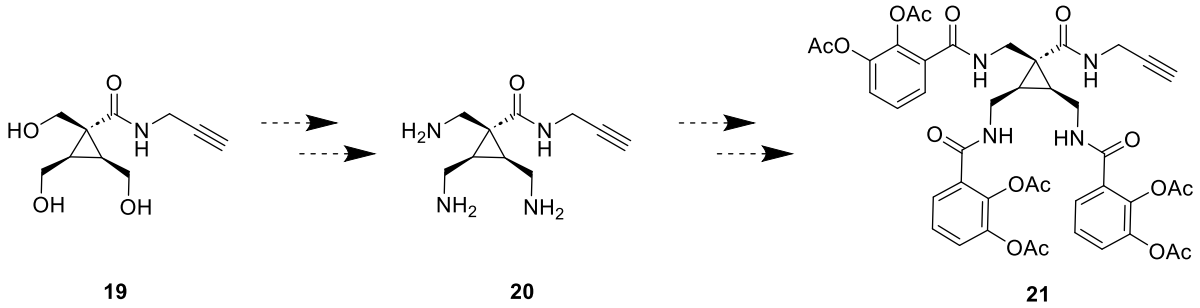

Scheme 5: Initial plan to convert triol **19** to tris(catecholate) cyclopropane-based siderophore **21** via triamine system **20**.

A plausible option to perform the initial transformation involves converting the alcohols to better leaving groups—mesylates, for instance. The subsequent alkylation of an "activated" ammonia—diformylamine or di-*tert*-butyl iminodicarbonate, for instance—with this trimesylate system would then result in a triamine-based system. This route could not be carried out since an insufficient amount of crude product was obtained during an attempt to convert the triol **19** to the trimesylate **22** (Scheme 6), which did not warrant further action.

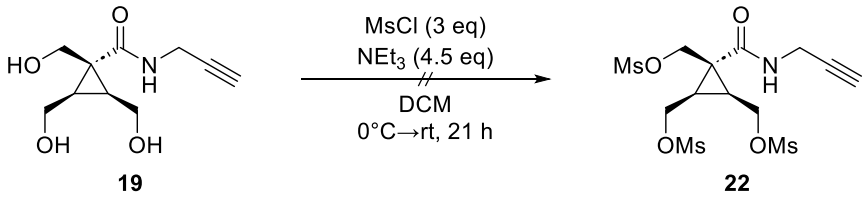

Scheme 6: Attempted mesylation of **19** to trimesylate **22**.

An alternative route was chosen to generate a triamine system from **19** via esterification of the triol with short linkers bearing both an acid and a protected amine. Subsequent deprotection would then afford the triamine system. Thus, **19** was coupled with commercially available Boc-β-Ala-OH **23** using EDC.HCl as a coupling reagent, catalysed by DMAP in the presence of NEt_3 as a base, to yield the protected triamine **24**. However, this could not be purified by silica gel column chromatography. It was nevertheless used further as an impure product; deprotection of **24** with TFA afforded the triamine **25** (Scheme 7).

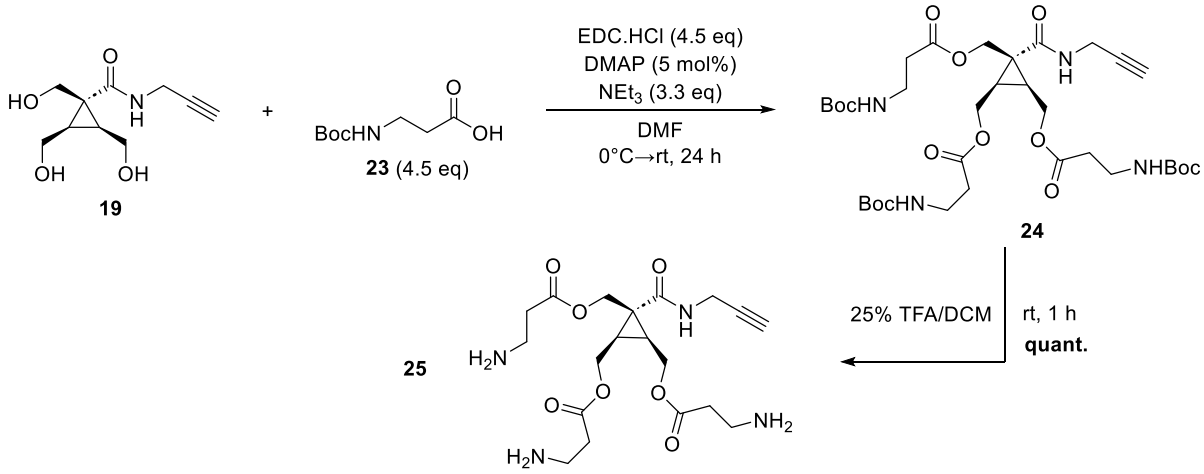

Scheme 7: Esterification of triol **19** with Boc-β-Ala-OH **23** to protected triamine **24** and subsequent deprotection to triamine **25**.

With the triamine synthesized, the catechol acid was then afforded in 2 steps from commercially available 2,3-dihydroxybenzoic acid **26**: acetylation of the phenol groups on **26** using acetic anhydride in the presence of catalytic DMAP yielded 2,3-diacetoxybenzoic acid **27**. This was converted to acid chloride **28** using oxalyl chloride in the presence of catalytic DMF (Scheme 8). **28** was used further as a crude product.

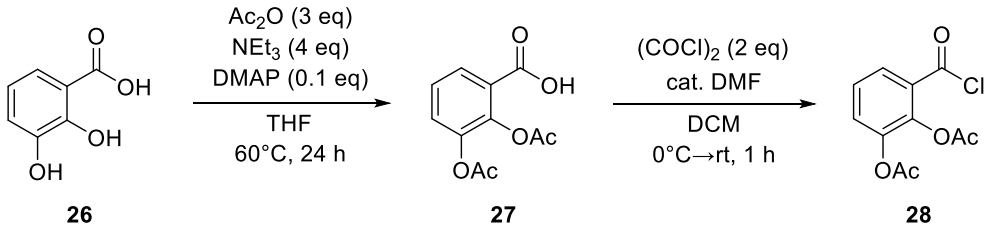

Scheme 8: Acetylation of 2,3-dihydroxybenzoic acid **26** to 2,3-diacetoxybenzoic acid **27** and conversion of **27** to acyl chloride **28**.

To ultimately synthesize the cyclopropane-based tris(catecholate) siderophore, a Schotten-Baumann amide coupling reaction between triamine **25** and acyl chloride **28** was performed. These were stirred with aq. potassium bicarbonate in dioxane at r.t. over 3 hours. Various degrees of de-acetylation were detected during the reaction, but the desired fully acetylated siderophore **29** could not be isolated upon purification via RP-HPLC. Instead, the completely de-acetylated siderophore **30** was isolated, although in a mere 7% yield (Scheme 9).

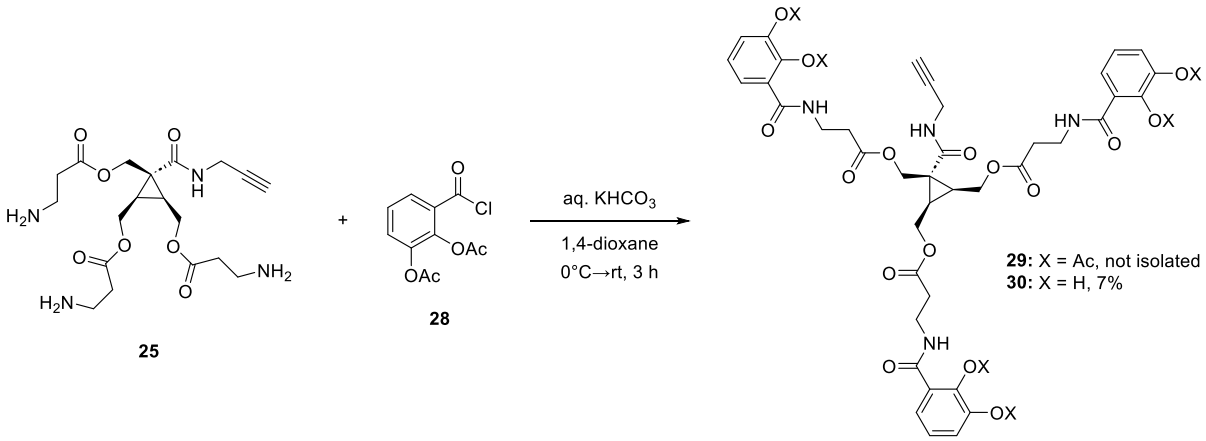

Scheme 9: Schotten-Baumann amide coupling of **25** with **28** to yield tris(catecholate) cyclopropane-based siderophore **30**.

While siderophore **30** was successfully synthesized, and siderophore **29** could potentially have also been isolated with a shorter reaction duration that minimized de-acetylation, the low yields and issues with purification in previous steps along the pathway to this siderophore remained to be addressed. Thus, efforts to overcome these limitations were subsequently focused on.

The formation of side products during conversion of the amide **16** to triol **19** was hypothesized to be influenced by the proximity of the amide carbonyl O to the alkyne. This proximity in case of a propargyl group could imply a partial withdrawal of electron density by this carbonyl O from the alkyne group, making it more electrophilic and thus more susceptible to reduction by the nucleophilic hydride species. In such a scenario, this effect could in principle be attenuated, or better yet, removed, by increasing the distance between the O and the alkyne—by including an extra -CH_2 unit between them, for instance (Fig. 10). This was thus attempted by first coupling mono-acid **14** with commercially available but-3-yn-1-amine **31** using HATU as a coupling reagent in the presence of DIPEA as a base to yield the corresponding

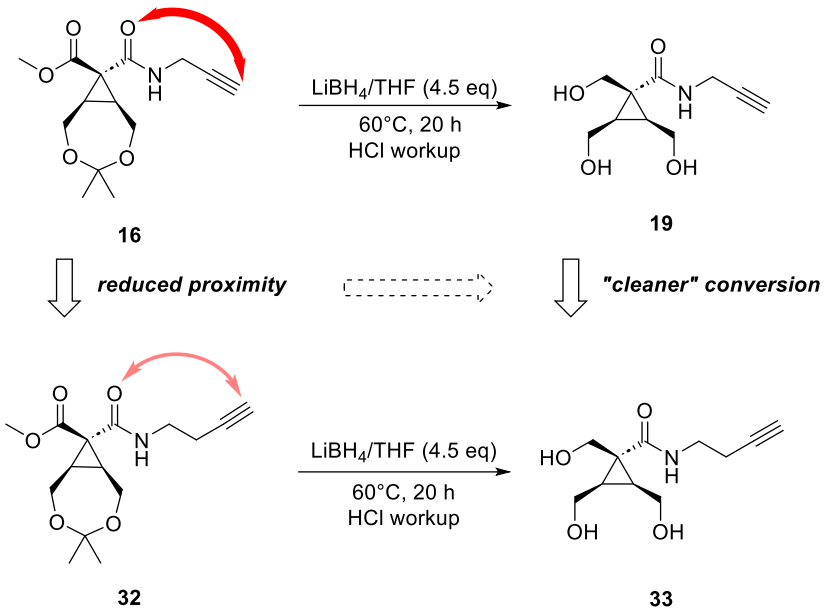

Figure 10: Hypothesized attenuation of electron-withdrawing influence by the carbonyl O on the alkyne in **16** upon increasing the distance between them, potentially minimizing the formation of side products.

amide **32**. This was then treated with $LiBH_4$ in THF at 60 °C overnight as before, to attempt a chemoselective reduction of the methyl ester on amide **32** to the corresponding triol **33** (Scheme 10). However, the crude mixture was observed to still contain a similar proportion of side products as before, so further action with this was not warranted; the proposed hypothesis was thus considered to be falsified.

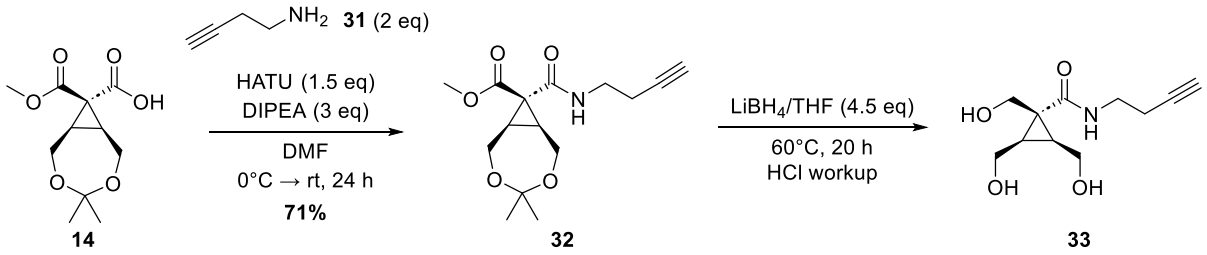

Scheme 10: Amide coupling of **14** to but-3-yn-1-amine **31** using HATU and DIPEA to yield amide **32** and a subsequent attempt to reduce **32** to triol **33** using $LiBH_4$.

Next, a chemoselective reduction of the methyl ester of **16** was attempted using *in-situ* generated alane. This was generated by stirring $LiAlH_4$ with trimethylsilyl chloride in THF for 2 h at 0 °C. Addition of **16** and stirring at r.t. for 2 days resulted in complete reduction of the ester to alcohol, amide to amine, and the alkyne to alkene. This was also observed in subsequent attempts at 0 °C in 2 hours and at -10 °C in 30 minutes (Scheme 11).

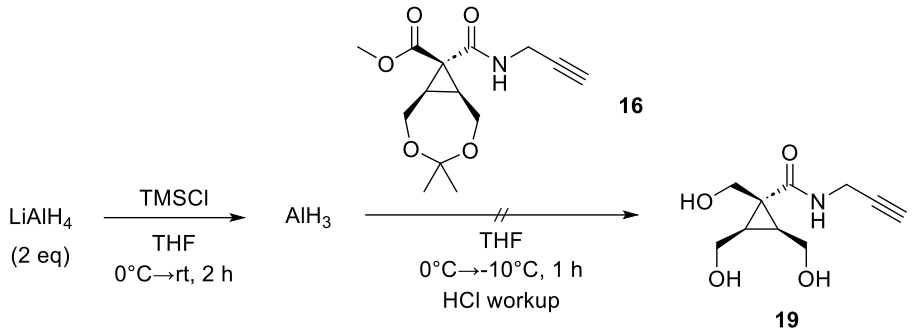

Scheme 11: An attempt to reduce **16** to **19** using *in-situ* generated alane.

In an attempt to selectively reduce the methyl ester of mono-acid **14**, it was treated with $LiBH_4$. Within 5 hours at 60 °C, the desired triol **34** was observed to have formed. However, both **14** was not consumed and formation of the desired product did not proceed further despite stirring overnight, subsequently heating the mixture to 80 °C, and also adding 2 drops of H_2O to it and stirring overnight (Scheme 12).

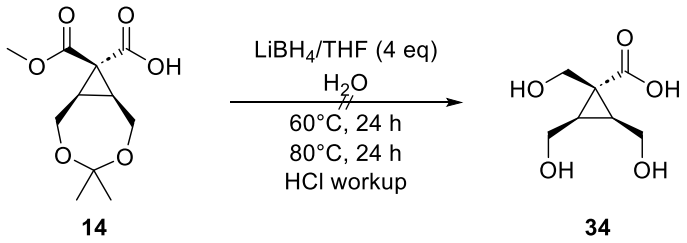

Scheme 12: Attempted reduction of **14** to triol **34** using $LiBH_4$.

$BF_3.Et_2O$ when used in conjunction with $NaBH_4$ can generate borane, BH_3, *in-situ*, which is known to selectively reduce carboxylic acids.[60] To attempt this, the mono-acid **14** was added to $NaBH_4$ and the mixture was stirred in THF at 0 °C. To this was added $BF_3.OEt_2$ to generate the borane, and the reaction mixture was stirred at r.t. overnight. No formation of **35** was observed (Scheme 13).

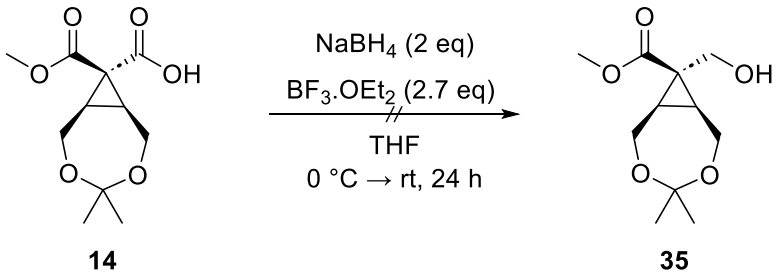

Scheme 13: Attempted reduction of **14** to **35** using $BF_3.Et_2O$ and $NaBH_4$.

Several unsuccessful attempts towards chemoselective reduction prompted a change in direction; A complete hydrolysis of both methyl esters on the cyclopropane core **13** was considered. In principle, this could be followed by selective esterification of the *trans*-oriented arm with an alcohol bearing an alkyne group, dictated by sterics—the face *trans* with respect to the 7-membrered ring would be more accessible to incoming nucleophiles. With this in mind, **13** was hydrolysed completely by treating with an excess of aq. NaOH in EtOH at 80 °C overnight. Acidification of the mixture to precipitate out the di-acid **36** was not practical, since this would also hydrolyse the ring ketal. The crude product was thus used further. Two attempts were made to couple commercially available but-3-yn-1-ol **37** to **36**, one using DCC as the coupling reagent and DMAP as the catalyst in the presence of NEt_3 as the base, and another using EDC·HCl as the coupling reagent with DMAP and NEt_3. In both cases, formation of the desired mono-ester **38** could not be detected (Scheme 14).

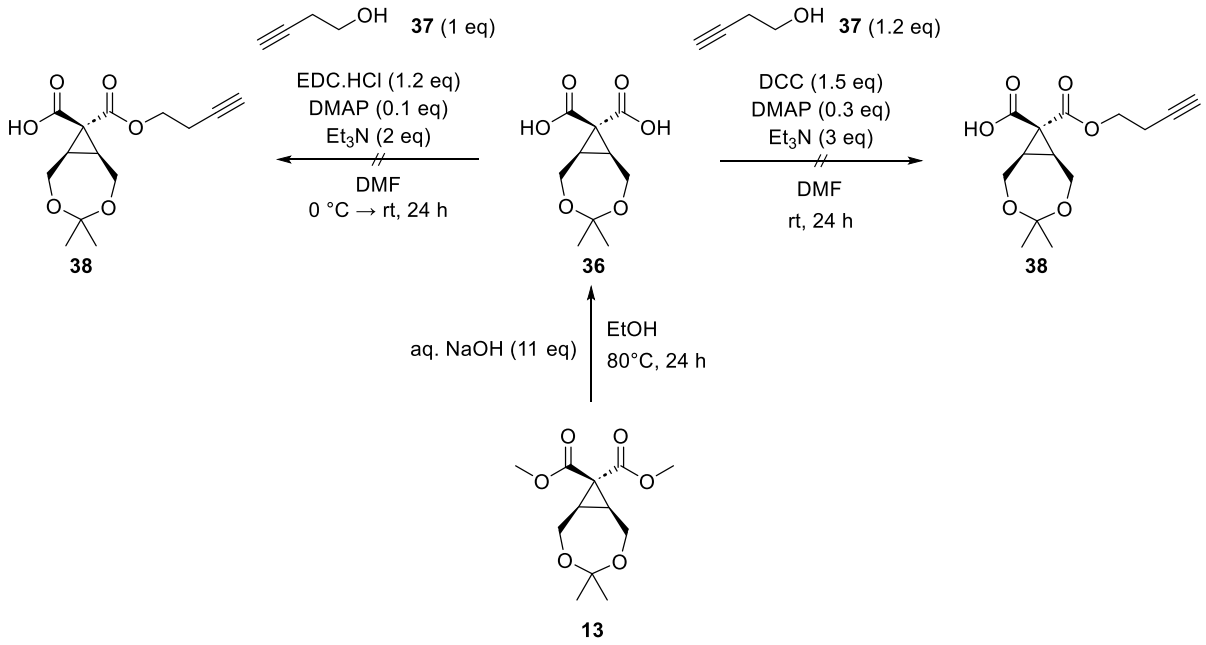

Scheme 14: Complete hydrolysis of both methyl esters of **13** to yield di-acid **36** and attempts to couple **36** with but-3-yn-1-ol **37** using EDC.HCl, and DCC as coupling reagents.

An analogous approach was considered; instead of attempting stereoselective attachment to a di-acid, the same was envisioned with a diol. A non-selective reduction of **13** to a diol could be followed by a stereoselective nucleophilic attack by the *trans*-oriented alcohol onto a halide to form a mono-ether via a Williamson ether synthesis. Thus, **13** was first reduced to the diol **39** using LAH. **39** was then treated

with commercially available 4-bromobut-1-yne **40** in the presence of NaH as the base and the mixture was stirred under reflux overnight (Scheme 15). A low crude weight and non-detection of the desired product **41** via ^{1}H NMR post-purification pointed to a) a probable decomposition of the product in the reaction mixture at high temperatures, and b) room for improvement in case of the reactivity of the halide electrophile.

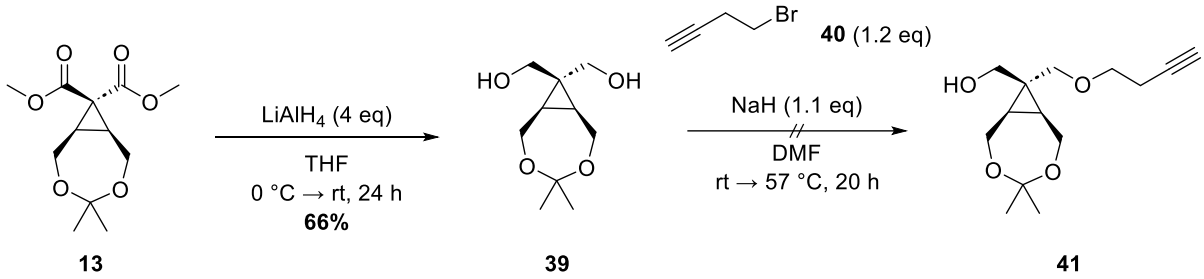

Scheme 15: Non-selective reduction of **13** to diol **39** and an attempt to alkylate 4-bromobut-1-yne **40** with **39**.

Thus, commercially available 3-bromoprop-1-yne **42** was added to **39** with KOH in DMSO. **42** is a better electrophile and more reactive than **40** since the electrophilic α-carbon on **42** may get stabilized via conjugation by a neighbouring π-bond; this is prevented in **40** by the extra –CH_2 separating them. It is interesting to note here that, during this reaction, KOH deprotonates DMSO, which may act as a base that deprotonates an alcohol on **39** to generate the nucleophile that attacks the electrophilic halide **42**. The educt **39** was completely consumed within 3 hours of stirring at r.t and the desired mono-ether **44** was isolated with a yield of 27%, along with side products **45** (5%) and **46** (4%) (Scheme 16).

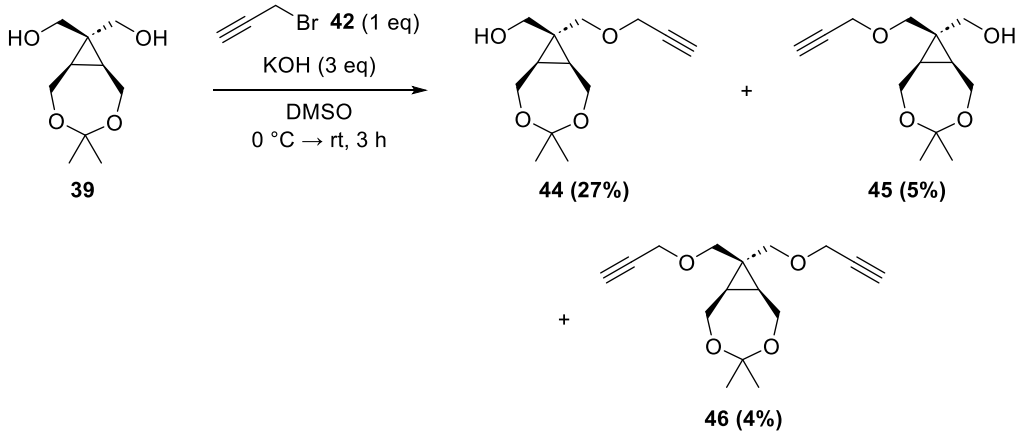

Scheme 16: Alkylation of 3-bromoprop-1-yne **42** with **39** using KOH in DMSO to yield **44**, **45** and **46**.

The discrepancy of 64% in total yield may be attributable to probable decomposition of the educt during the reaction. With regards to ^{1}H NMR spectra of both **44** and **45**, while H_B are expected to correspond to a 2H singlet, H_C could correspond to either a 2H singlet or a 2H doublet, depending on whether they show $^{3}J_{H,H}$ coupling with $H_{O\text{-}H}$ (Fig. 11). This uncertainty is attributed to commonly observed solvent interactions with the –OH protons.

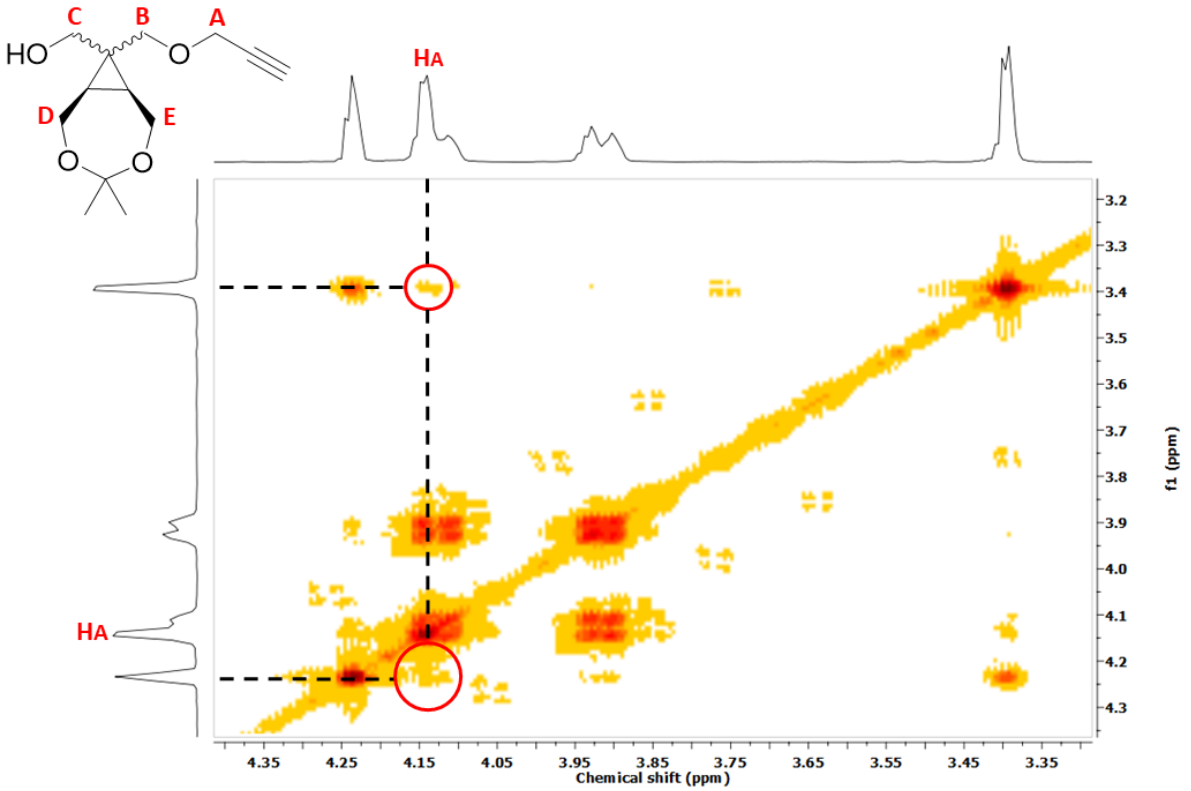

Figure 11: ^{1}H-^{1}H COSY spectrum of the major product (Scheme 16) ($CDCl_3$, 500 MHz). Carbon atoms labelled in red. H_A indicates protons attached to carbon A.

Initially in the absence of this coupling, ^{1}H NMR peak assignments for H_B and H_C were ambiguous, since both corresponded to 2H singlets with similar chemical shifts. Although a ^{1}H-^{1}H COSY experiment was performed with the major product to distinguish these signals, correlations were apparent for both pairs H_A-H_B and H_A-H_C; although, in principle, the former must be observed and the latter is highly unlikely. Fortunately, an additional ^{1}H NMR experiment in the same solvent as previously ($CDCl_3$), subsequently revealed a new 2H doublet besides a new 1H triplet, which was assigned to the –OH proton. Since all other signals remained approximately unchanged, this new 2H doublet was assigned to H_C, thus distinguishing it from the 2H singlet corresponding to H_B (Fig. 12).

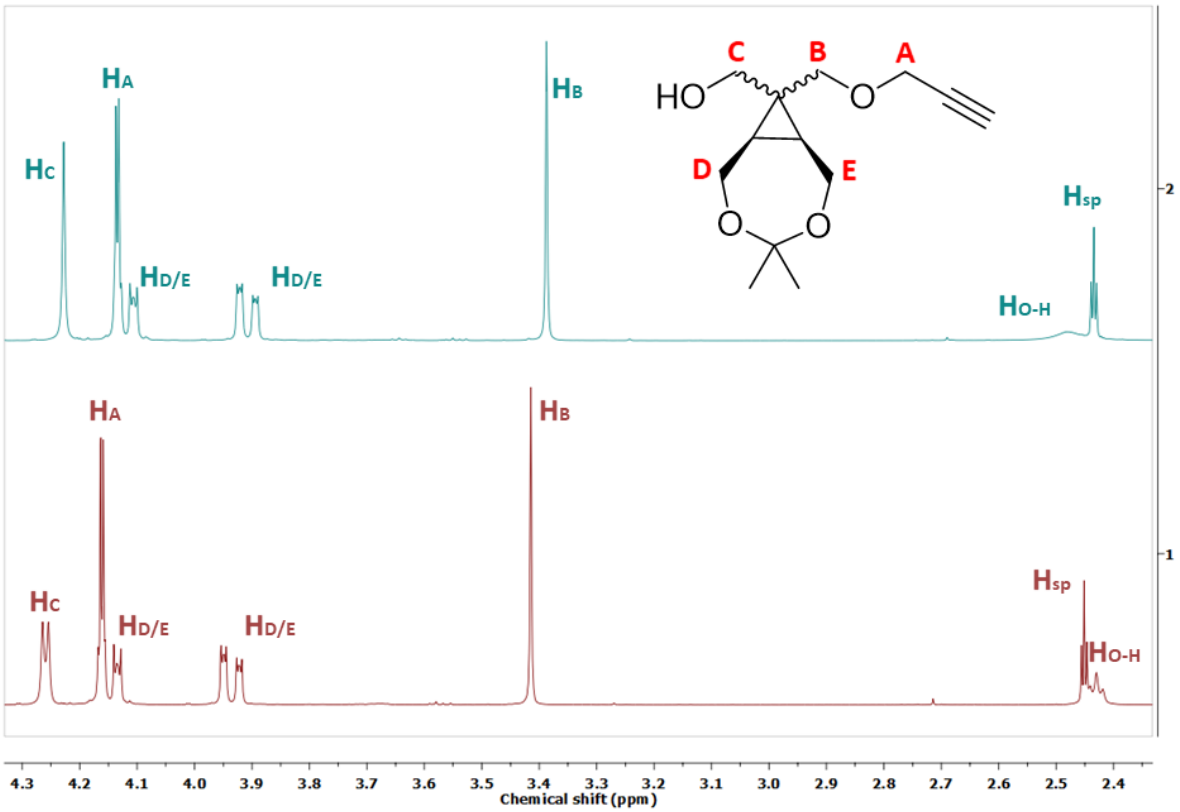

Figure 12: ^{1}H NMR spectra of the major product (scheme 16) without (above) and with (below) $^{3}J_{H,H}$ coupling between H_C and $H_{O\text{-}H}$ ($CDCl_3$, 500 MHz).

^{1}H-^{1}H NOESY experiments were performed for both isomers (Fig. 13). Important correlations $H_{O\text{-}H}$-$H_{D/E}$ and H_C-$H_{D/E}$ were observed clearly for the major product in DMSO-d_6, indicating that it is indeed isomer **44**. Correlations between ^{1}H NMR signals near 4.25 ppm for the minor isomer could not be resolved via ^{1}H-^{1}H COSY. Thus, a ^{1}H-^{13}C HSQC experiment was performed to determine ^{13}C NMR peak assignments. Subsequently, a ^{1}H-^{13}C HMBC experiment was performed to determine ^{1}H NMR peak assignments (Appendix). Among two ambiguous ^{1}H 2H singlets, the one that correlated with the ^{13}C NMR peak of A was assigned to H_B, while the other that did not, was assigned to H_C. In accordance with these peak assignments, the ^{1}H-^{1}H NOESY spectrum of the minor isomer revealed a clear H_B-$H_{D/E}$ correlation, corroborating its identity as isomer **45**.

Owing to the low yield of **44** (27%), attempts to optimize the transformation of **39** to **44** were made (Scheme 17). Accordingly, the base, reaction temperature, and reaction duration were varied (Table 1).

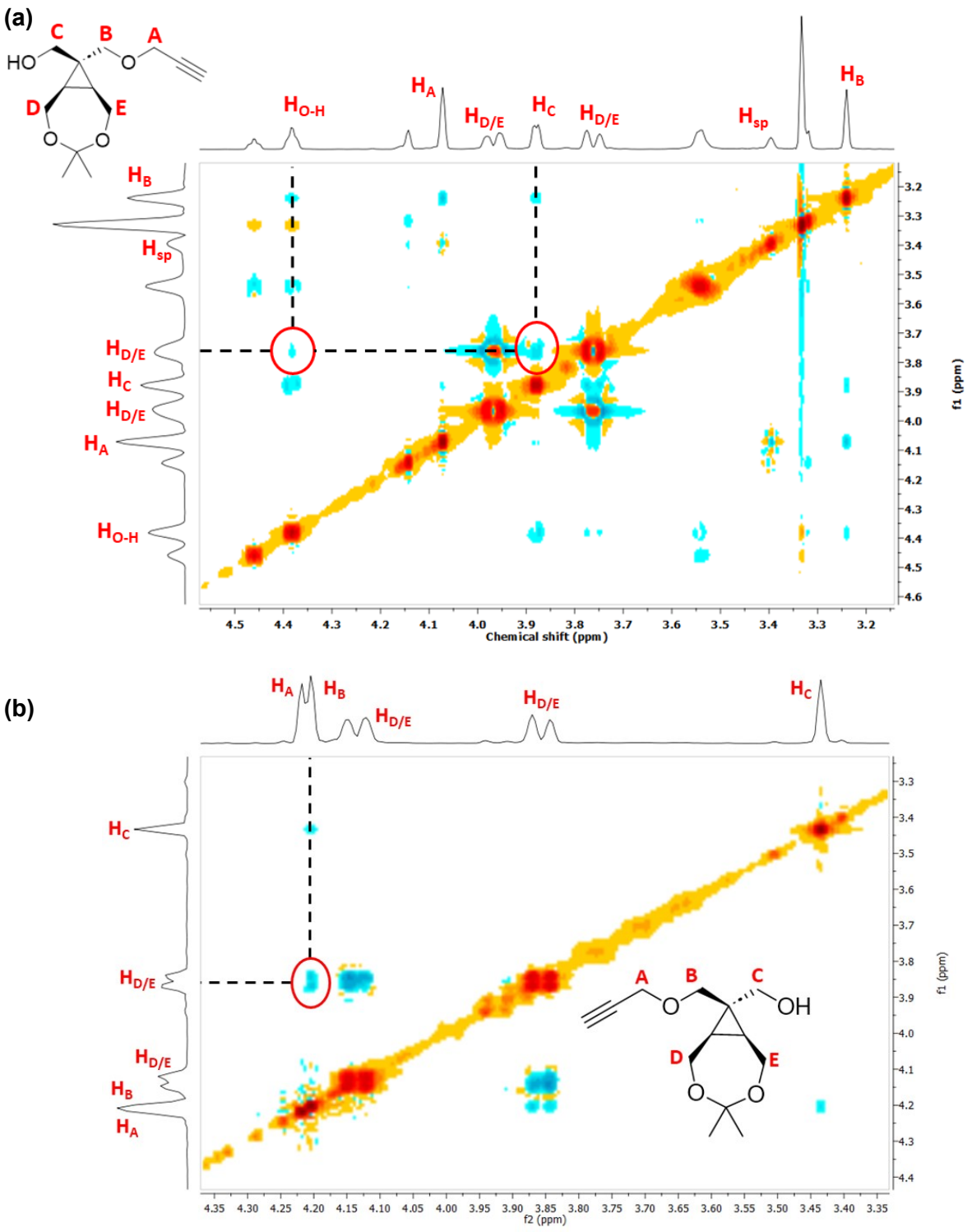

Figure 13: NOESY experiments to distinguish isomers **44** and **45**. **(a)** NOESY spectrum of major isomer **44**. **(b)** NOESY spectrum of minor isomer **45**.

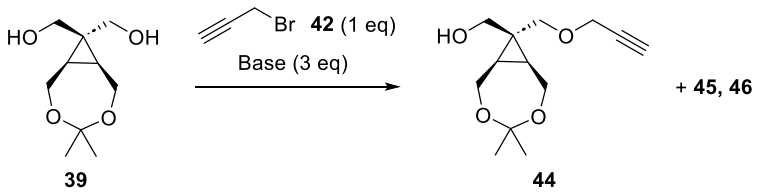

Scheme 17: General scheme for optimization of the transformation of **39** to **44**.

Base	Solvent	Duration (h)	Temp. (°C)	Yield (%)	*de* (approx., %)
KOH	DMF	3	0 → r.t.	27	68
tBuOK	DMF	1	0 → r.t.	30	66
KHMDS	THF	3	-78	23	80
Cs_2CO_3	DMF	4	0 → r.t.	N/A	N/A

Table 1: Conditions used for optimization of the transformation of **39** to **44**. Diastereomeric excess (*de*) of **44** was calculated w.r.t its diastereomer **45**.

3 equivalents of base were used for all attempts. In each case, complete consumption of educt **39** was confirmed via TLC. Although it resulted in a low yield, the alkylation was robust over several repeats with KOH as the base.

A change of base to potassium *tert*-butoxide provided a yield and *de* similar to that with KOH, with a shorter reaction duration of 1 h. Using KHMDS at -78 °C resulted in no significant improvements. Finally, the crude weight upon workup of the alkylation with cesium carbonate was deemed insufficient for purification; the crude product was thus discarded in this case. Thus, alkylating **39** using tBuOK in DMF over 1 h was the best out of the tested options.

With the cyclopropane core established with 1 *trans* and 3 *cis*-oriented arms, the idea was to then install short linkers to the 3 *cis* arms on **44**, followed by attachment of catechols, to complete the synthesis of the tris(catecholate) siderophore. Thus, in a manner similar to the synthesis of **24** from **19** (Scheme 7), the ring ketal on **44** was first hydrolysed to generate the triol **47**. As a crude product, **47** was coupled to Boc-β-Ala-OH **23** using EDC.HCl as a coupling reagent, catalysed by DMAP, and in the presence of NEt_3 as a base, to yield the protected triamine **48**. Deprotection of **48** by TFA afforded the triamine **49** (Scheme 18)

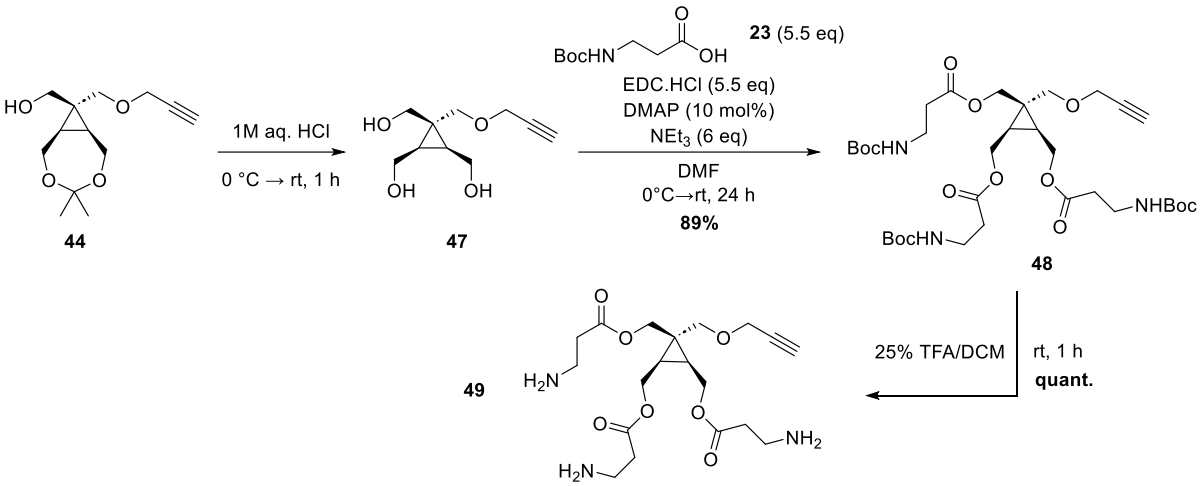

Scheme 18: Hydrolysis of **44** to triol **47**, esterification of **47** with Boc-β-Ala-OH **23** to protected triamine **48** and subsequent deprotection to triamine **49**.

49 was then coupled to acid chloride **28** (Scheme 19) in a manner similar to that in Scheme 9. However, this coupling was complete in a shorter duration, and with an improved yield compared to that in Scheme 9. Most importantly, the fully acetylated tris(catecholate) siderophore **50** was isolated.

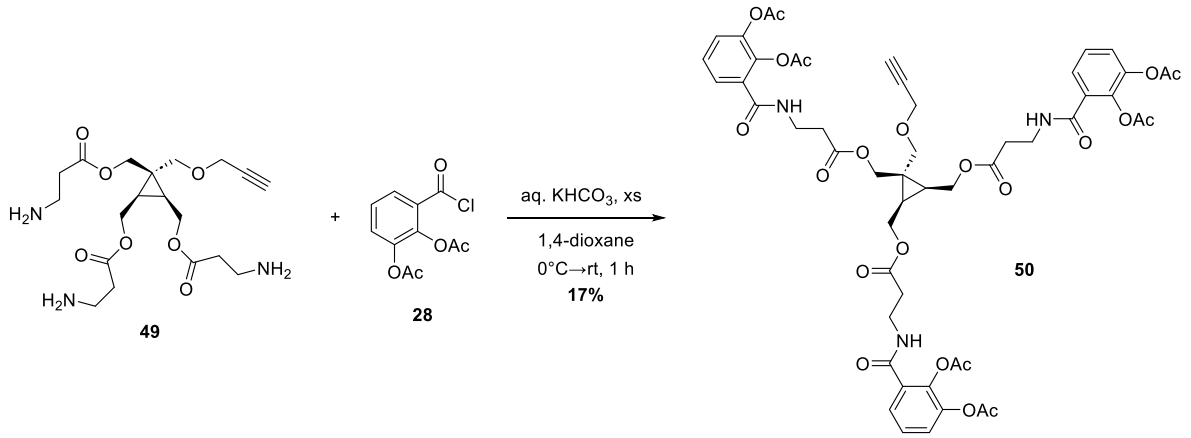

Scheme 19: Schotten-Baumann amide coupling of **49** with **28** to yield tris(catecholate) cyclopropane-based siderophore **50**.

To enable a study of the effect of acetylation of the siderophore catechols on iron binding and uptake in bacteria, **50** was hydrolysed using NEt_3 to afford **51**, its fully de-acetylated derivative (Scheme 20).

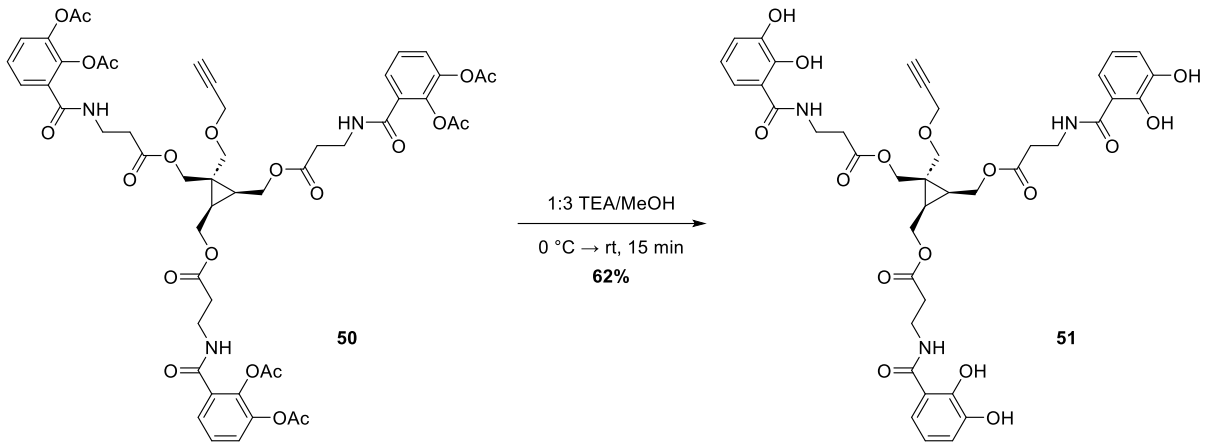

Scheme 20: De-acetylation of siderophore **50** using NEt_3 to afford fully de-acetylated siderophore **51**.

Ampicillin was the first choice of antibiotic for conjugation to **50** primarily since: it a) is active against numerous strains of Gram-negative bacteria, b) is commercially available and inexpensive, c) is amenable to functionalization, and d) has its target enzyme transpeptidase accessible from the periplasm.

The plan was to conjugate the siderophore to the antibiotic via Cu(I)-catalysed Azide Alkyne Cycloaddition (CuAAC). While the alkyne was installed on the siderophore, the azide had to be installed on Ampicillin. Thus, commercially available 3-bromopropanoic acid **52** was treated with sodium azide to afford 3-azidopropanoic acid **53**. This was then used to functionalize Ampicillin **54** via amide coupling, i.e., by first treating **53** with IBCF in the presence of NMM as a base to convert it into the active ester **55**, which was then coupled with **54** to yield functionalized Ampicillin **56** (Scheme 21).

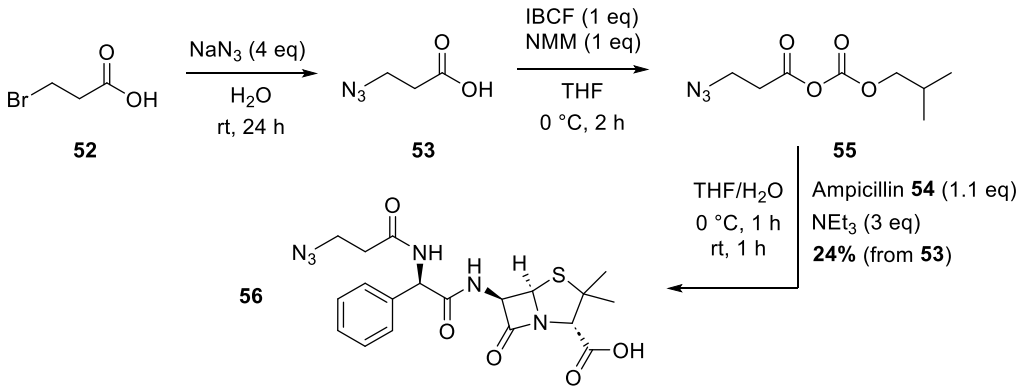

Scheme 21: Azidation of **52** to **53**, activation of **53** by IBCF to active ester **55**, and amide coupling of **55** with Ampicillin **54** to afford functionalized Ampicillin **56**.

Then, azide **56** was conjugated to alkyne **50** via CuAAC, i.e., using $CuSO_4.5H_2O$ as a source of Cu (II) for catalysis, sodium ascorbate as a reducing agent to generate catalytically active Cu(I), and THPTA as a ligand to retain Cu(I) availability for catalysis. The siderophore-antibiotic conjugate (SAC) **57** was thus isolated (Scheme 22).

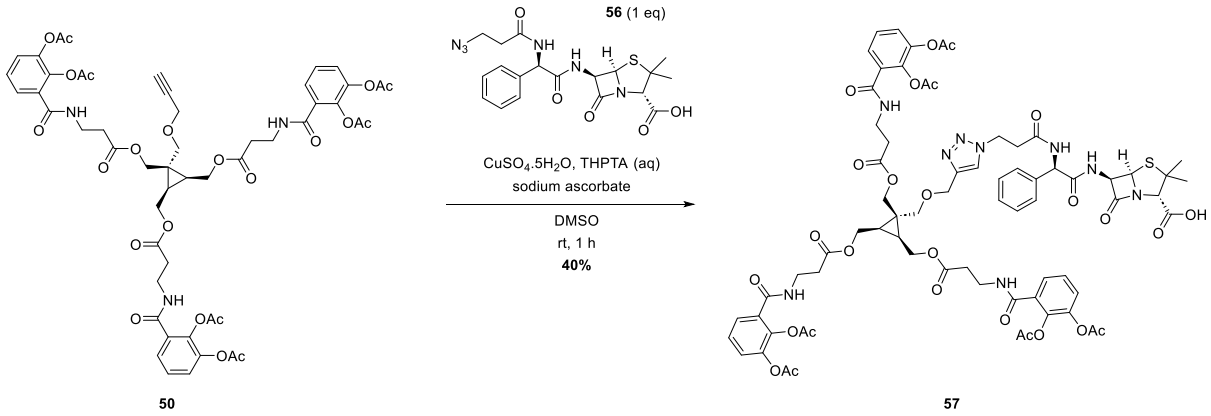

Scheme 22: Conjugation of **50** with **56** via CuAAC to afford SAC **57**.

In order to conjugate **50** to another antibiotic, Amoxicillin **58** was chosen, for similar reasons as above, and additionally since it had previously been conjugated to siderophores via CuAAC. To functionalize **58** with an azide moiety, **53** was treated with IBCF in the presence of NMM as a base to convert it into the active ester **55**, which was then coupled with **58** to yield functionalized Amoxicillin **59** (Scheme 23).

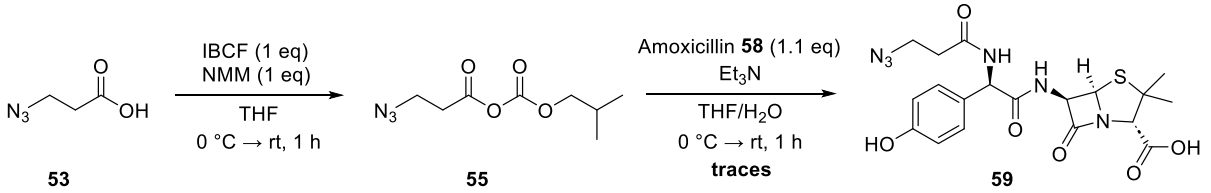

Scheme 23: Activation of **53** by IBCF to active ester **55**, and amide coupling of **55** with Amoxicillin **58** to afford functionalized Amoxicillin **59**.

Since the yield of **59** was negligible, a different route was attempted subsequently. **53** was treated with HATU as a coupling reagent and DIPEA as a base, followed by **58** (Scheme 24). The desired amide **59** could be detected only in traces, therefore conjugation to **58** was abandoned.

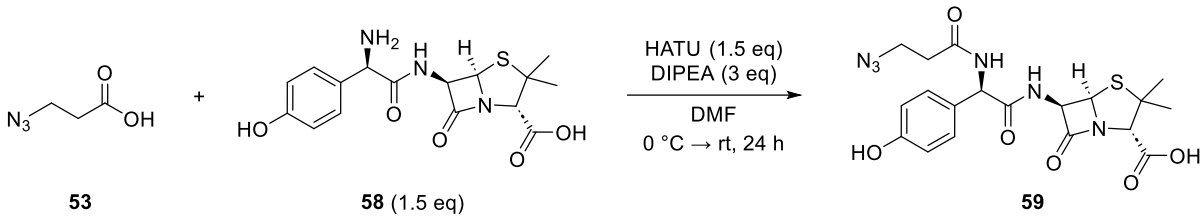

53 **58** (1.5 eq) **59**

Scheme 24: Attempted HATU amide coupling of **53** and **58** to amide **59** in the presence of DIPEA.

The siderophores **30**, **50** and **51** synthesized thus far include linkers between catechols and the cyclopropyl core containing ester groups. These are inherently prone to cleavage by esterases in the context of bacterial cells. These siderophores were thus designed and synthesized for an initial proof-of-concept, i.e., to probe iron binding, bacterial uptake and antibacterial activity in preliminary experiments.

Accordingly, in an effort to circumvent the potential esterase-mediated cleavage, a siderophore including linkers containing ether groups was envisioned (Scheme 25).

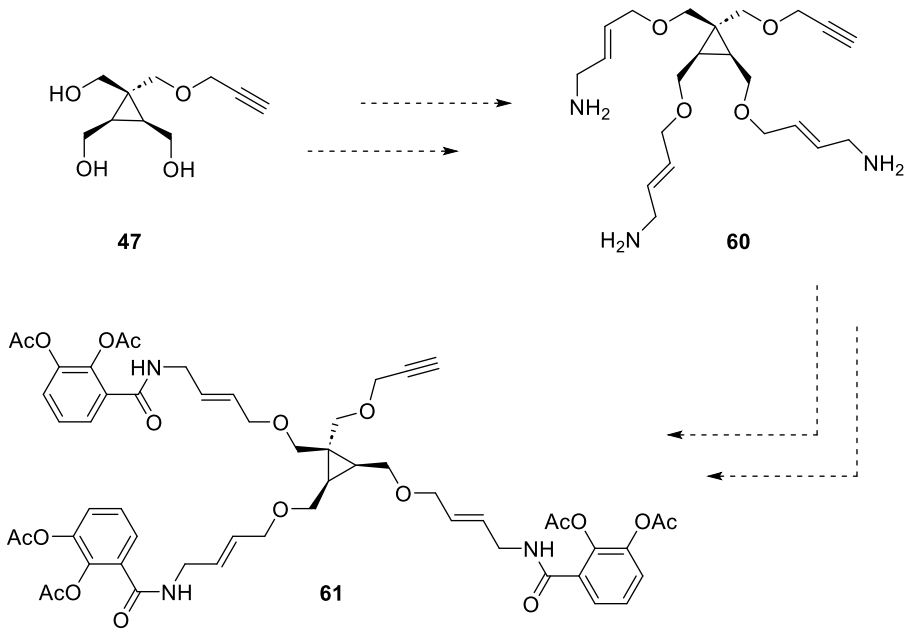

47 **60** **61**

Scheme 25: Plan to synthesize siderophore **61** including linkers containing ether groups, from **47** via intermediate **60**.

The plan was to install these ether-based linkers onto **47** via a Williamson ether synthesis. The instability of **47** necessitated the usage of an activated halide for this purpose—an allyl bromide, for instance.

Thus, (*E*)-1,4-dibromobut-2-ene **62** was used to alkylate *tert*-butyl carbamate **63** (both commercially available) to yield *tert*-butyl (*E*)-(4-bromobut-2-en-1-yl)carbamate **64** via two methods: using (a) K_3PO_4 as a base and *n*-Bu_4NBr as a phase-transfer catalyst, and (b) using NaH as a base (Scheme 26, Table 2).

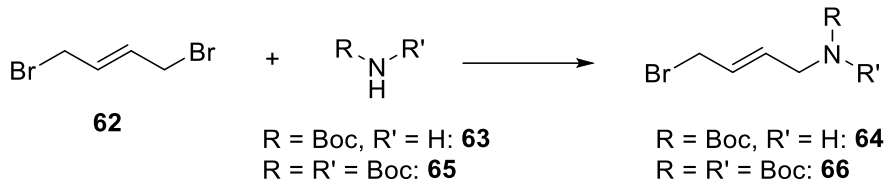

Scheme 26: Synthesis of halide precursors **64** and **66** for ether-based linkers via alkylation of **63** and **65** using dibromide **62**.

The yields of alkylated amine **64** obtained were deemed insufficient—13% and 15% respectively, prompting a change in the choice of halide. Thus, **62** was treated with commercially available di-*tert*-butyl iminodicarbonate **65** using cesium carbonate as a base to afford *tert*-butyl (*E*)-(4-bromobut-2-en-1-yl)(*tert*-butoxycarbonyl)carbamate **66** in 60% yield (Scheme 26, Table 2).

R, R’	Eq. of 62 added	Reagents	Solvent	Duration (h)	Temp. (°C)	Yield (%)
Boc, H	3	K_3PO_4, *n*-Bu_4NBr	MeCN	18	50	13
Boc, H	3	NaH	THF	18	r.t.	15
Boc, Boc	5	Cs_2CO_3	DMF	18	r.t.	60

Table 2: Summary of alkylation reactions performed to afford compounds **64** and **66**.

Then, triol **47** was treated with halide precursor **66** in the presence of NaH as a base in DMF. However, although the tri-ether **67** could be detected in the reaction mixture, it could not be isolated (Scheme 27). This reaction is currently being optimized.

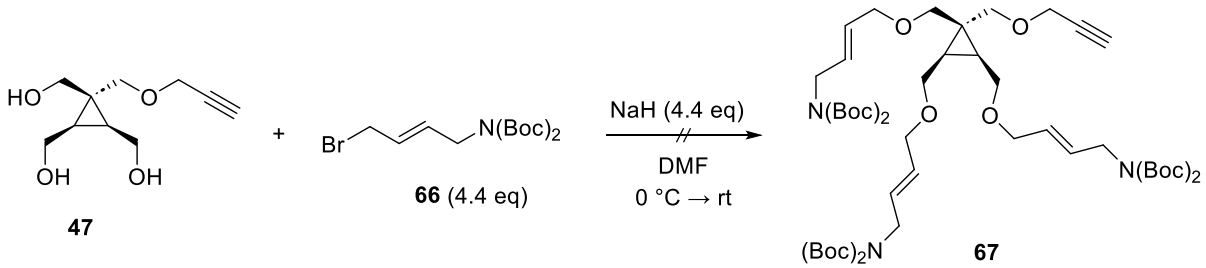

Scheme 27: Attempted Williamson ether synthesis between **47** and **66** to yield tri-ether **67**.

3.2. CAS Assay to Evaluate Fe(III) Binding Ability

Upon equilibration after 24 h in the dark, the Fe(CAS) solutions prepared and inoculated with compounds **30**, **50**, **51** and **57** displayed varied results (Fig. 14). Fully de-acetylated siderophore **51** resulted in the largest reduction in absorbance at 630 nm among the four tested compounds, which was nearly identical to that produced by the positive control, enterobactin. Thus **51** is able to chelate ferric ions. This result may be rationalized by the complete availability of all 6 phenolates for chelation to Fe(III). Fully acetylated siderophore **50** and its corresponding ampicillin conjugate **57** resulted in a moderate absorbance reduction when compared to enterobactin and DMSO, the negative control. In the context of the tested compounds, this points to a moderate ability of **50** and **57** to chelate Fe(III). Two important interpretations arise: (a) The masking of phenolates in siderophores by acetylation partially reduces their ability to chelate Fe(III), corresponding to a reduced availability of the phenolate O for binding, and (b) a similarity in results for **50** and **57** indicates that conjugation to ampicillin does not affect the iron-binding ability of these siderophores. Finally, fully de-acetylated siderophore **30** resulted in a minimal absorbance reduction. This was not anticipated, since it is a siderophore with three free catecholates. This anomaly may be attributed to either (a) an error in preparation of the stock solution of **30**, or (b) an error in pipetting the stock solution of **30** into the wells of the assay plate.

(a)

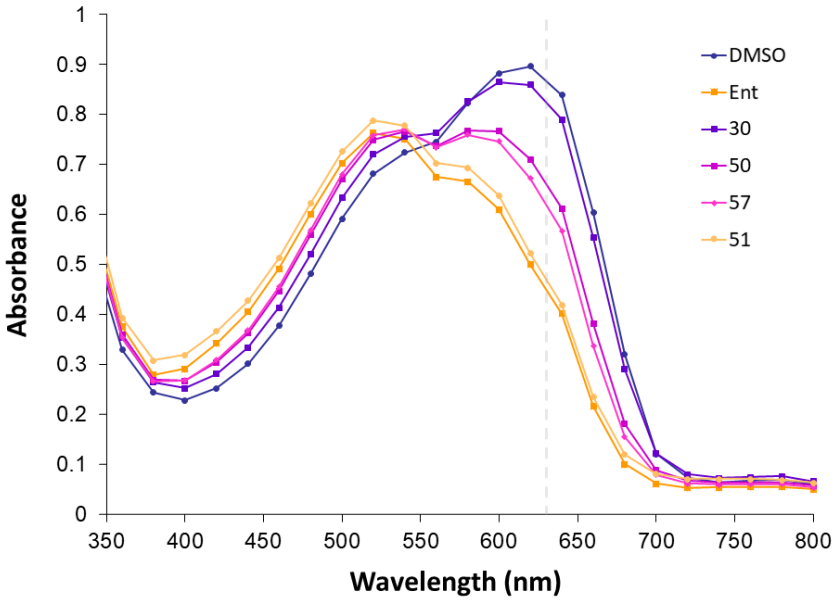

(b)

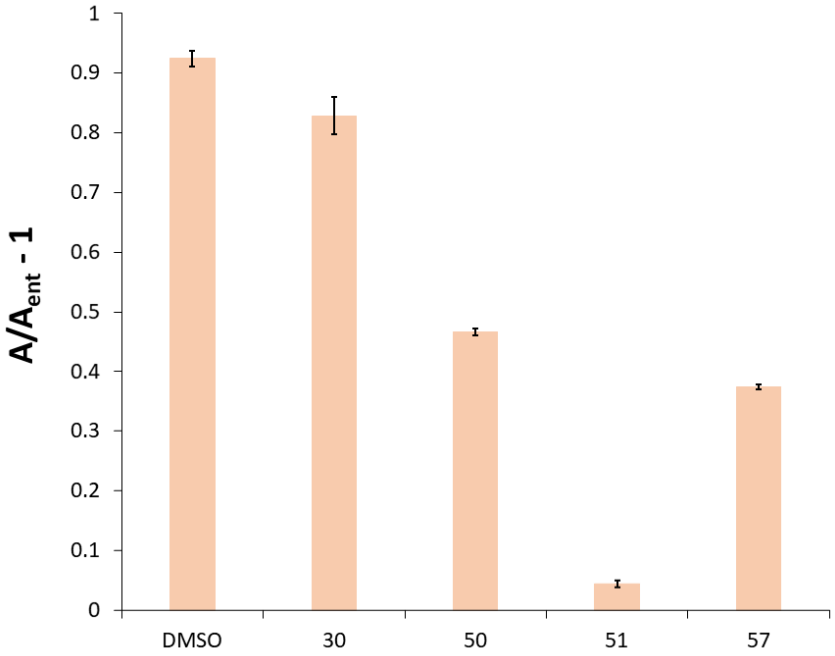

Figure 14: A study of the iron-binding ability of siderophores using the CAS assay. (a) Absorption spectra of a Fe(III)-CAS solution upon equilibration with tested compounds, DMSO (-ve control), and enterobactin (+ve control). (b) A comparison of the iron-binding ability of tested compounds (A = absorbance with compound, A_{ent} = absorbance with enterobactin). Error bars represent standard deviation of 8 replicates.

4. Conclusions

In accordance with the initial objective, 1,1,2,3-tetrasubstituted, cyclopropane-based artificial siderophores **30** and **50** were synthesized. Siderophore **30** was not pursued further due to low yields in the preceding steps to this compound. A de-acetylated derivative **51** of siderophore **50** was prepared to enable studies of the influence of catechol acetylation on iron binding, antibacterial activity and bacterial uptake. While siderophore **50** was conjugated to ampicillin to yield SAC **57**, its conjugation to amoxicillin could not be achieved. In an effort to circumvent the potential esterase-mediated cleavage of siderophores containing ester groups, precursor compounds towards ether group-based linkers for these siderophores were synthesized. Owing to time constraints, the synthesis along this route remains incomplete. The ability of the synthesized siderophores to form stable complexes with Fe(III) was evaluated and compared in a qualitative manner via a CAS-based colorimetric assay.

As part of initial efforts towards microbiological characterization, these compounds were tested for their ability to (a) aid growth recovery of Δ*entA E. coli* (enterobactin deletion mutant) in iron-deficient conditions, and (b) determine their minimum inhibitory concentrations (MICs) in Δ*entA E. coli* in iron-deficient conditions, both by Felix Schwenke. The MIC of SAC **57** was found to be 0.60 μM—enhanced appreciably compared to that of free ampicillin, which exhibited a MIC of 13.46 μM.

5. References

(1) Ikuta *et al.* Global Mortality Associated with 33 Bacterial Pathogens in 2019: A Systematic Analysis for the Global Burden of Disease Study 2019. *Lancet* **2022**, *400* (10369), 2221–2248.

(2) Perry, J.; Waglechner, N.; Wright, G. The Prehistory of Antibiotic Resistance. *Cold Spring Harb. Perspect. Med.* **2016**, *6* (6), a025197.

(3) *A Scientific Roadmap for Antibiotic Discovery*. http://pew.org/26ZYUqA (accessed 2024-02-11).

(4) World Health Organization. WHO Report on Surveillance of Antibiotic Consumption: 2016-2018 Early Implementation; World Health Organization: Geneva, 2018.

(5) Pulingam, T.; Parumasivam, T.; Gazzali, A. M.; Sulaiman, A. M.; Chee, J. Y.; Lakshmanan, M.; Chin, C. F.; Sudesh, K. Antimicrobial Resistance: Prevalence, Economic Burden, Mechanisms of Resistance and Strategies to Overcome. *Eur. J. Pharm. Sci.* **2022**, *170*, 106103.

(6) Murray, C. J. L. *et al.* Global Burden of Bacterial Antimicrobial Resistance in 2019: A Systematic Analysis. *Lancet* **2022**, *399* (10325), 629–655.

(7) O'Neill, J. *Tackling Drug-Resistant Infections Globally: Final Report and Recommendations*; Report; Government of the United Kingdom, 2016. https://apo.org.au/node/63983 (accessed 2024-02-11).

(8) Tacconelli, E. *et al.* Discovery, Research, and Development of New Antibiotics: The WHO Priority List of Antibiotic-Resistant Bacteria and Tuberculosis. *Lancet Infect. Dis.* **2018**, *18* (3), 318–327.

(9) Ventola, C. L. The Antibiotic Resistance Crisis. *Pharm. Ther.* **2015**, *40* (4), 277–283.

(10) Palmer, K. L.; Kos, V. N.; Gilmore, M. S. Horizontal Gene Transfer and the Genomics of Enterococcal Antibiotic Resistance. *Curr. Opin. Microbiol.* **2010**, *13* (5), 632–639.

(11) Kell, D. B.; Pretorius, E. On the Translocation of Bacteria and Their Lipopolysaccharides between Blood and Peripheral Locations in Chronic, Inflammatory Diseases: The Central Roles of LPS and LPS-Induced Cell Death. *Integr. Biol.* **2015**, *7* (11), 1339–1377.

(12) Whittle, E. E.; McNeil, H. E.; Trampari, E.; Webber, M.; Overton, T. W.; Blair, J. M. A. Efflux Impacts Intracellular Accumulation Only in Actively Growing Bacterial Cells. *mBio* **2021**, *12* (5), e02608-21.

(13) Wong, J. L. C.; Romano, M.; Kerry, L. E.; Kwong, H.-S.; Low, W.-W.; Brett, S. J.; Clements, A.; Beis, K.; Frankel, G. OmpK36-Mediated Carbapenem Resistance Attenuates ST258 Klebsiella Pneumoniae in Vivo. *Nat. Commun.* **2019**, *10* (1), 3957.

(14) Fernández, L.; Hancock, R. E. W. Adaptive and Mutational Resistance: Role of Porins and Efflux Pumps in Drug Resistance. *Clin. Microbiol. Rev.* **2012**, *25* (4), 661–681.

(15) Lou, H.; Chen, M.; Black, S. S.; Bushell, S. R.; Ceccarelli, M.; Mach, T.; Beis, K.; Low, A. S.; Bamford, V. A.; Booth, I. R.; Bayley, H.; Naismith, J. H. Altered Antibiotic Transport in OmpC Mutants Isolated from a Series of Clinical Strains of Multi-Drug Resistant E. Coli. *PLOS ONE* **2011**, *6* (10), e25825.

(16) Nazarov, P. A. MDR Pumps as Crossroads of Resistance: Antibiotics and Bacteriophages. *Antibiotics* **2022**, *11* (6), 734.

(17) Darby, E. M.; Trampari, E.; Siasat, P.; Gaya, M. S.; Alav, I.; Webber, M. A.; Blair, J. M. A. Molecular Mechanisms of Antibiotic Resistance Revisited. *Nat. Rev. Microbiol.* **2023**, *21* (5), 280–295.

(18) Wright, G. Bacterial Resistance to Antibiotics: Enzymatic Degradation and Modification. *Adv. Drug Deliv. Rev.* **2005**, *57* (10), 1451–1470.

(19) Schaenzer, A. J.; Wright, G. D. Antibiotic Resistance by Enzymatic Modification of Antibiotic Targets. *Trends Mol. Med.* **2020**, *26* (8), 768–782.

(20) Then, R. L. Mechanisms of Resistance to Trimethoprim, the Sulfonamides, and Trimethoprim-Sulfamethoxazole. *Clin. Infect. Dis.* **1982**, *4* (2), 261–269.

(21) Koteva, K.; Cox, G.; Kelso, J. K.; Surette, M. D.; Zubyk, H. L.; Ejim, L.; Stogios, P.; Savchenko, A.; Sørensen, D.; Wright, G. D. Rox, a Rifamycin Resistance Enzyme with an Unprecedented Mechanism of Action. *Cell Chem. Biol.* **2018**, *25* (4), 403-412.e5.

(22) Yasir, M.; Turner, A. K.; Bastkowski, S.; Baker, D.; Page, A. J.; Telatin, A.; Phan, M.-D.; Monahan, L.; Savva, G. M.; Darling, A.; Webber, M. A.; Charles, I. G. TraDIS-Xpress: A High-Resolution Whole-Genome Assay Identifies Novel Mechanisms of Triclosan Action and Resistance. *Genome Res.* **2020**, *30* (2), 239–249.

(23) Smith, W. P. J.; Wucher, B. R.; Nadell, C. D.; Foster, K. R. Bacterial Defences: Mechanisms, Evolution and Antimicrobial Resistance. *Nat. Rev. Microbiol.* **2023**, 1–16.

(22) Miethke, M.; Marahiel, M. A. Siderophore-Based Iron Acquisition and Pathogen Control. *Microbiol. Mol. Biol. Rev.* **2007**, *71* (3), 413–451.

(25) Andreini, C.; Bertini, I.; Cavallaro, G.; Holliday, G. L.; Thornton, J. M. Metal Ions in Biological Catalysis: From Enzyme Databases to General Principles. *J. Biol. Inorg. Chem.* **2008**, *13* (8), 1205–1218.

(26) Hider, R. C.; Kong, X. Chemistry and Biology of Siderophores. *Nat. Prod. Rep.* **2010**, *27* (5), 637.

(27) Behnsen, J.; Raffatellu, M. Siderophores: More than Stealing Iron. *mBio* **2016**, *7* (6), e01906-16.

(28) Weinberg, E. D. Nutritional Immunity: Host's Attempt to Withhold Iron From Microbial Invaders. *JAMA* **1975**, *231* (1), 39–41.

(29) Sheldon, J. R.; Laakso, H. A.; Heinrichs, D. E. Iron Acquisition Strategies of Bacterial Pathogens. *Microbiol. Spectr.* **2016**, *4* (2), 4.2.05.

(30) Schalk, I. J. Metal Trafficking via Siderophores in Gram-Negative Bacteria: Specificities and Characteristics of the Pyoverdine Pathway. *J. Inorg. Biochem.* **2008**, *102* (5), 1159–1169.

(31) Hood, M. I.; Skaar, E. P. Nutritional Immunity: Transition Metals at the Pathogen–Host Interface. *Nat. Rev. Microbiol.* **2012**, *10* (8), 525–537.

(32) Noinaj, N.; Guillier, M.; Barnard, T. J.; Buchanan, S. K. TonB-Dependent Transporters: Regulation, Structure, and Function. *Annu. Rev. Microbiol.* **2010**, *64* (1), 43–60.

(33) Ferreira, K.; Hu, H.-Y.; Fetz, V.; Prochnow, H.; Rais, B.; Müller, P. P.; Brönstrup, M. Multivalent Siderophore–DOTAM Conjugates as Theranostics for Imaging and Treatment of Bacterial Infections. *Angew. Chem. Int. Ed.* **2017**, *56* (28), 8272–8276.

(34) Fritsch, S.; Gasser, V.; Peukert, C.; Pinkert, L.; Kuhn, L.; Perraud, Q.; Normant, V.; Brönstrup, M.; Schalk, I. J. Uptake Mechanisms and Regulatory Responses to MECAM- and DOTAM-Based Artificial Siderophores and Their Antibiotic Conjugates in *Pseudomonas Aeruginosa*. *ACS Infect. Dis.* **2022**, *8* (6), 1134–1146.

(35) Peukert, C.; Gasser, V.; Orth, T.; Fritsch, S.; Normant, V.; Cunrath, O.; Schalk, I. J.; Brönstrup, M. Trojan Horse Siderophore Conjugates Induce *Pseudomonas Aeruginosa* Suicide and Qualify the TonB Protein as a Novel Antibiotic Target. *J. Med. Chem.* **2023**, *66* (1), 553–576.

(36) Ghosh, M.; Miller, P. A.; Möllmann, U.; Claypool, W. D.; Schroeder, V. A.; Wolter, W. R.; Suckow, M.; Yu, H.; Li, S.; Huang, W.; Zajicek, J.; Miller, M. J. Targeted Antibiotic Delivery: Selective Siderophore Conjugation with Daptomycin Confers Potent Activity against Multidrug Resistant Acinetobacter Baumannii Both in Vitro and in Vivo. *J. Med. Chem.* **2017**, *60* (11), 4577–4583.

(37) Pinkert, L.; Lai, Y.-H.; Peukert, C.; Hotop, S.-K.; Karge, B.; Schulze, L. M.; Grunenberg, J.; Brönstrup, M. Antibiotic Conjugates with an Artificial MECAM-Based Siderophore Are Potent Agents against Gram-Positive and Gram-Negative Bacterial Pathogens. *J. Med. Chem.* **2021**, *64* (20), 15440–15460.

(38) Peukert, C.; Rox, K.; Karge, B.; Hotop, S.-K.; Brönstrup, M. Synthesis and Characterization of DOTAM-Based Sideromycins for Bacterial Imaging and Antimicrobial Therapy. *ACS Infect. Dis.* **2023**, *9* (2), 330–341.

(39) Zhao, S.; Wang, Z.-P.; Lin, Z.; Wei, G.; Wen, X.; Li, S.; Yang, X.; Zhang, Q.; Jing, C.; Dai, Y.; Guo, J.; He, Y. Drug Repurposing by Siderophore Conjugation: Synthesis and Biological Evaluation of Siderophore-Methotrexate Conjugates as Antibiotics. *Angew. Chem. Int. Ed.* **2022**, *61* (36), e202204139.

(40) Zähner, H.; Diddens, H.; Keller-Schierlein, W.; Nägeli, H. U. Some Experiments with Semisynthetic Sideromycins. *Jpn. J. Antibiot.* **1977**, *30 Suppl*, 201–206.

(41) Miller, M. J.; Malouin, F. Microbial Iron Chelators as Drug Delivery Agents: The Rational Design and Synthesis of Siderophore-Drug Conjugates. *Acc. Chem. Res.* **1993**, *26* (5), 241–249.

(42) Negash, K. H.; Norris, J. K. S.; Hodgkinson, J. T. Siderophore–Antibiotic Conjugate Design: New Drugs for Bad Bugs? *Molecules* **2019**, *24* (18), 3314.

(43) Ohi, N.; Aoki, B.; Shinozaki, T.; Moro, K.; Noto, T.; Nehashi, T.; Okazaki, H.; Matsunaga, I. Semisynthetic β-Lactam Antibiotics I. Synthesis and Antibacterial Activity of New Ureidopenicillin Derivatives Having Catechol Moieties. *J. Antibiot. (Tokyo)* **1986**, *39* (2), 230–241.

(44) Cefiderocol: Discovery, Chemistry, and In Vivo Profiles of a Novel Siderophore Cephalosporin | Clinical Infectious Diseases | Oxford Academic. https://academic.oup.com/cid/article/69/Supplement_7/S538/5624004 (accessed 2024-02-13).

(45) Heinisch, L.; Wittmann, S.; Stoiber, T.; Hofmann, I.; Dr. Ankel-Fuchs, D.; Möllmann, U. Synthesis and Biological Activity of Trisand Tetrakiscatecholate Siderophores Based on Poly-Aza Alkanoic Acids or Alkylbenzoic Acids and Their Conjugates with β-Lactam Antibiotics. *Arzneimittelforschung.* **2003**, *53*, 188–195.

(46) Boyce, J. H.; Dang, B.; Ary, B.; Edmondson, Q.; Craik, C. S.; DeGrado, W. F.; Seiple, I. B. Platform to Discover Protease-Activated Antibiotics and Application to Siderophore-Antibiotic Conjugates. *J. Am. Chem. Soc.* **2020**, *142* (51), 21310–21321.

(47) Guo, C.; Nolan, E. M. Heavy-Metal Trojan Horse: Enterobactin-Directed Delivery of Platinum(IV) Prodrugs to Escherichia Coli. *J. Am. Chem. Soc.* **2022**, *144* (28), 12756–12768.

(48) Ji, C.; Miller, M. J. Siderophore-Fluoroquinolone Conjugates Containing Potential Reduction-Triggered Linkers for Drug Release: Synthesis and Antibacterial Activity. *BioMetals* **2015**, *28* (3), 541–551.

(49) Juárez-Hernández, R. E.; Miller, P. A.; Miller, M. J. Syntheses of Siderophore–Drug Conjugates Using a Convergent Thiol–Maleimide System. *ACS Med. Chem. Lett.* **2012**, *3* (10), 799–803.

(50) Md-Saleh, S. R.; Chilvers, E. C.; Kerr, K. G.; Milner, S. J.; Snelling, A. M.; Weber, J. P.; Thomas, G. H.; Duhme-Klair, A.-K.; Routledge, A. Synthesis of Citrate–Ciprofloxacin Conjugates. *Bioorg. Med. Chem. Lett.* **2009**, *19* (5), 1496–1498.

(51) Ghosh, M.; Miller, P. A.; Miller, M. J. Antibiotic Repurposing: Bis-Catechol- and Mixed Ligand (Bis-Catechol-Mono-Hydroxamate)-Teicoplanin Conjugates Are Active against Multidrug Resistant Acinetobacter Baumannii. *J. Antibiot. (Tokyo)* **2020**, *73* (3), 152–157.

(52) Rayner, B.; Verderosa, A. D.; Ferro, V.; Blaskovich, M. A. T. Siderophore Conjugates to Combat Antibiotic-Resistant Bacteria. *RSC Med. Chem.* **2023**, 10.1039.D2MD00465H.

(53) Schwyn, B.; Neilands, J. B. Universal Chemical Assay for the Detection and Determination of Siderophores. *Anal. Biochem.* **1987**, *160* (1), 47–56.

(54) Wiputra, F. Synthesis of Novel Cyclopropane-Based Siderophore. Master Thesis, Technisches Universität Braunschweig, Braunschweig, Germany, 2022.

(55) Baum, J. S.; Shook, D. A.; Davies, H. M. L.; Smith, H. D. Diazotransfer Reactions with P-Acetamidobenzenesulfonyl Azide. *Synth. Commun.* **1987**, *17* (14), 1709–1716.

(56) Bell-Tyrer, J. J.; Hume, P. A.; Grant, P. S.; Brimble, M. A.; Furkert, D. P. Azide–Enolate Cycloaddition-Rearrangement Enables Direct α-Amination of Amides and Enelactam Synthesis from Esters**. *Chem. Eur. J.* **2023**, *29* (31), e202300261.

(57) Peukert, C.; Langer, L. N. B.; Wegener, S. M.; Tutov, A.; Bankstahl, J. P.; Karge, B.; Bengel, F. M.; Ross, T. L.; Brönstrup, M. Optimization of Artificial Siderophores as 68Ga-Complexed PET Tracers for In Vivo Imaging of Bacterial Infections. *J. Med. Chem.* **2021**, *64* (16), 12359–12378.

(58) Pinkert, L. Synthese von Siderophor-Antibiotika-Konjugaten als neuartige antibakterielle Wirkstoffe, Gottfried Wilhelm Leibniz Universität Hannover, Braunschweig, Germany, 2020.

(59) Müller, P.; Ghanem, A. Rh(II)-Catalyzed Enantioselective Cyclopropanation of Olefins with Dimethyl Malonate via in Situ Generated Phenyliodonium Ylide. *Org. Lett.* **2004**, *6* (23), 4347–4350.

(60) Yoon, N. M.; Pak, C. S.; Brown Herbert C.; Krishnamurthy, S.; Stocky, T. P. Selective Reductions. XIX. Rapid Reaction of Carboxylic Acids with Borane-Tetrahydrofuran. Remarkably Convenient Procedure for the Selective Conversion of Carboxylic Acids to the Corresponding Alcohols in the Presence of Other Functional Groups. *J. Org. Chem.* **1973**, *38* (16), 2786–2792.

6. Appendix

Dimethyl 2-Diazomalonate (**11**)

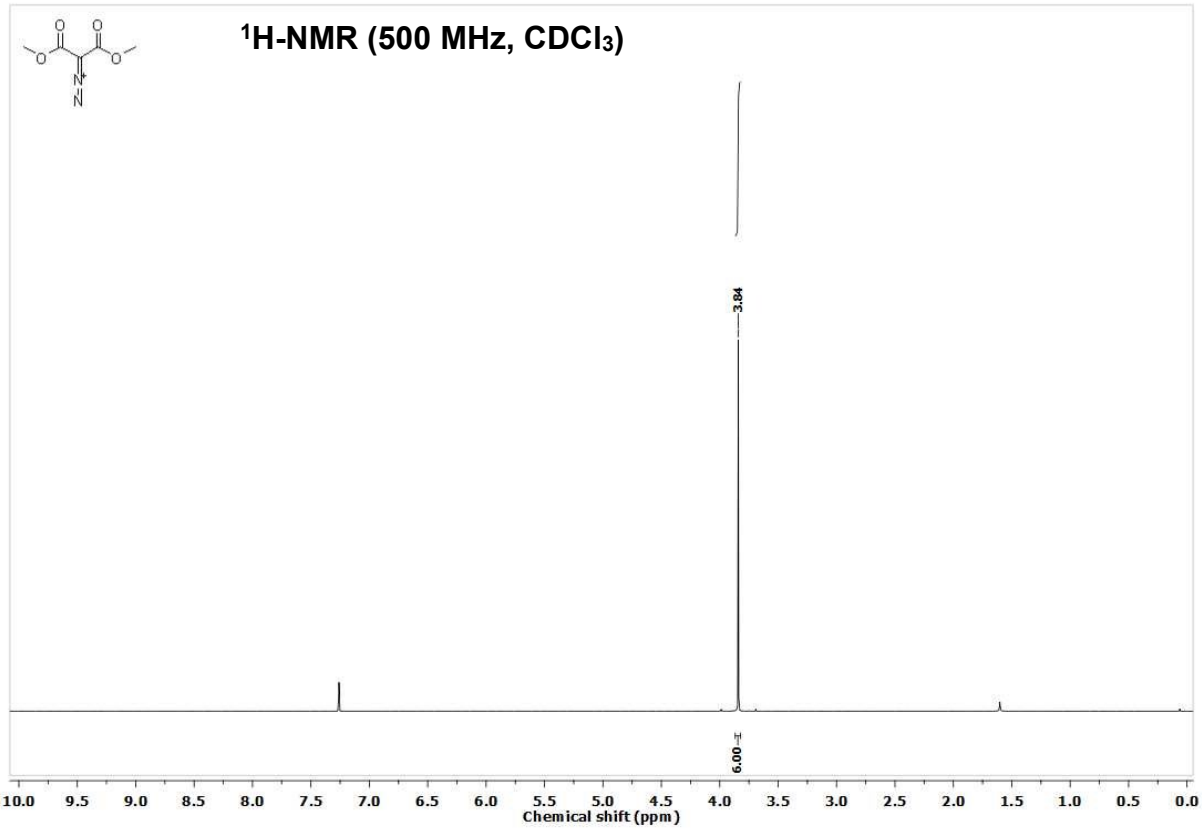

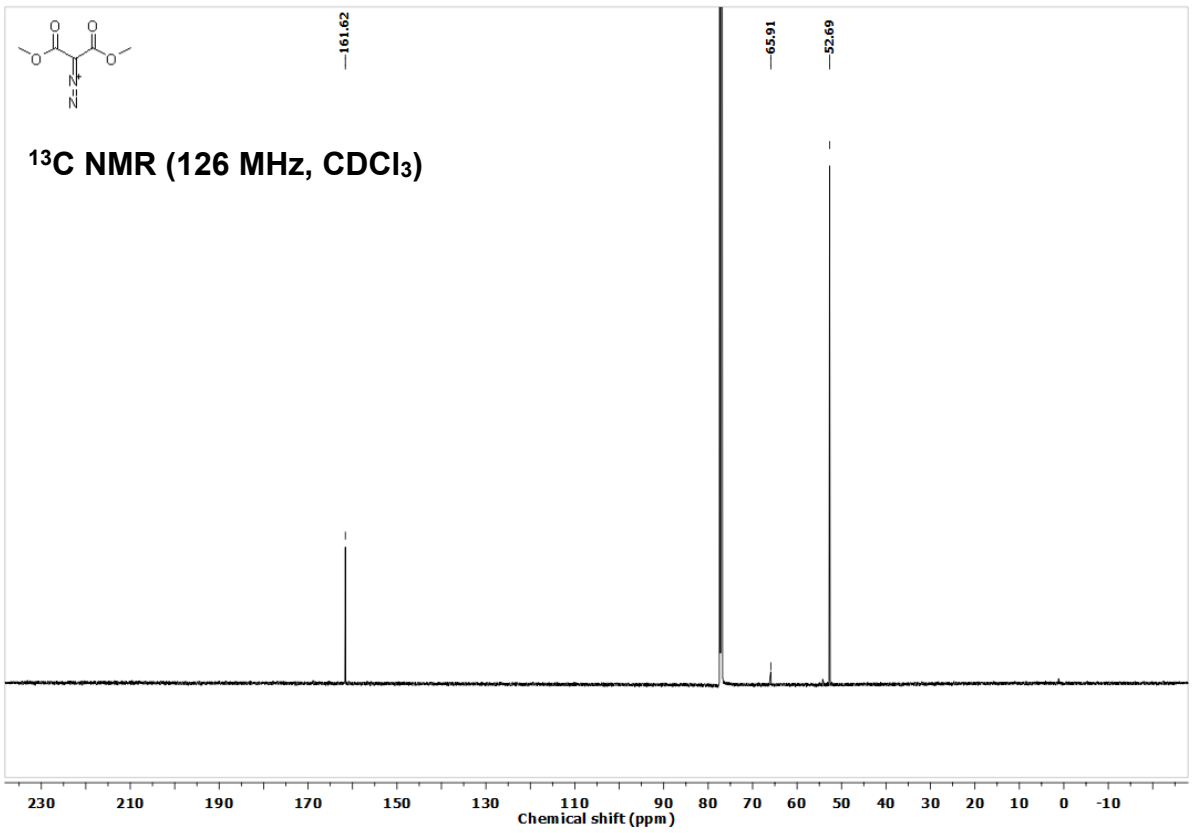

Dimethyl (1*R**,7*S**)-4,4-Dimethyl-3,5-dioxabicyclo[5.1.0]octane-8,8-dicarboxylate (**13**)

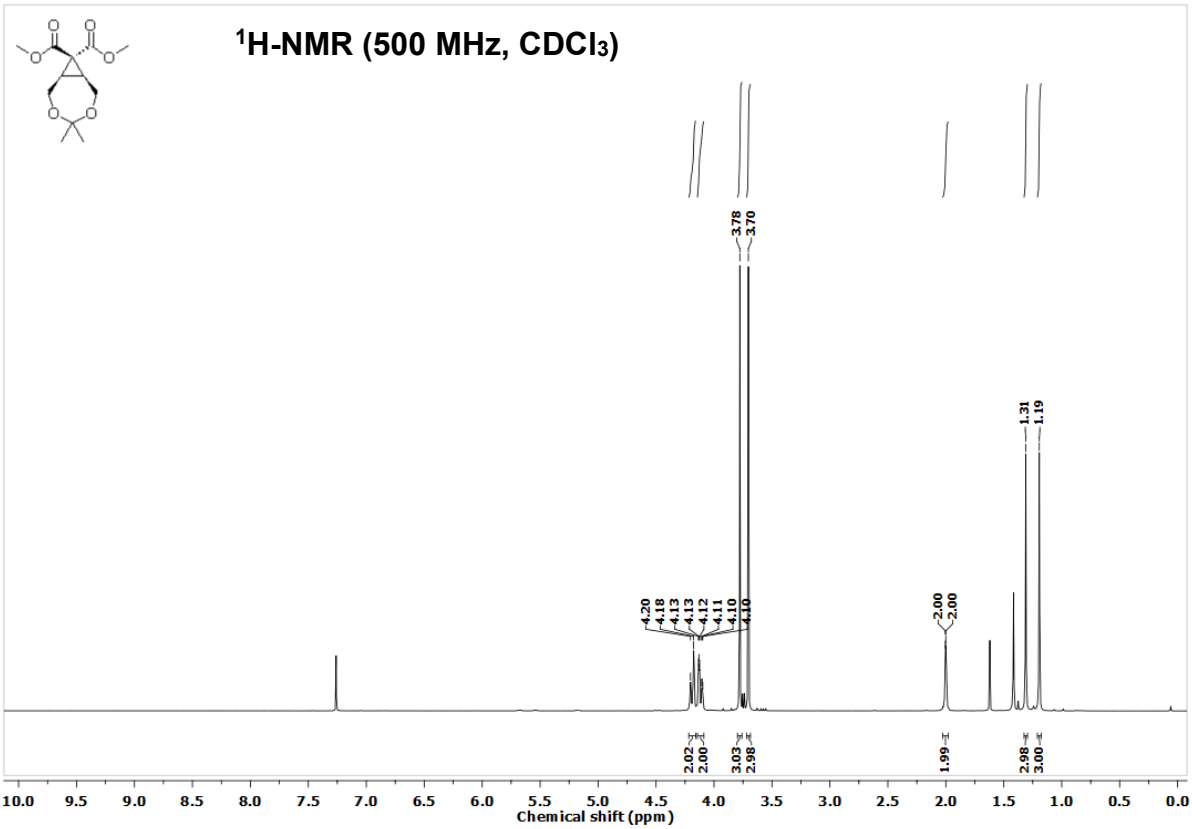

Methyl (1*R**,7*S**,8*s*)-4,4-Dimethyl-8-(Prop-2-yn-1-ylcarbamoyl)-3,5-Dioxabicyclo [5.1.0]octane-8-carboxylate (**16**)

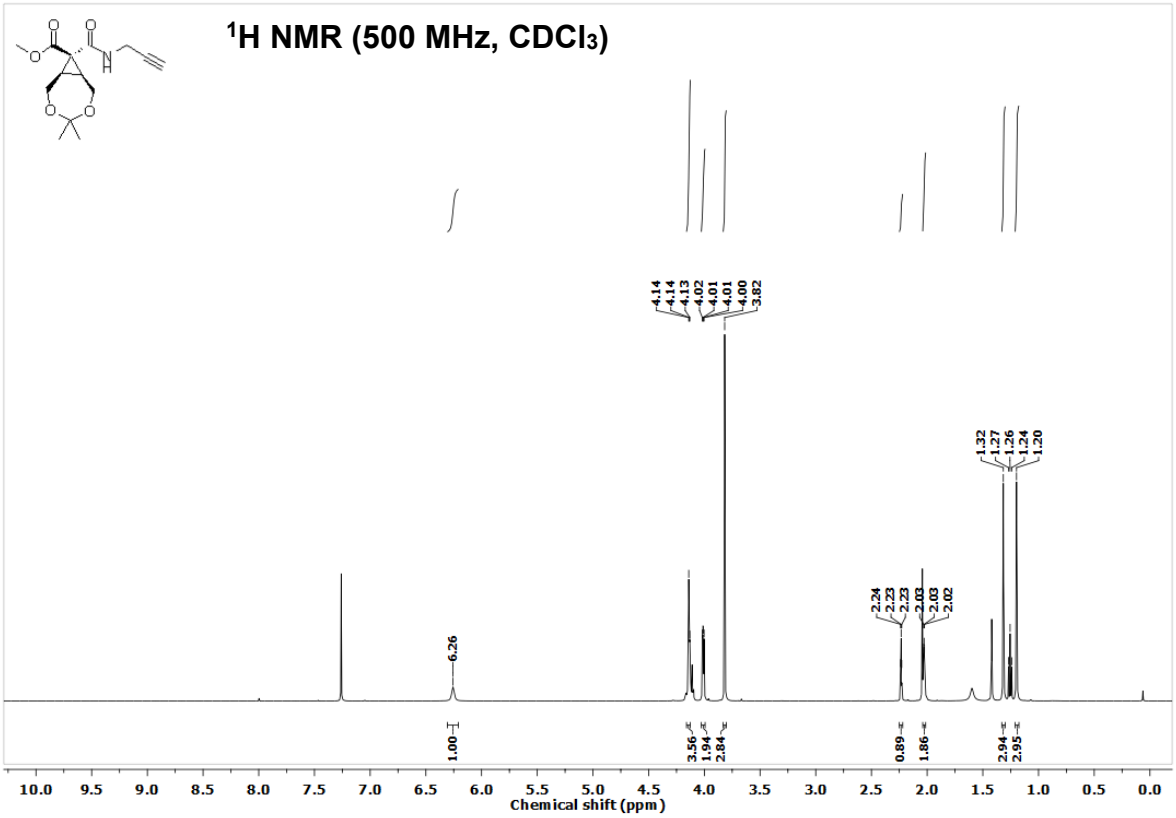

Methyl (1*R**,7*S**,8*s*)-8-(Allylcarbamoyl)-4,4-dimethyl-3,5-dioxabicyclo[5.1.0]octane-8-carboxylate (**17**)

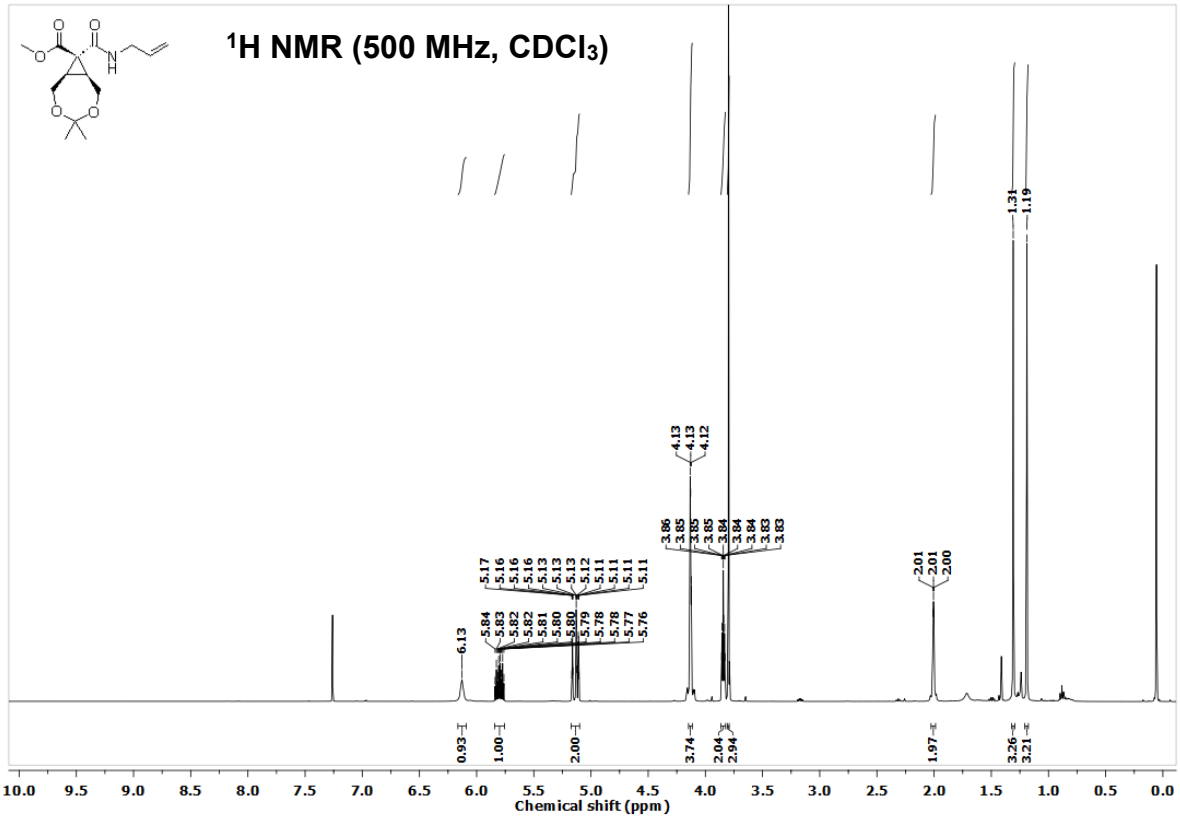

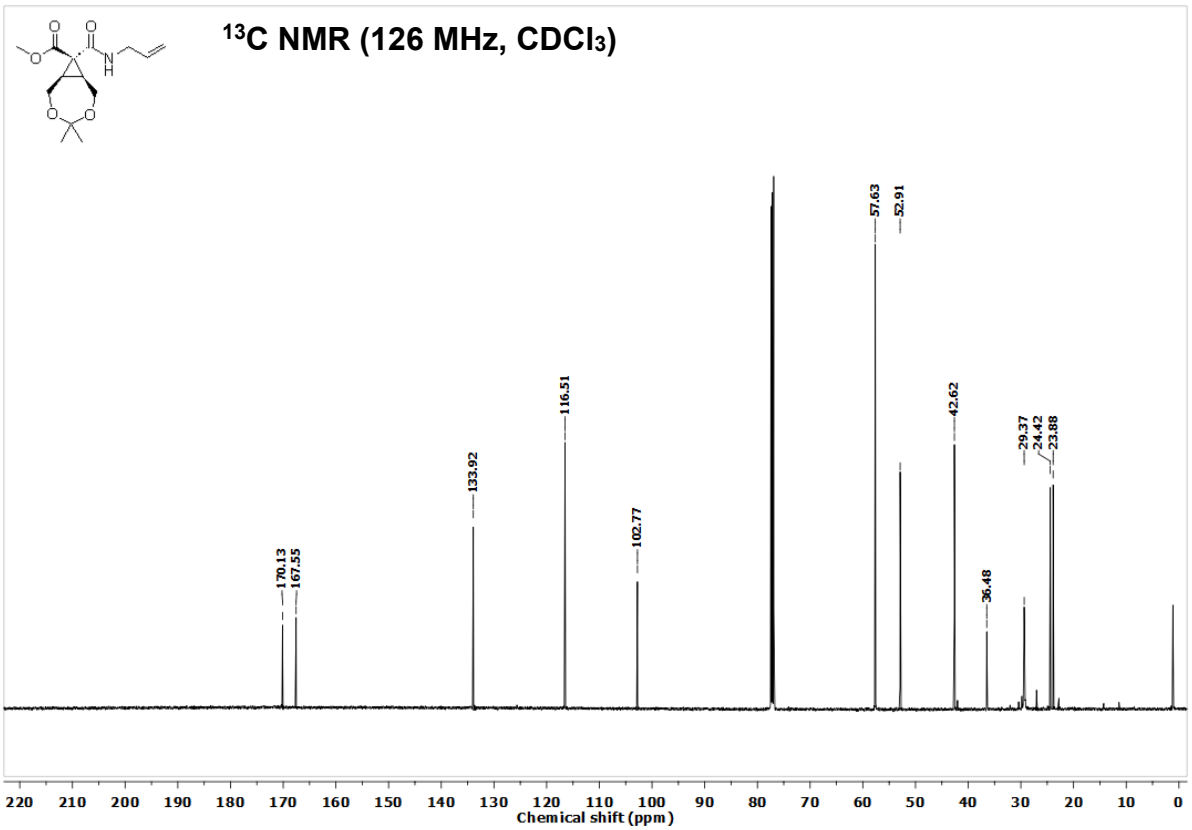

2,3-Diacetoxybenzoic acid (**27**)

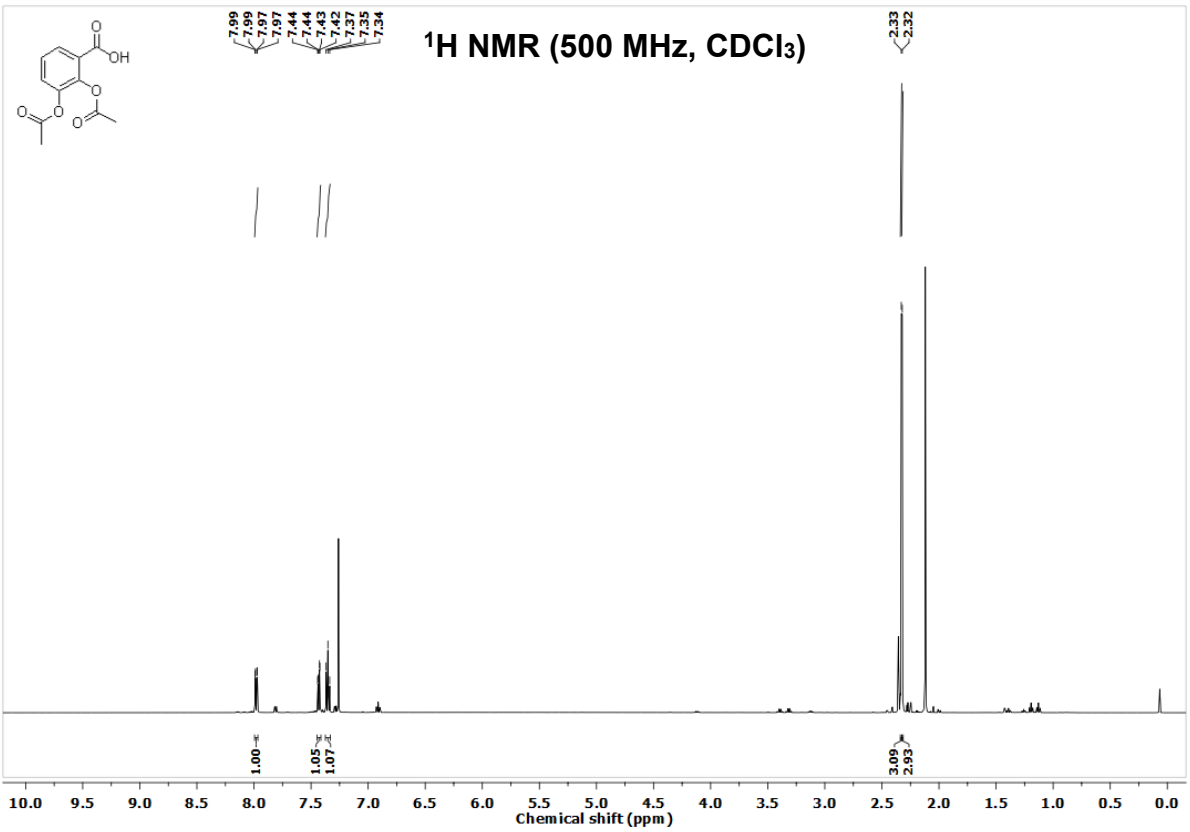

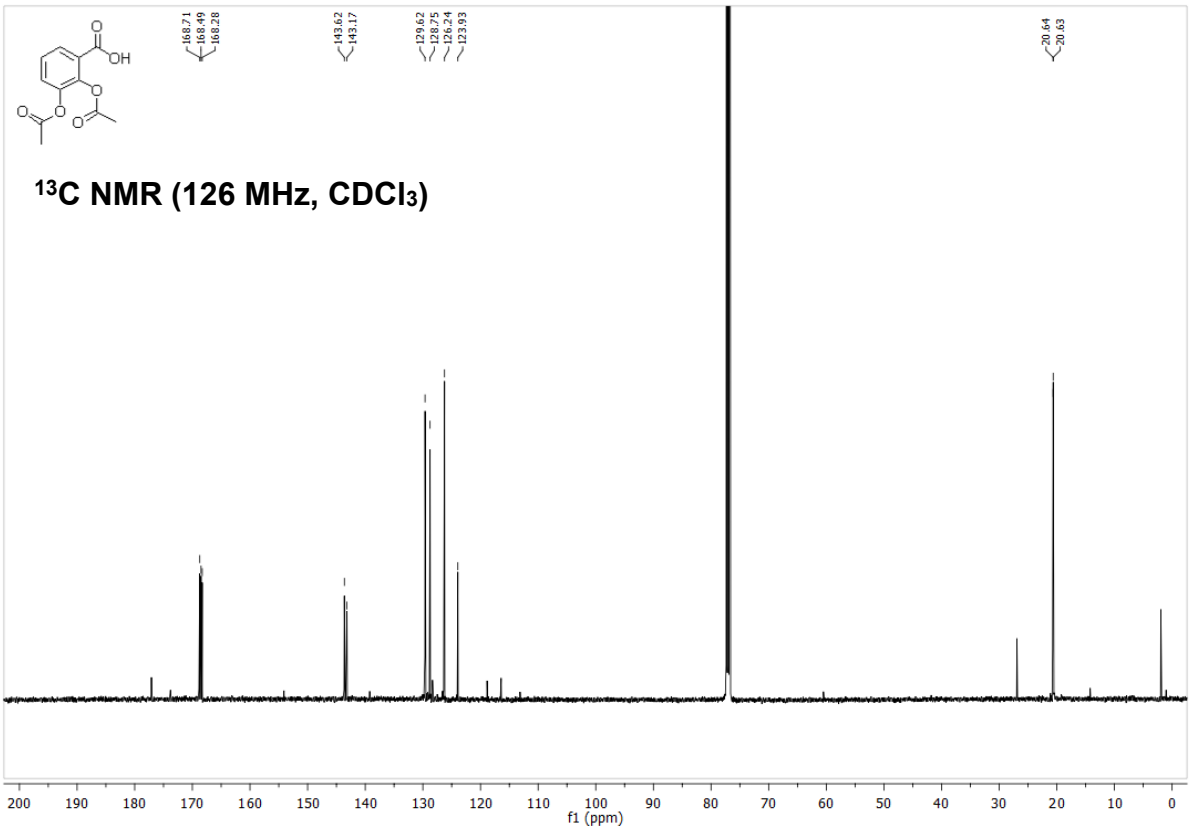

((1*r*,2*R**,3*S**)-1-(Prop-2-yn-1-ylcarbamoyl)cyclopropane-1,2,3-triyl)tris(methylene) Tris(3-(2,3-dihydroxybenzamido)propanoate) (**30**)

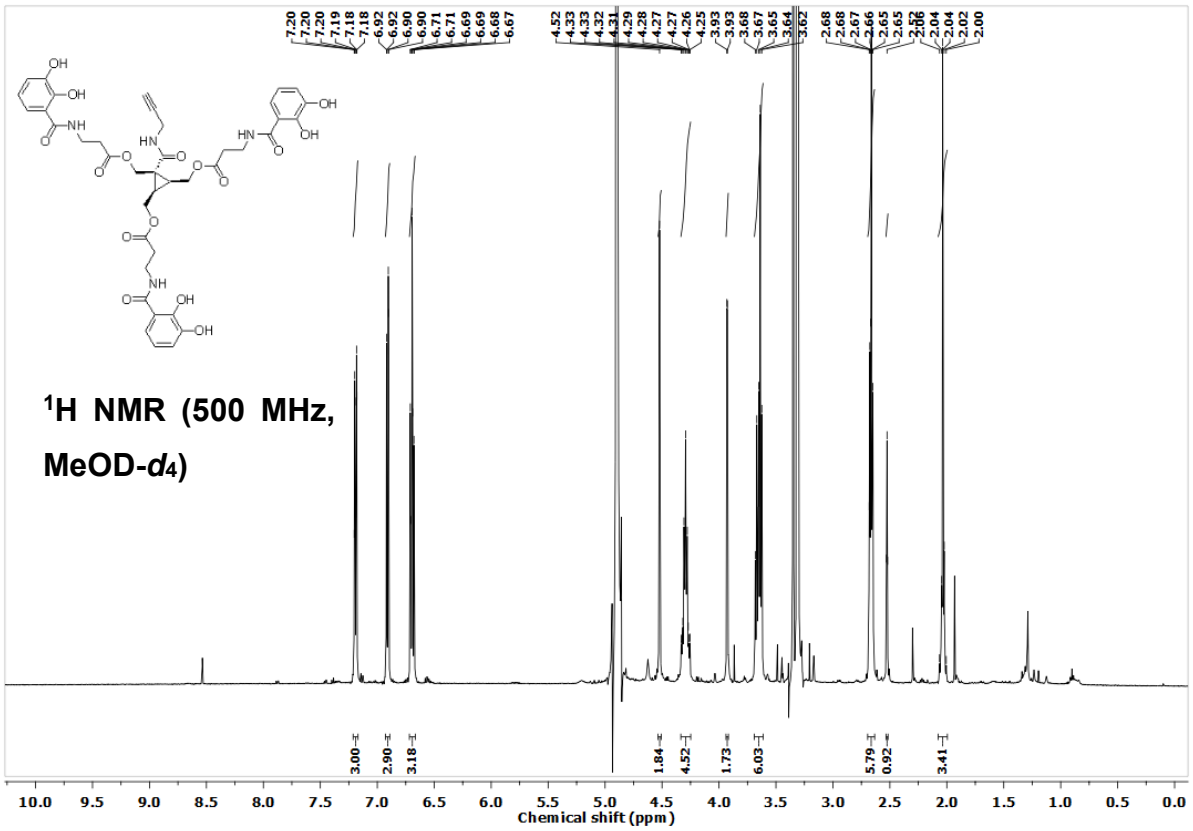

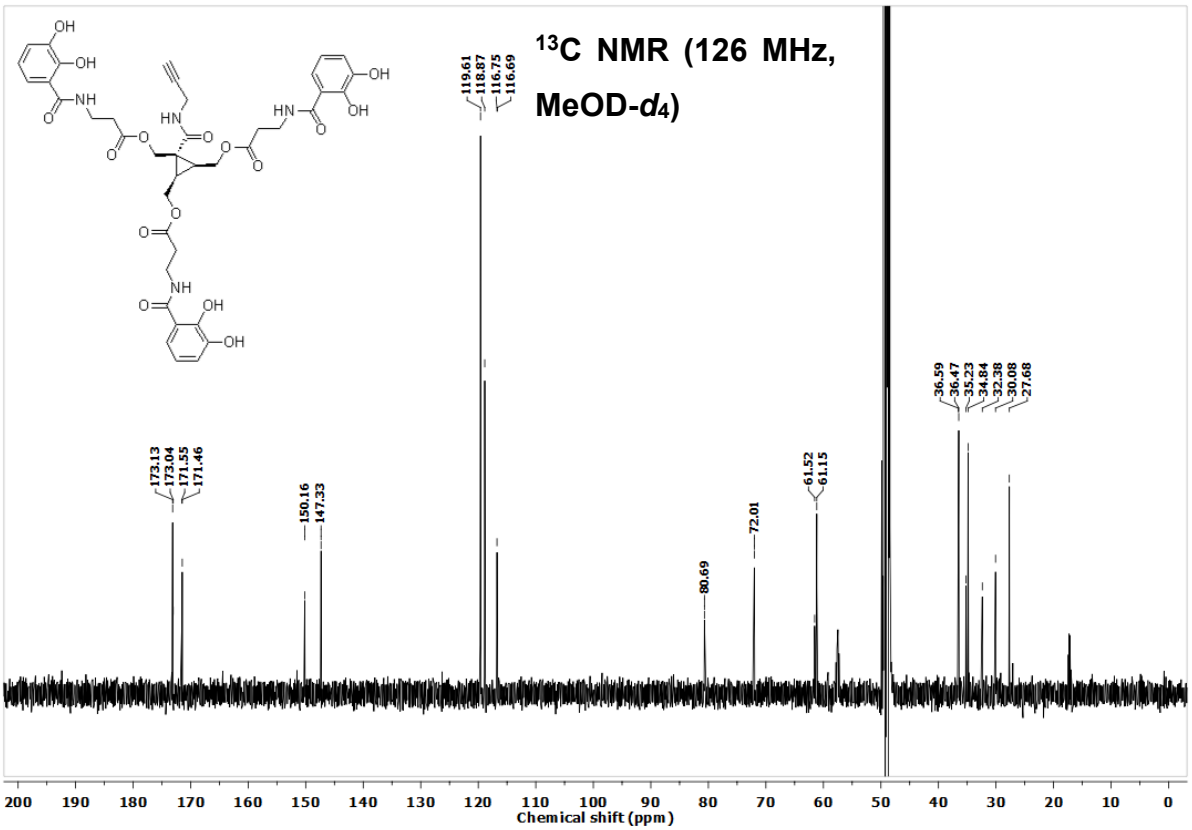

Methyl (1*R**,7*S**,8*s*)-8-(But-3-yn-1-ylcarbamoyl)-4,4-dimethyl-3,5-dioxabicyclo[5.1.0] octane-8-carboxylate (**32**)

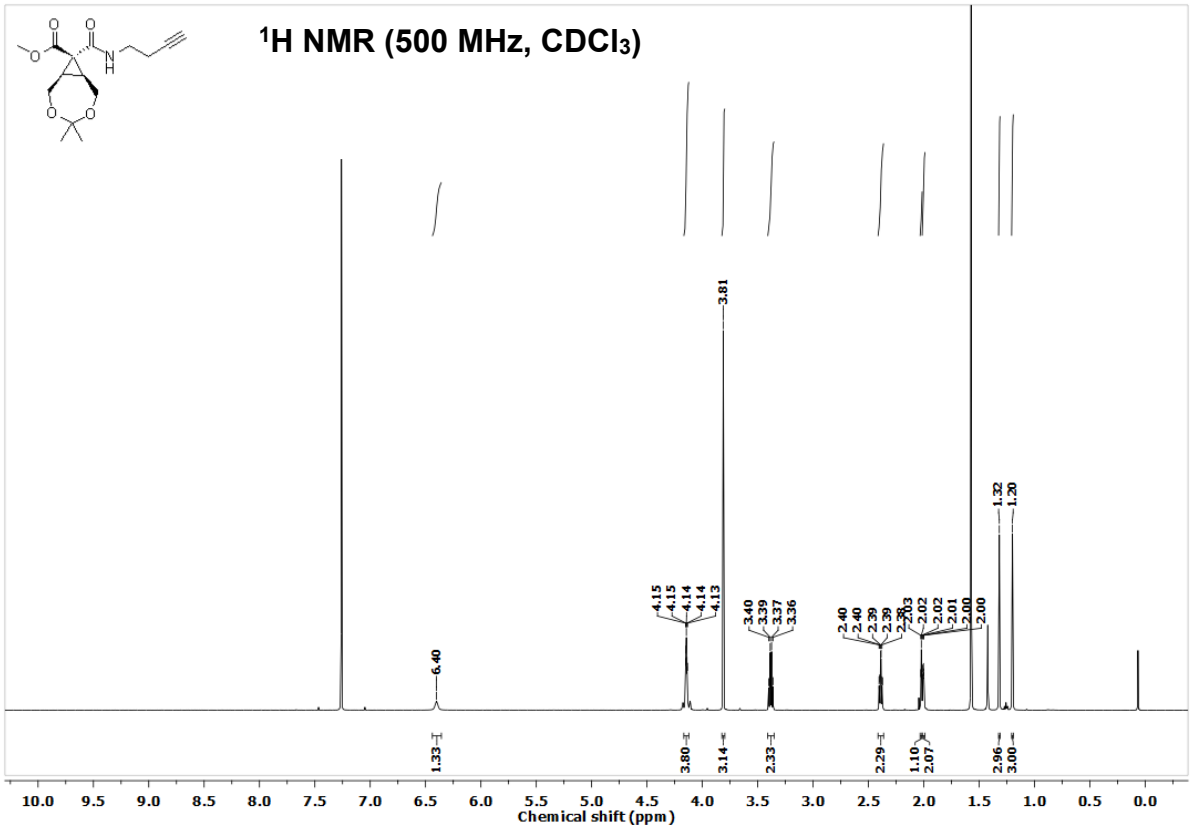

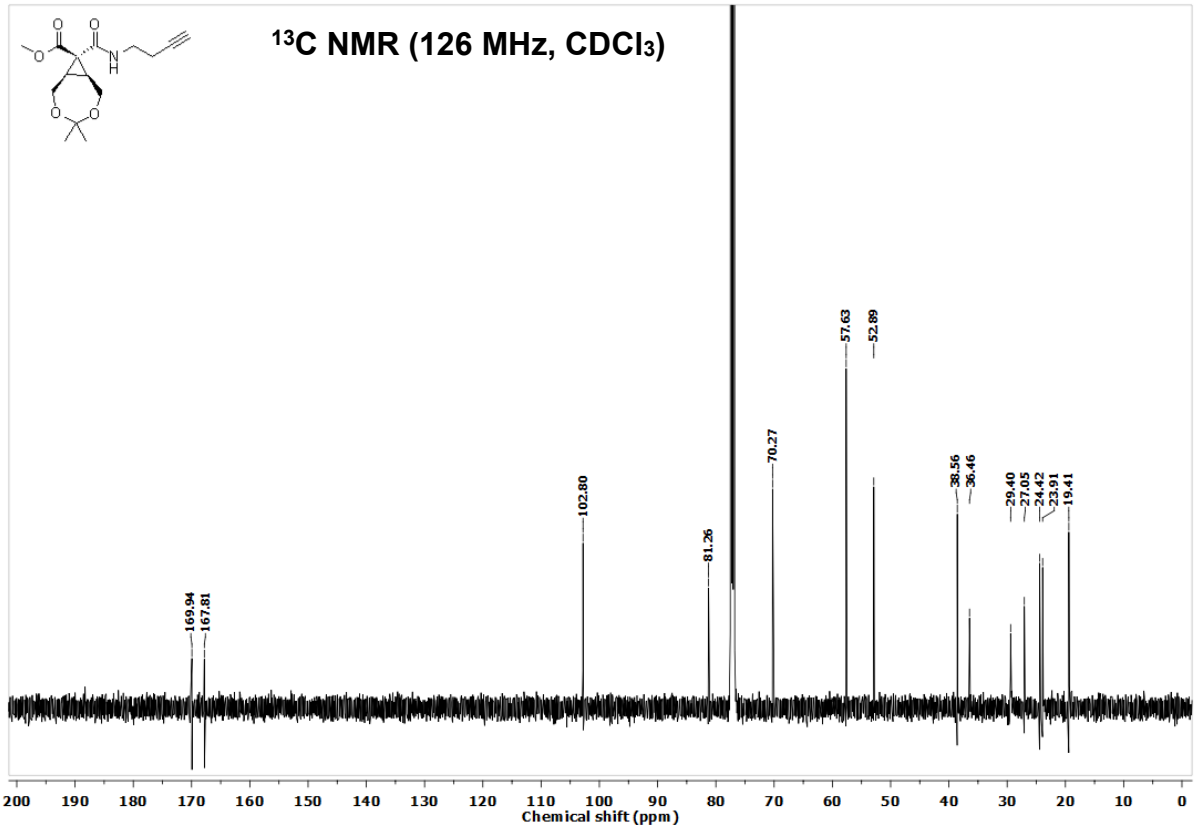

((1*R**,7*S**)-4,4-Dimethyl-3,5-dioxabicyclo[5.1.0]octane-8,8-diyl)Dimethanol (**39**)

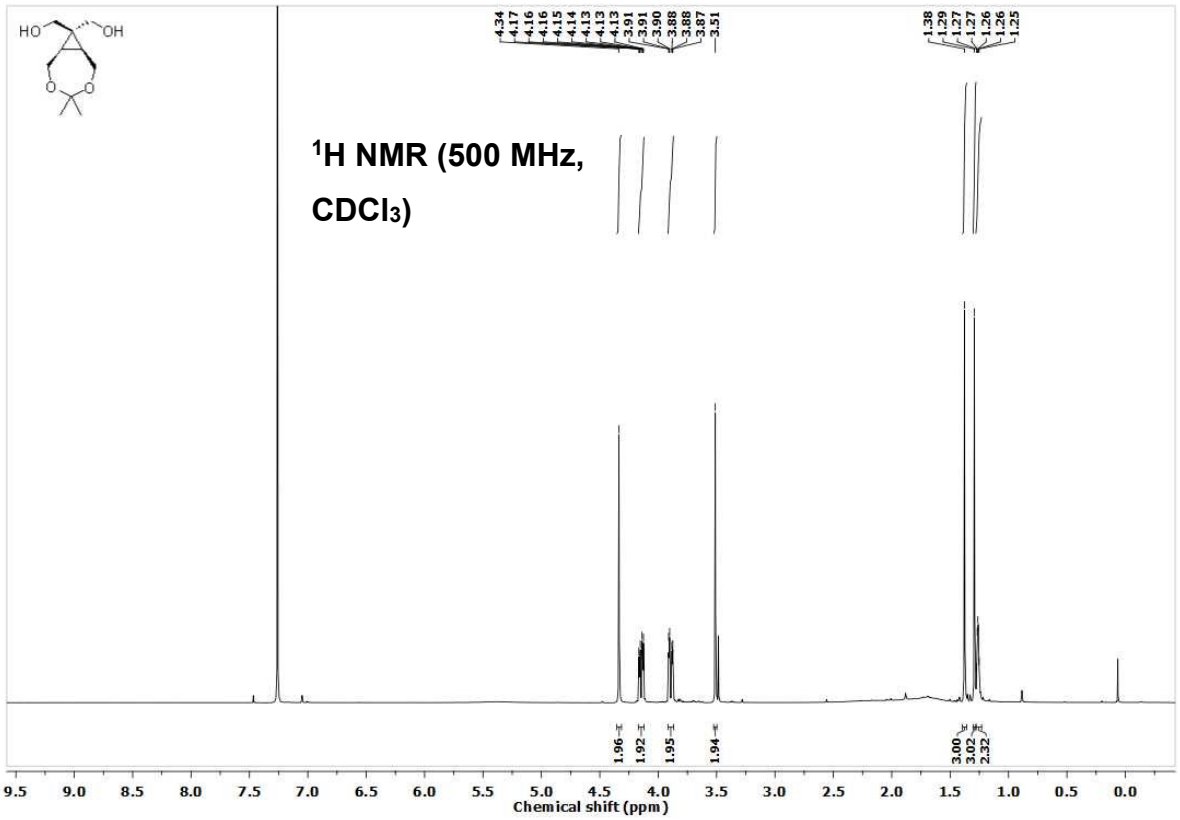

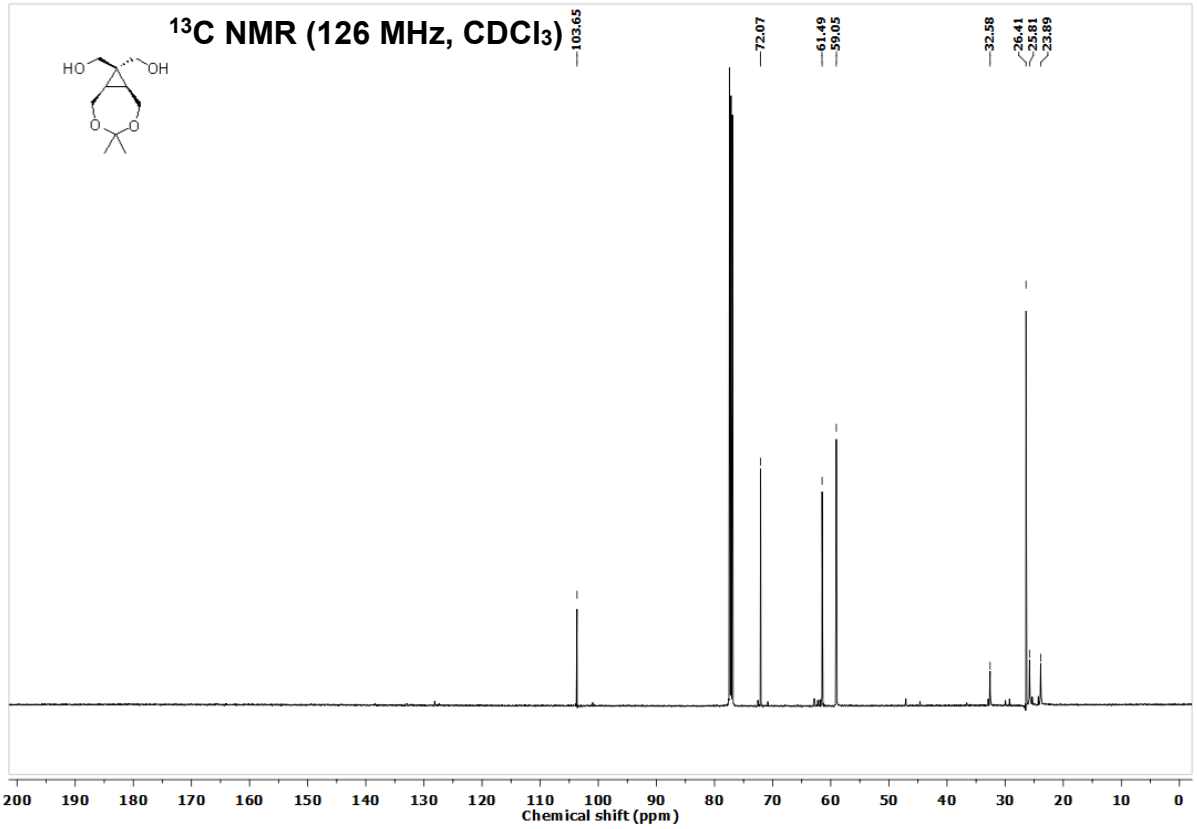

((1*R**,7*S**,8*r*)-4,4-Dimethyl-8-((prop-2-yn-1-yloxy)methyl)-3,5-dioxabicyclo[5.1.0] octan-8-yl)Methanol (**44**)

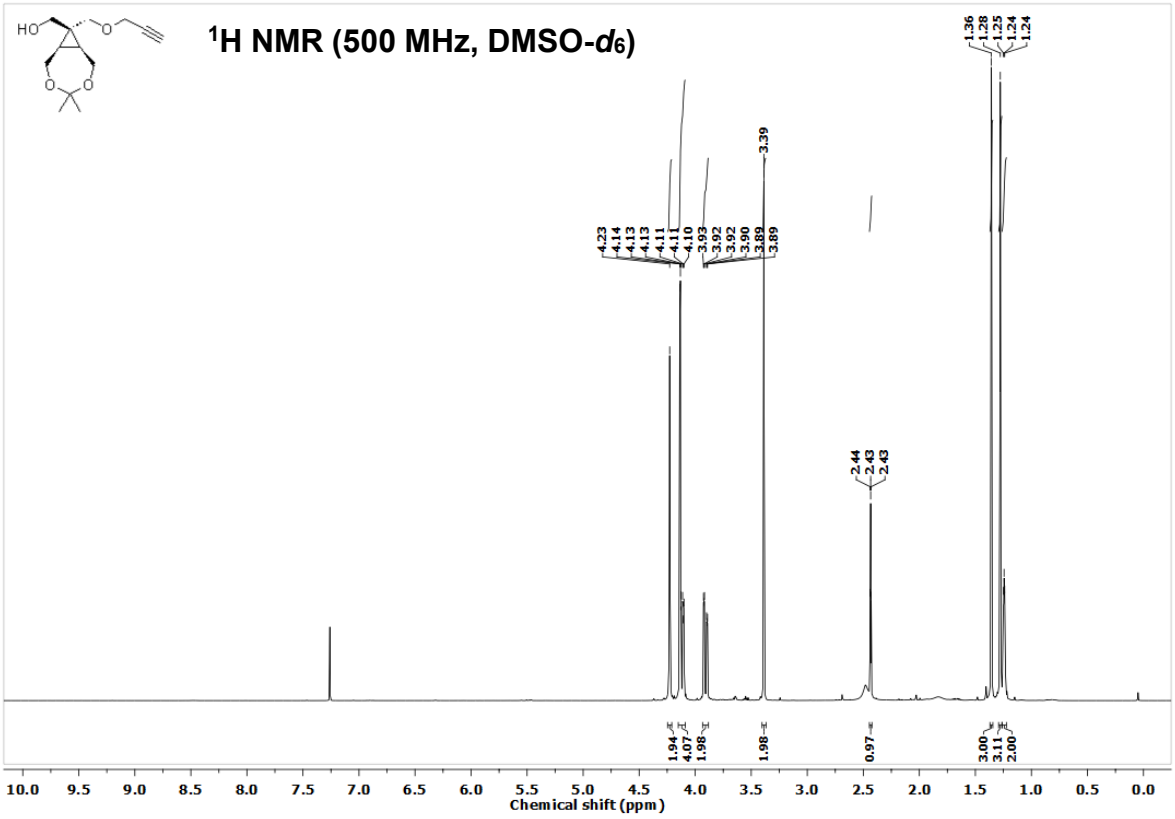

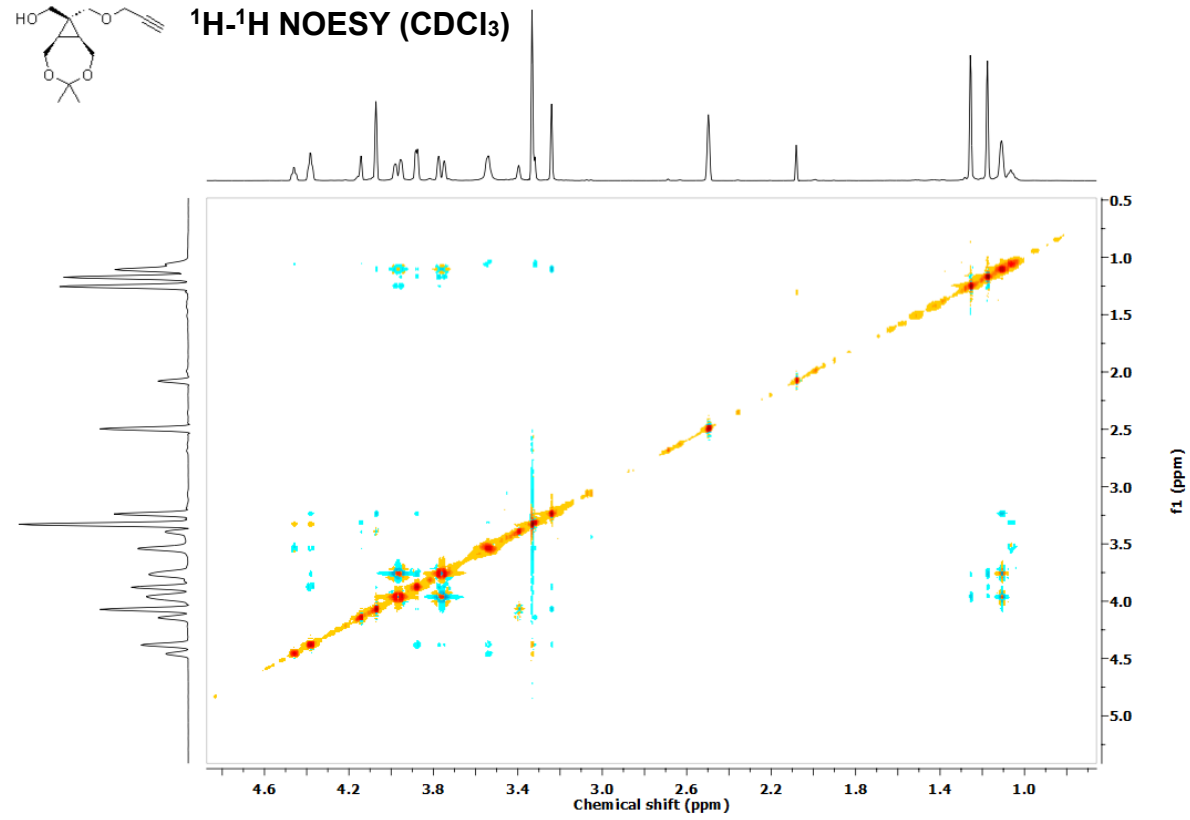

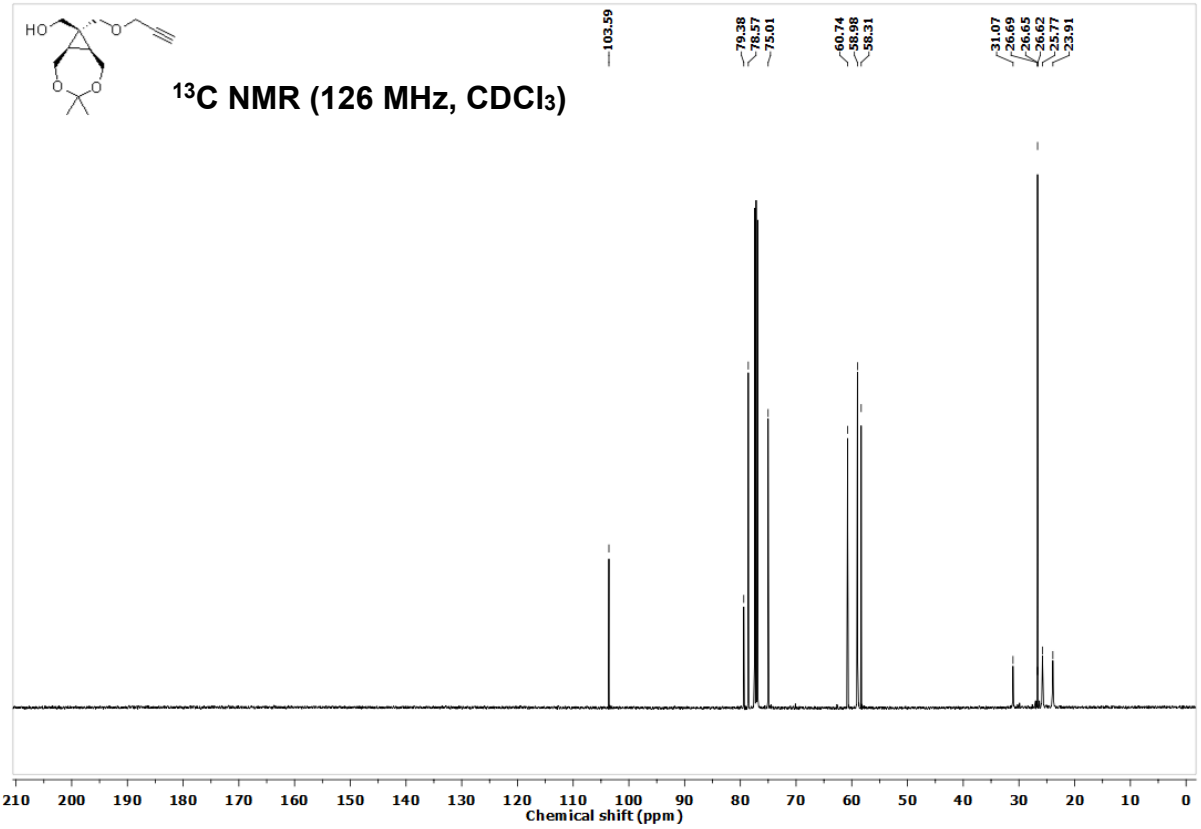

((1*R**,7*S**,8*s*)-4,4-Dimethyl-8-((prop-2-yn-1-yloxy)methyl)-3,5-dioxabicyclo[5.1.0] octan-8-yl)methanol (**45**)

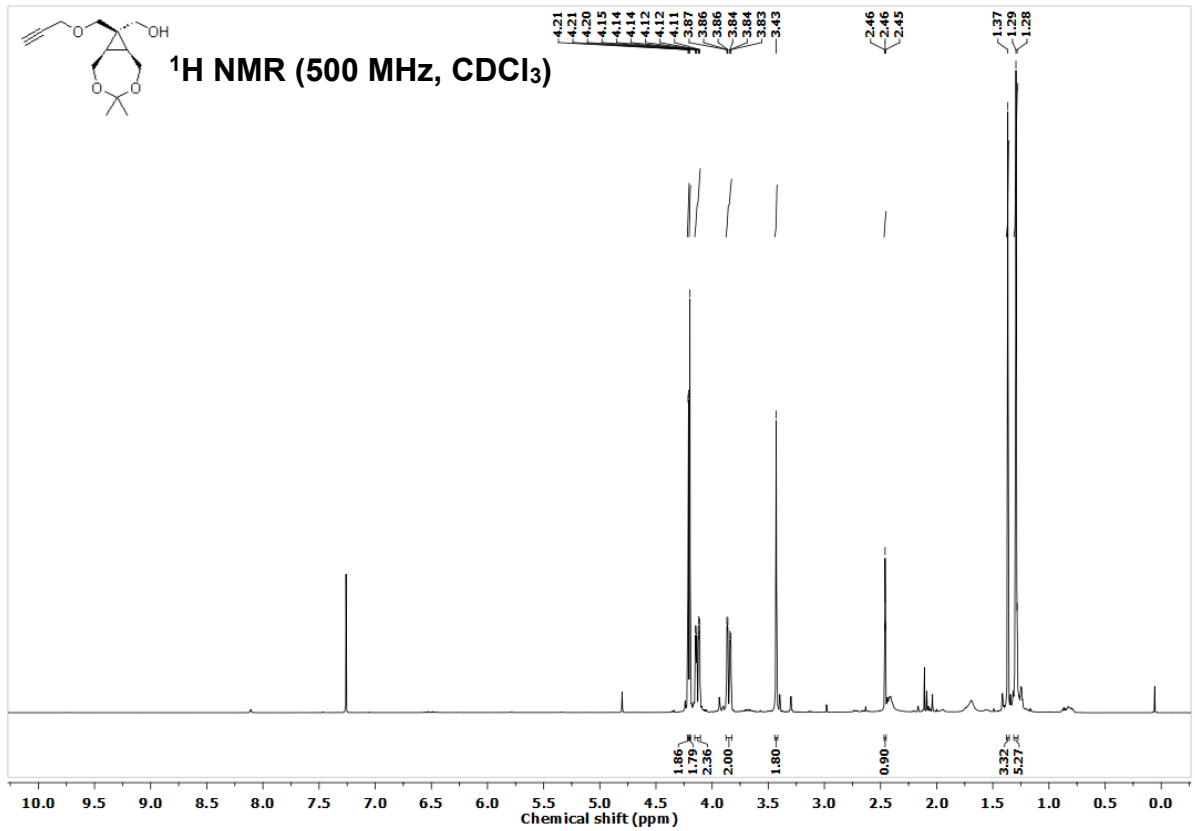

^{1}H-^{1}H NOESY ($CDCl_3$)

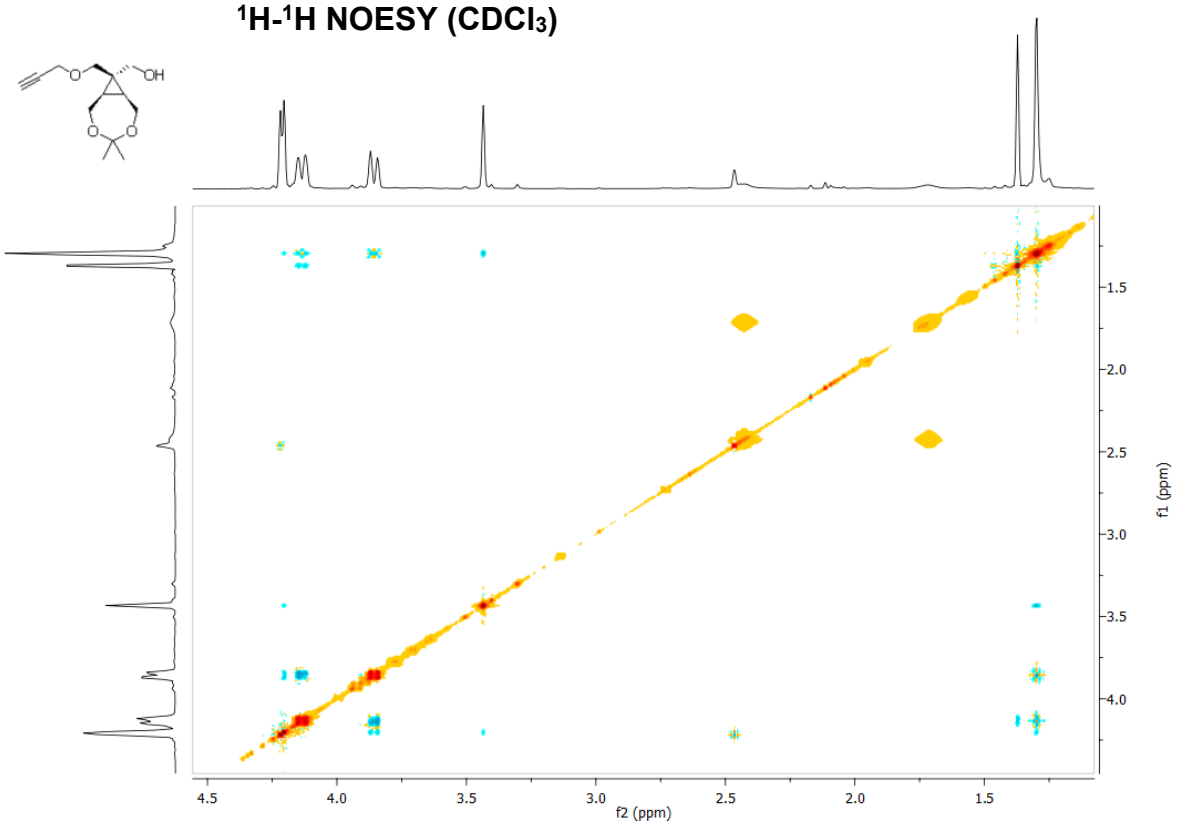

^{13}C NMR (126 MHz, $CDCl_3$)

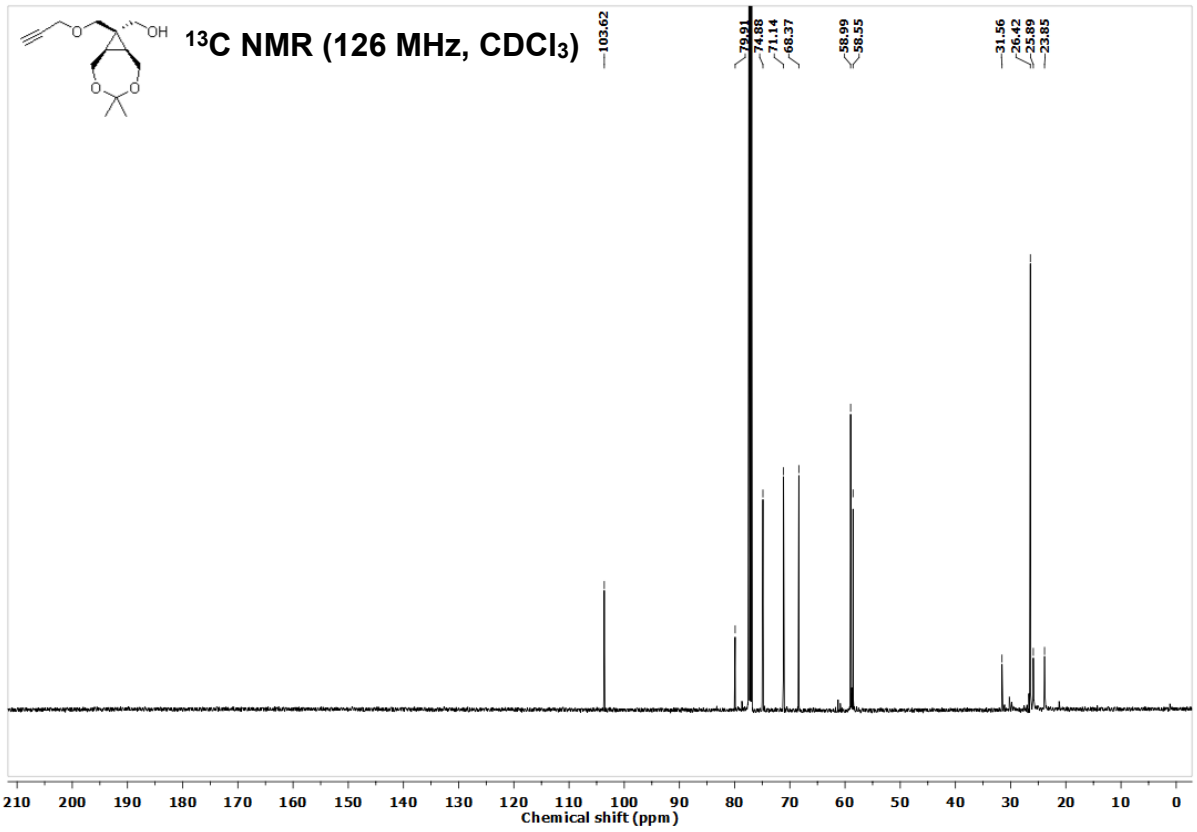

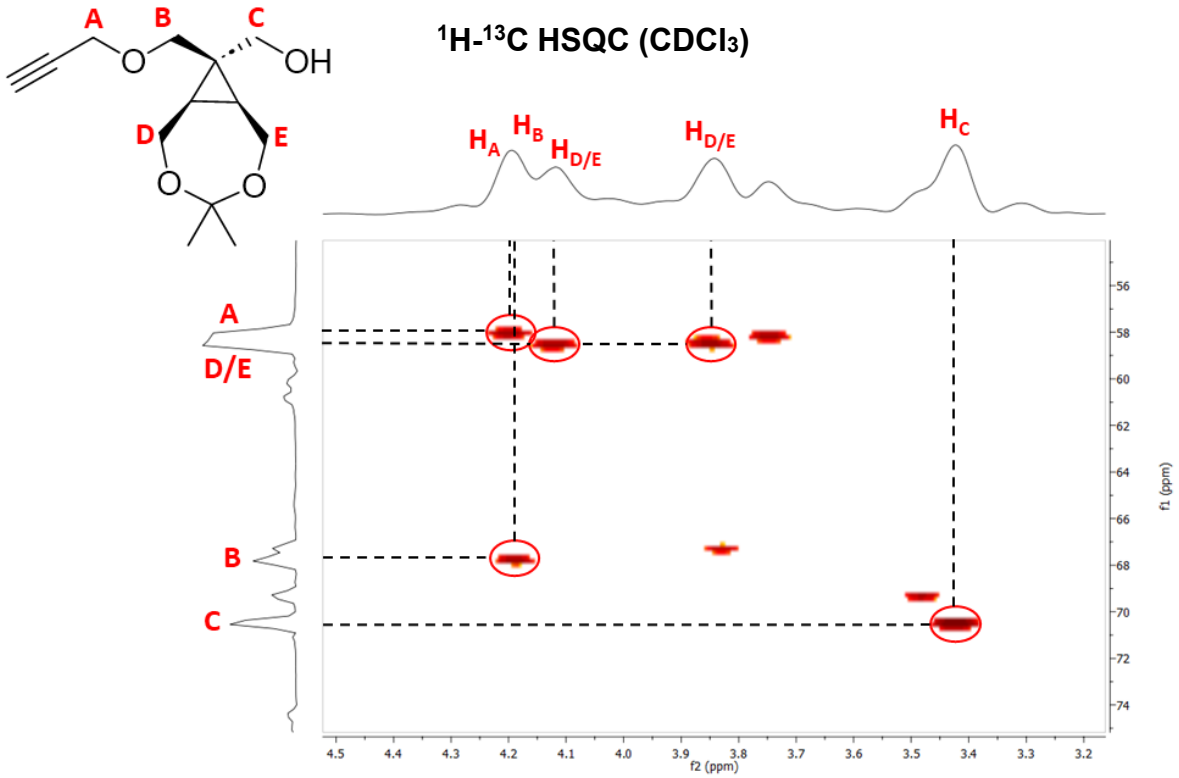
A
B
C
OH
D
E
O
O
^{1}H-^{13}C HSQC (CDCl$_3$)
H_A
H_B
$H_{D/E}$
$H_{D/E}$
H_C
A
D/E
B
C
f1 (ppm)
f2 (ppm)

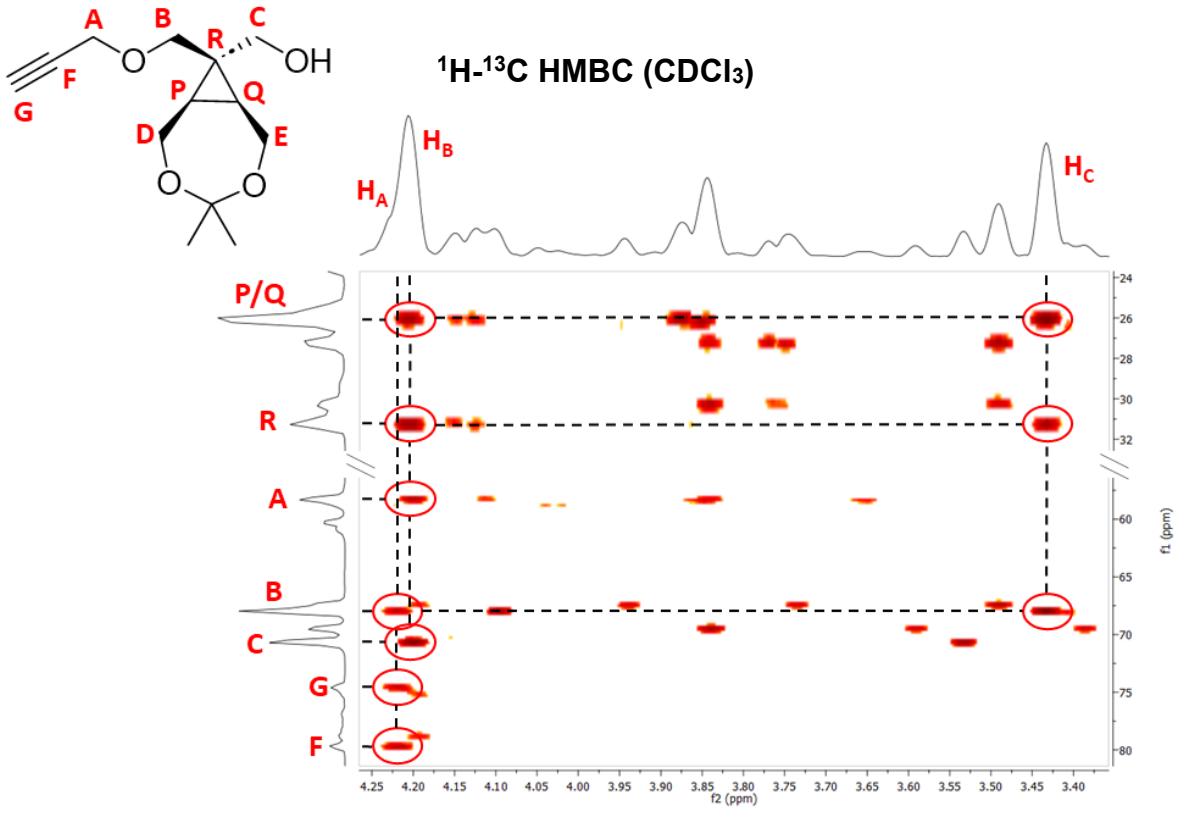
A
B
R
C
OH
F
G
P
Q
D
E
O
O
^{1}H-^{13}C HMBC (CDCl$_3$)
H_A
H_B
H_C
P/Q
R
A
B
C
G
F
f1 (ppm)
f2 (ppm)

(1*R**,7*S**)-4,4-Dimethyl-8,8-bis((prop-2-yn-1-yloxy)methyl)-3,5-dioxabicyclo[5.1.0] octane (**46**)

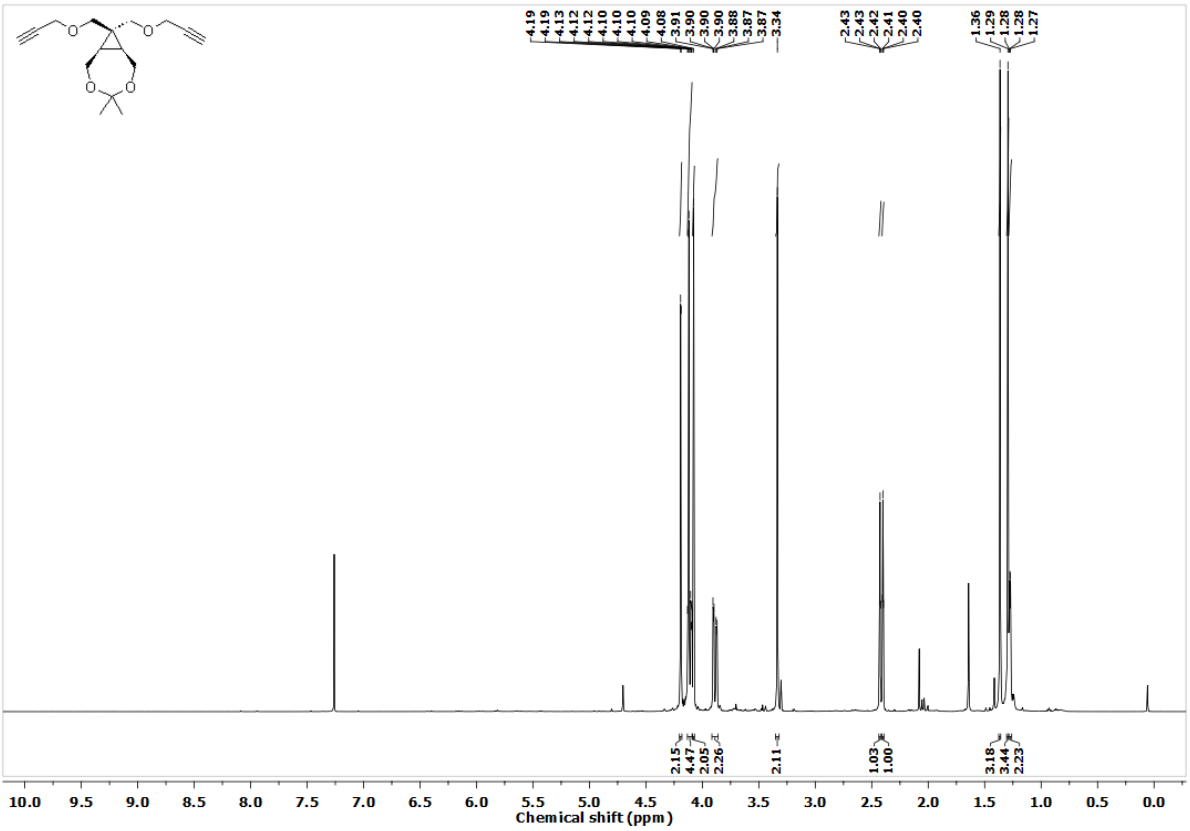

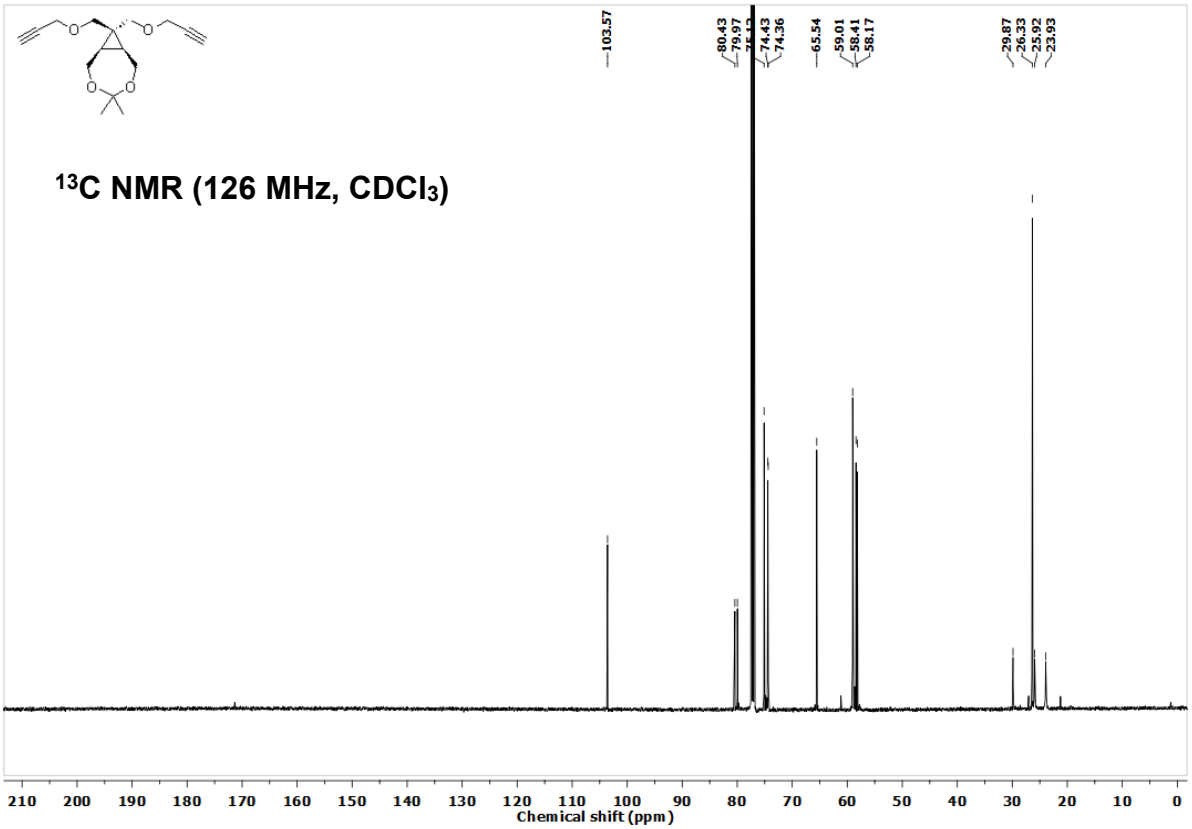

((1*s*,2*R**,3*S**)-1-((Prop-2-yn-1-yloxy)methyl)cyclopropane-1,2,3-triyl)tris(methylene) Tris(3-((*tert*-butoxycarbonyl)amino)propanoate) (**48**)

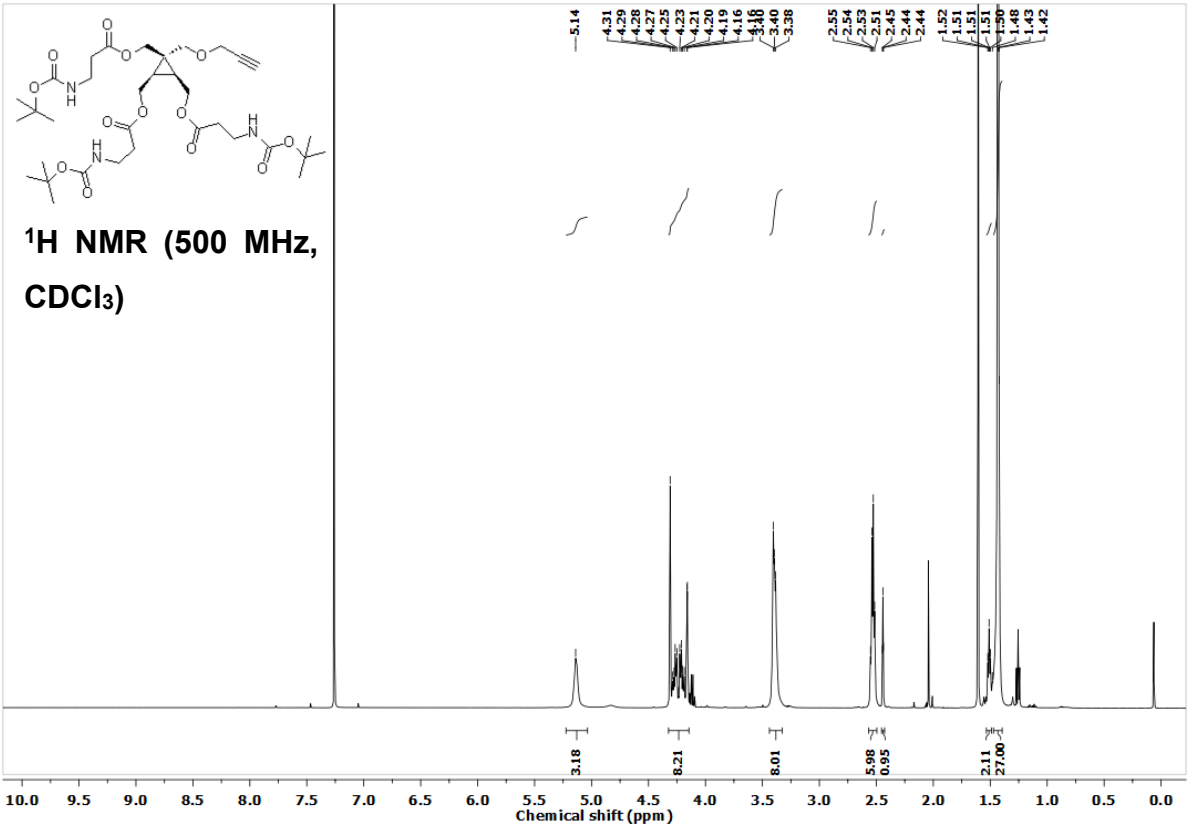

^{1}H NMR (500 MHz, $CDCl_3$)

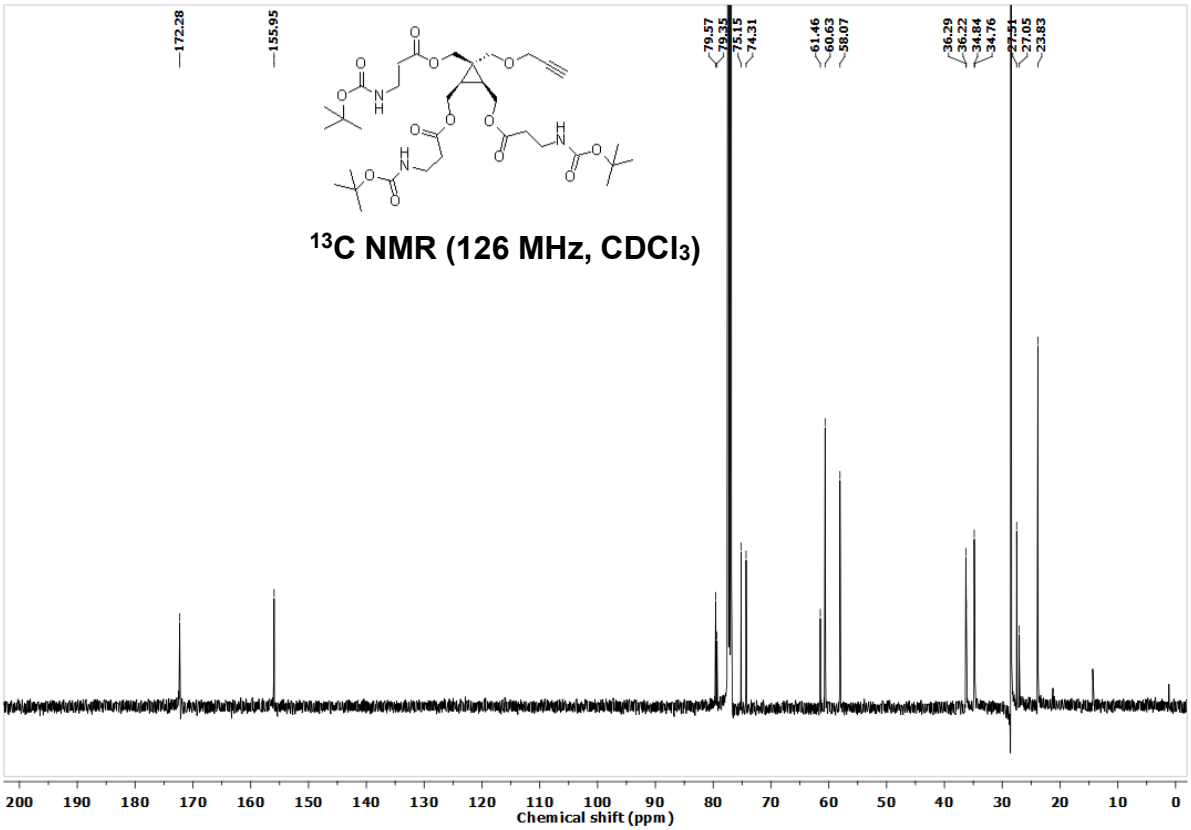

^{13}C NMR (126 MHz, $CDCl_3$)

((1*s*,2*R**,3*S**)-2,3-Bis((2-(2,3-bis(methylcarbonyloxy)phenylcarbonylamino) ethylcarbonyloxy)methyl)-1-((prop-2-ynyloxy)methyl)cyclopropyl)methyl 3-(2,3-Bis (methylcarbonyloxy)phenylcarbonylamino)Propanoate (**50**)

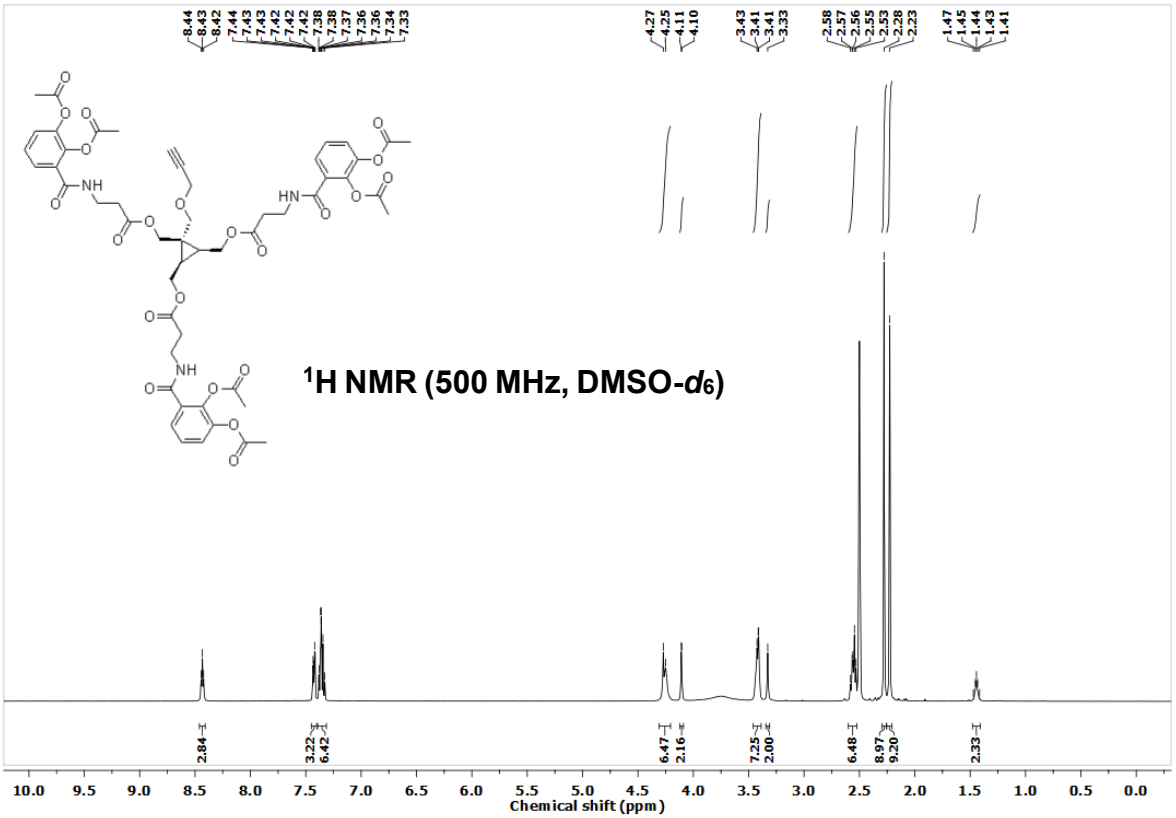

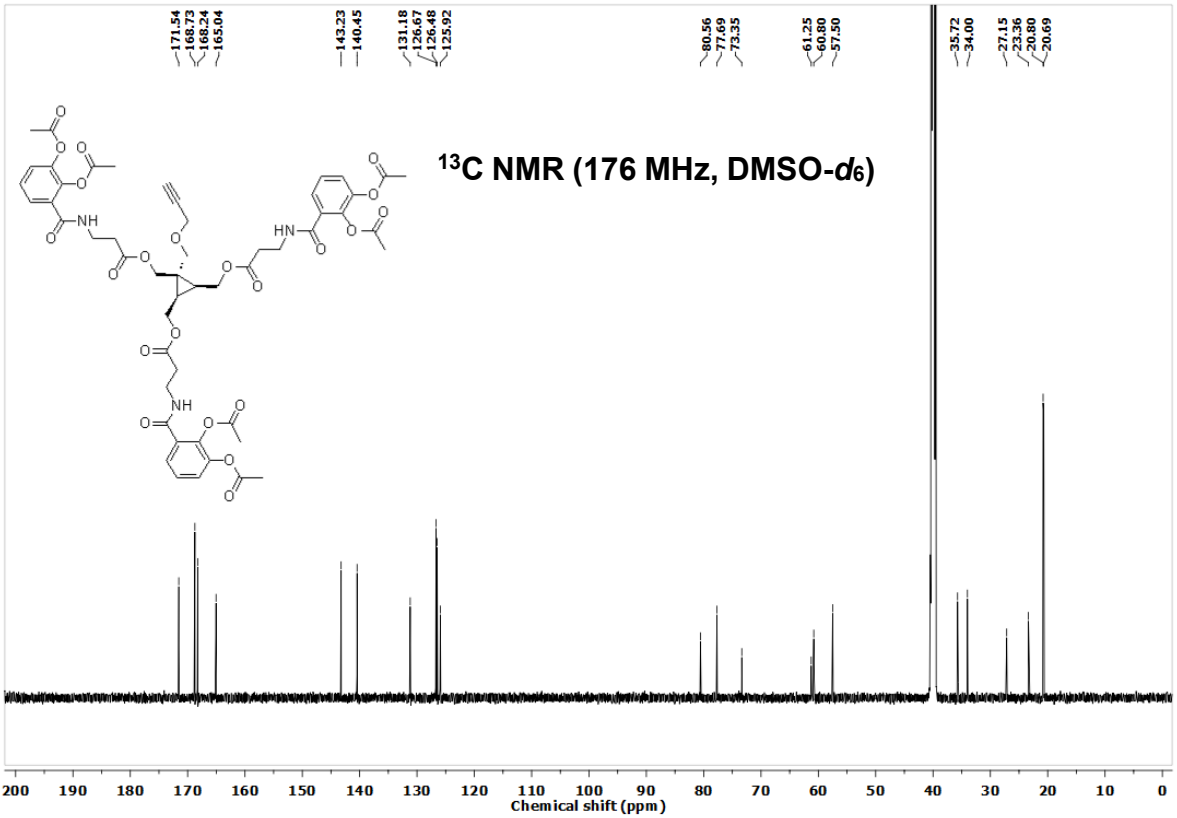

tert-Butyl (*E*)-(4-Bromobut-2-en-1-yl)Carbamate (**64**)

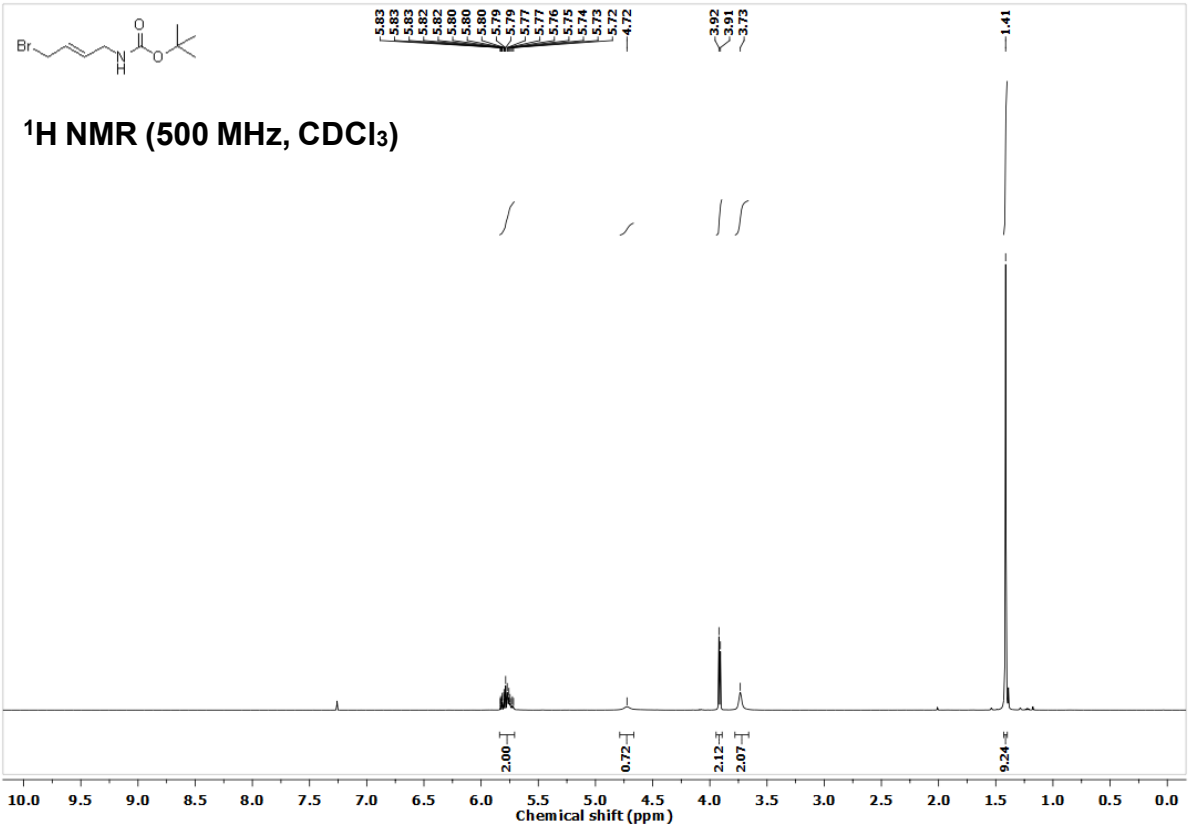

^{1}H NMR (500 MHz, $CDCl_3$)

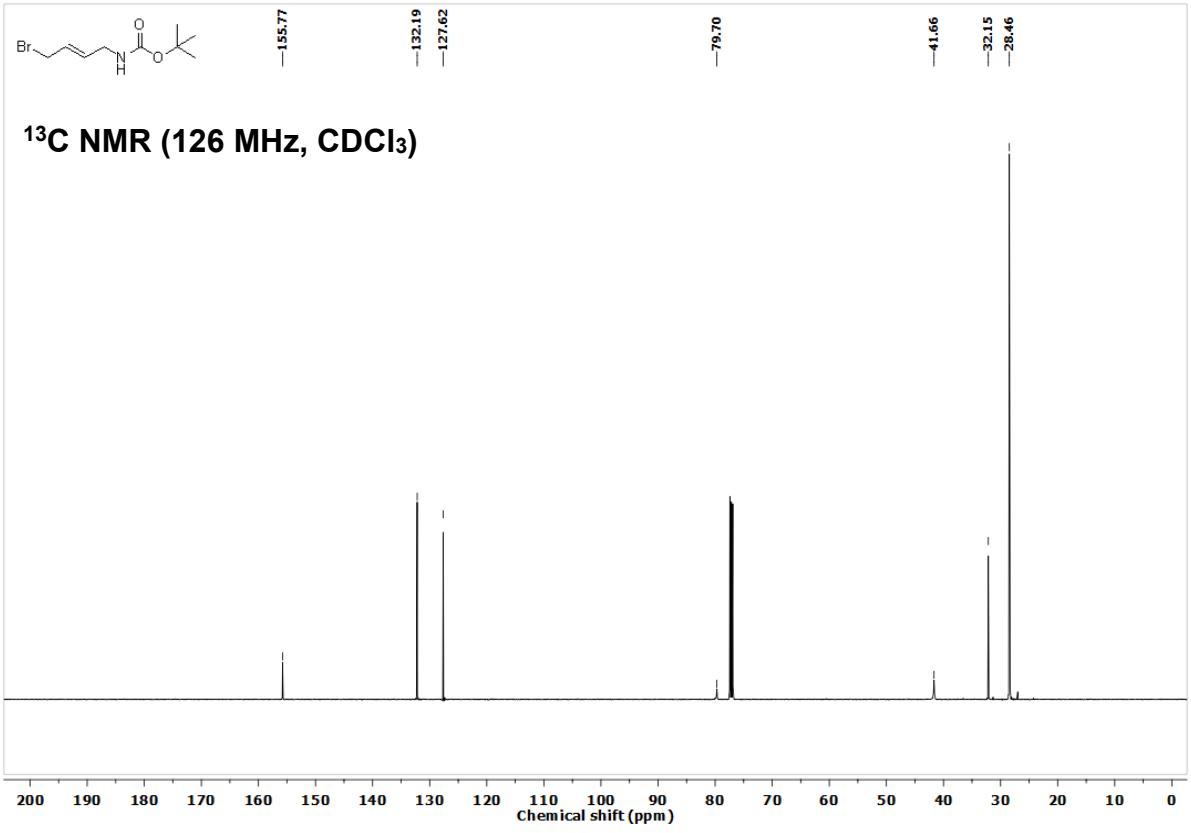

^{13}C NMR (126 MHz, $CDCl_3$)

(2*S*,5*R*,6*R*)-6-((*R*)-2-(3-Azidopropanamido)-2-phenylacetamido)-3,3-dimethyl-7-oxo-4-thia-1-azabicyclo[3.2.0]heptane-2-carboxylic acid (**56**)

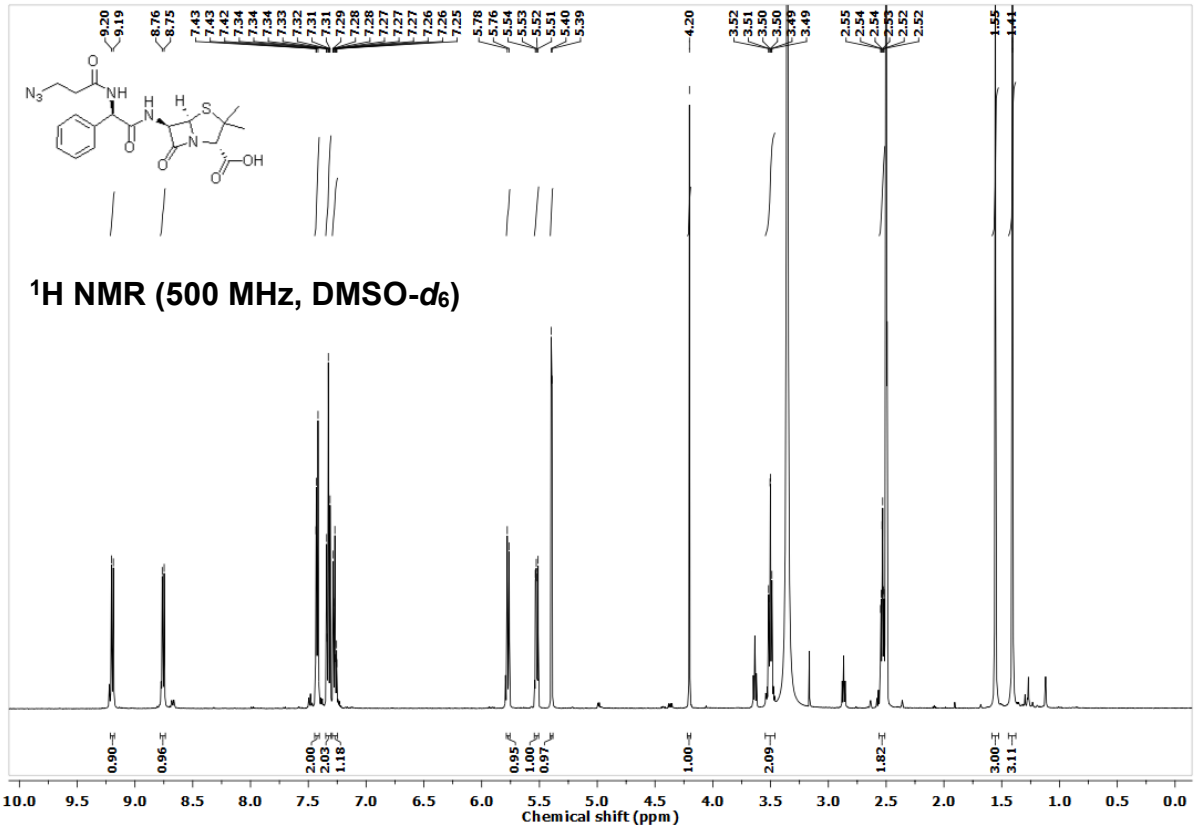

^{1}H NMR (500 MHz, DMSO-d_6)

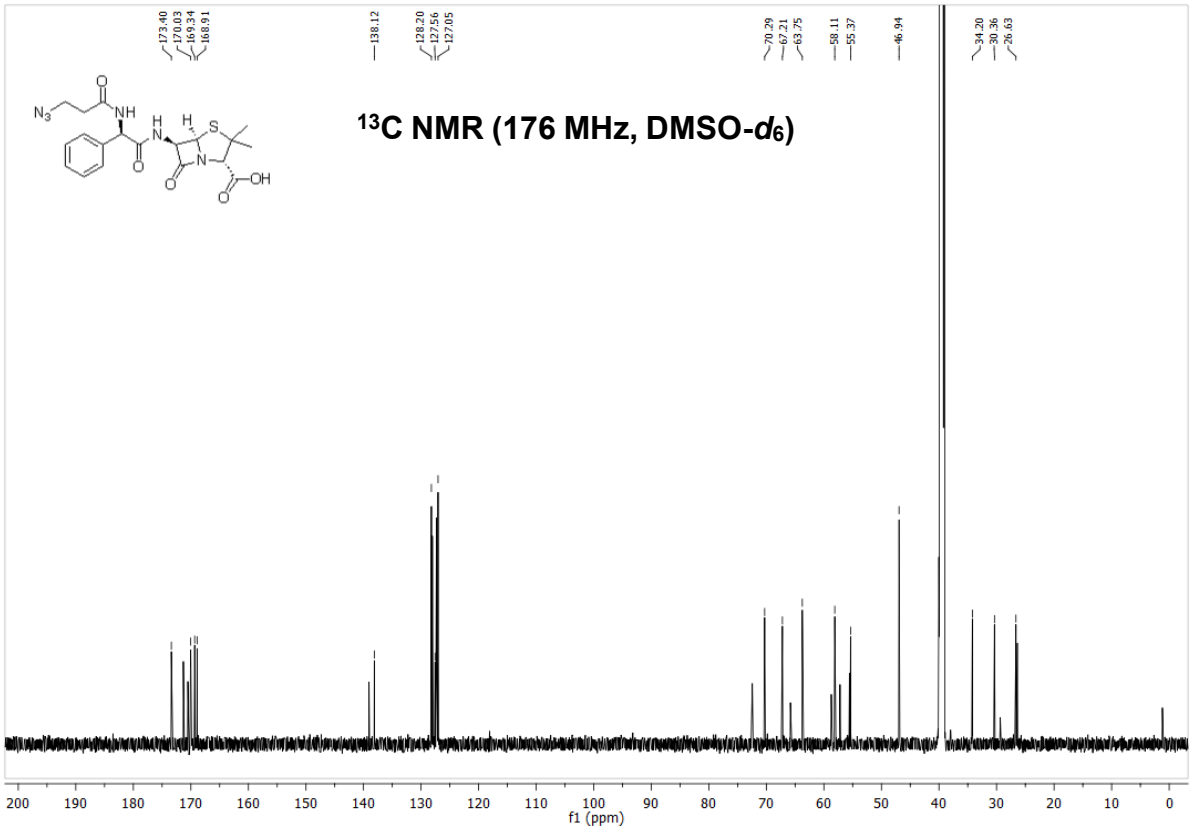

^{13}C NMR (176 MHz, DMSO-d_6)

2*S*,5*R*,6*R*)-3,3-Dimethyl-7-oxo-6-((*R*)-2-phenyl-2-(3-(4-((((1*s*,2*R**,3*S**)-1,2,3-tris(((3-(2,3-diacetoxybenzamido)propanoyl)oxy)methyl)cyclopropyl)methoxy)methyl)-1*H*-1,2,3-triazol-1-yl)propanamido)acetamido)-4-thia-1-azabicyclo[3.2.0]heptane-2-carboxylic acid (**57**)

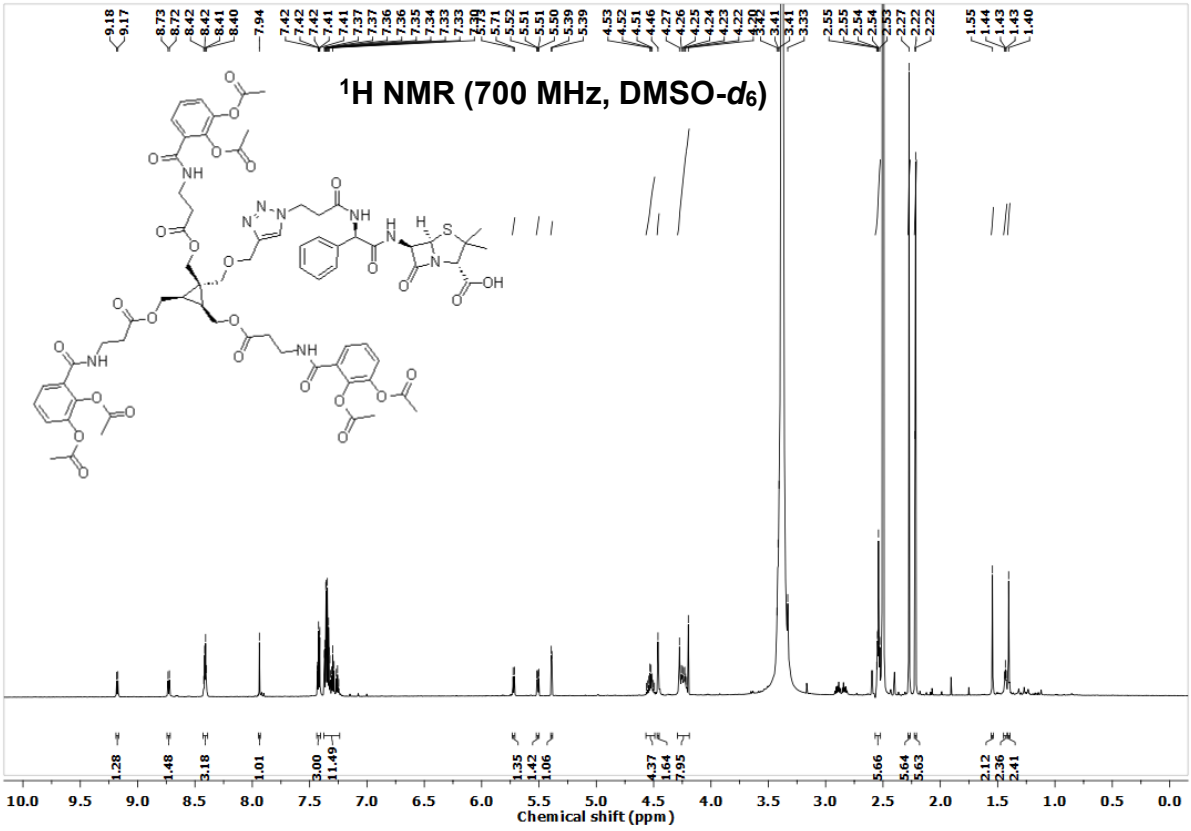

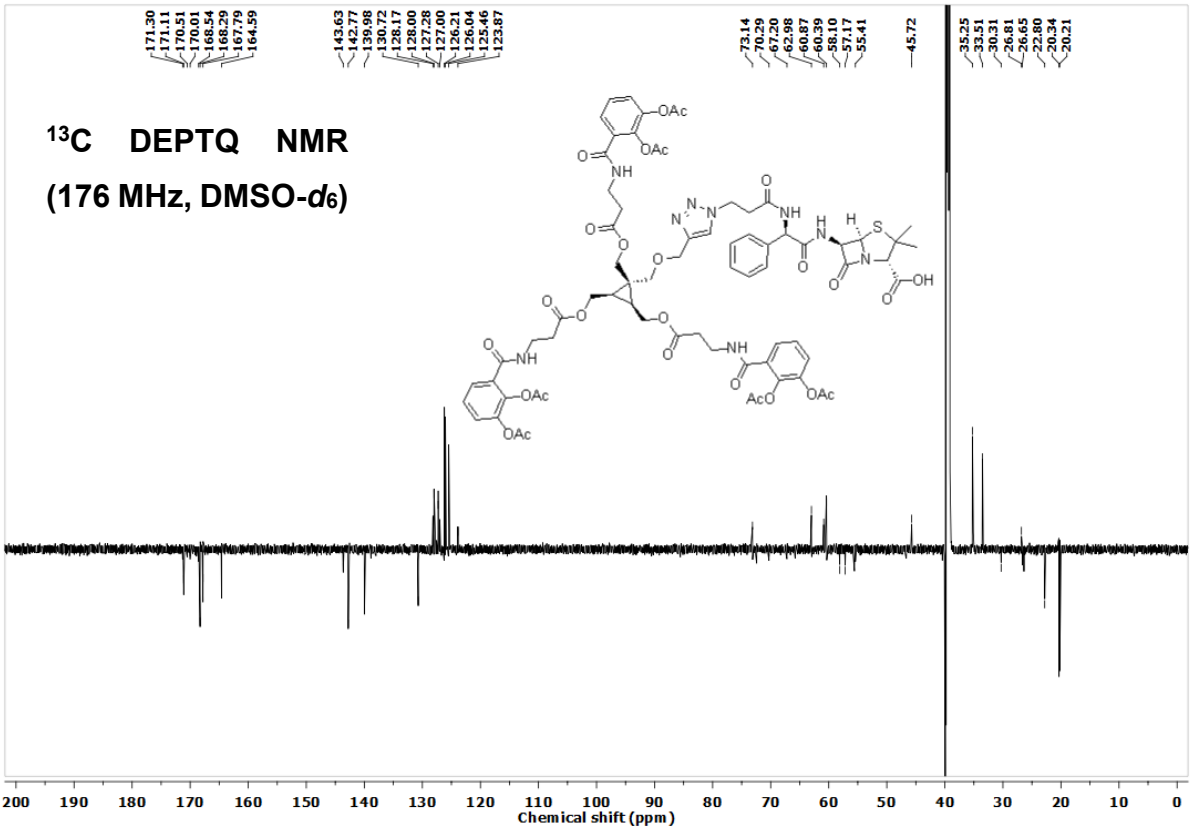

tert-Butyl (*R*)-(4-Bromobut-2-en-1-yl)(*tert*-Butoxycarbonyl)Carbamate (**66**)

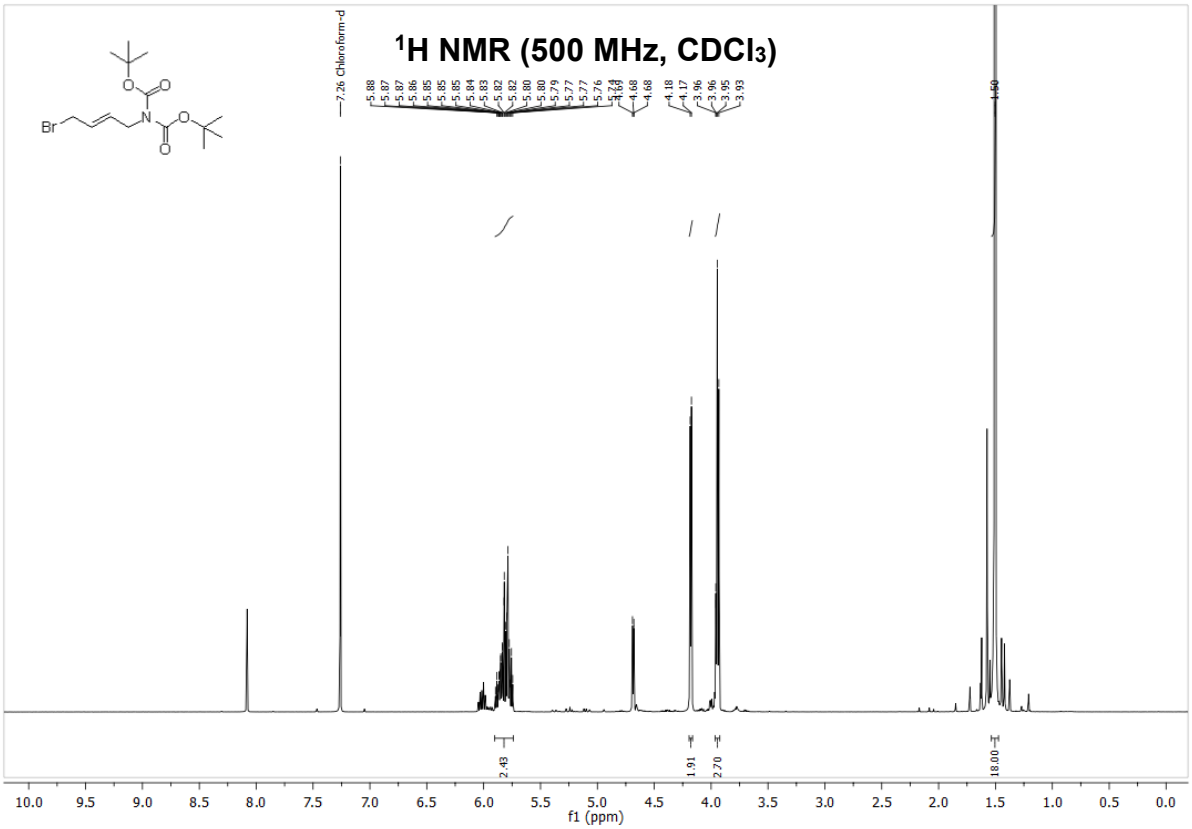

((1*s*,2*R**,3*S**)-1-((Prop-2-yn-1-yloxy)methyl)cyclopropane-1,2,3-triyl)tris(methylene) Tris(3-(2,3-dihydroxybenzamido)propanoate) (**51**)

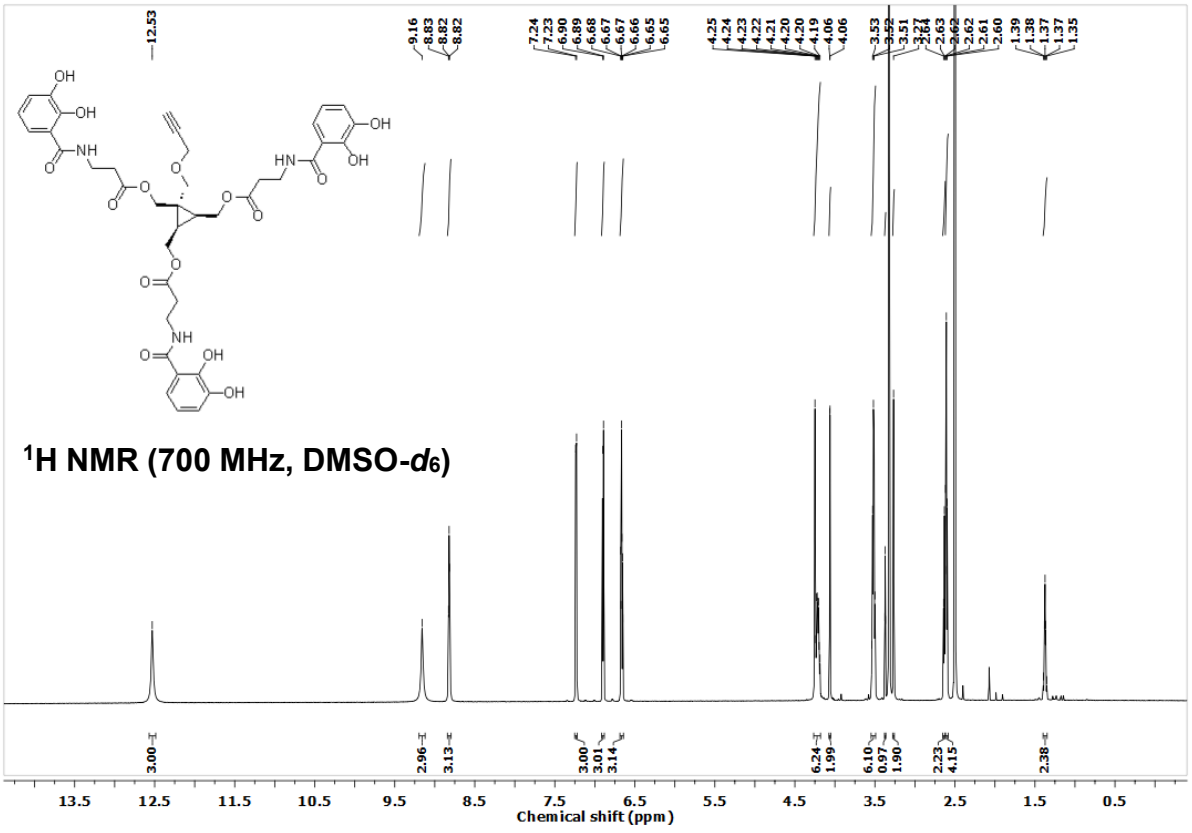

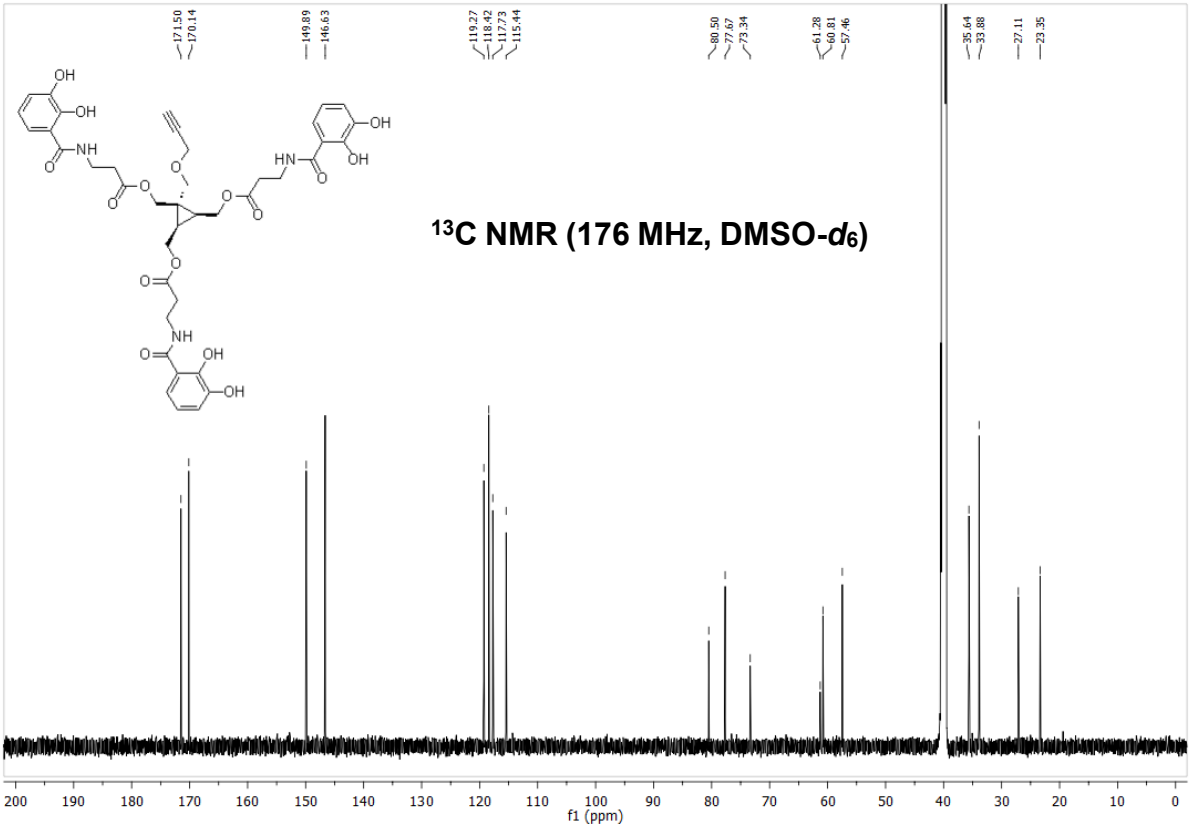
171.50
170.14
149.89
146.63
119.27
118.42
117.73
115.44
80.50
77.67
73.34
61.28
60.81
57.46
35.64
33.88
27.11
23.35
OH
OH
NH
O
O
O
O
O
HN
OH
OH
O
O
O
NH
O
OH
OH
13C NMR (176 MHz, DMSO-d6)
200
190
180
170
160
150
140
130
120
110
100
90
80
70
60
50
40
30
20
10
0
f1 (ppm)